

Bridging Microscopic Constructions and Continuum Topological Field Theory of Three-Dimensional Non-Abelian Topological Order

Yizhou Huang^{1,*}, Zhi-Feng Zhang^{2,*}, Qing-Rui Wang^{3,†} and Peng Ye^{1,‡}

¹*Guangdong Provincial Key Laboratory of Magnetoelectric Physics and Devices,
State Key Laboratory of Optoelectronic Materials and Technologies,
and School of Physics, Sun Yat-sen University, Guangzhou, 510275, China*

²*Max Planck Institute for the Physics of Complex Systems, Nöthnitzer Straße 38, Dresden 01187, Germany*

³*Yau Mathematical Sciences Center, Tsinghua University, Haidian, Beijing, China*

(Dated: Thursday 12th March, 2026)

Continuum field-theoretical descriptions of topological order *at long distances*, philosophically similar to Ginzburg–Landau field theory for symmetry-breaking phases, are guided by a small set of fundamental principles—such as gauge invariance, locality, symmetry considerations, expected response, and topological invariance—without explicit reference to microscopic realizations *at short distances*. A paradigmatic example is provided by Chern–Simons field theories, where varying choices of gauge groups and coefficients generate a broad family of incompressible fractional quantum Hall states. In addition to such anyonic systems, continuum topological field theories have emerged as a powerful framework for three-dimensional topological orders, capturing particle and loop excitations along with their braiding, fusion, and shrinking processes, as well as the associated diagrammatic rules and stringent *fusion-shrinking consistency* relations required for anomaly-free theories. Despite the progress made over the past years, a long-standing and heavily scrutinized question remains whether these long-distance field-theoretical descriptions admit faithful microscopic counterparts equipped with tensor-product local Hilbert spaces and short-range interactions, and whether the diagrammatic rules and consistency relations previously discovered at long distances still hold valid and complete at short distances. In this paper, we bridge this gap systematically by establishing an explicit correspondence between continuum topological field theory and microscopic lattice constructions of three-dimensional non-Abelian topological orders. While Wilson operators defined by gauge-field holonomies represent topological excitations at long distances, we explicitly construct microscopic lattice operators that create, fuse, and shrink particle and loop excitations, derive their fusion and shrinking rules microscopically, and show how non-Abelian shrinking channels are selectively controlled through the internal degrees of freedom of loop creation operators. Crucially, we demonstrate that the lattice shrinking rules satisfy the *fusion-shrinking consistency* relations previously identified at long distances, thereby establishing these relations as a general, microscopically verifiable principle. Moreover, by computing the complete excitation spectrum alongside all fusion and shrinking data microscopically, we establish a correspondence between the \mathbb{D}_4 quantum double lattice model and the BF field theory with an AAB twist and gauge group $(\mathbb{Z}_2)^3$. Through the precise microscopic construction of the $BF + AAB$ field theory, this work definitively addresses the long-standing skepticism regarding its microscopic realizability, which has persisted over the past years. Finally, our work bridges the gap between theories at long and short distances, taking a crucial step toward a more complete microscopic construction of topological data previously identified at long distances, including braiding, pentagon relations, and fusion–shrinking hexagon relations. This progress holds the potential to deepen our understanding of quantum matter across all length scales and foster collaboration between researchers from diverse fields and approaches.

CONTENTS

I. Introduction	2	A. Hamiltonian on a lattice	10
II. Field-theoretical consistency conditions and diagrammatics of fusion and shrinking rules	6	B. Particle excitations	12
A. Consistent fusion and shrinking rules	6	C. Loop excitations	13
B. Diagrammatics	8	IV. Fusion rules and quantum dimensions	16
III. Excitation creation	9	A. General consideration	16
		B. Abelian fusion rules	18
		C. Non-Abelian fusion rules	18
		V. Shrinking rules and fusion-shrinking consistency	19
		A. General consideration	19
		B. Abelian shrinking rules	21
		C. Non-Abelian shrinking rules	22
		D. Controlling non-Abelian shrinking channels	23

* These authors contributed equally.

† wangqr@mail.tsinghua.edu.cn

‡ yepeng5@mail.sysu.edu.cn

E. Consistency relations between fusion and shrinking	24
VI. Microscopic construction of the BF field theory with an AAB twist	24
A. Overview	24
B. BF field theory with AAB twisted term as a Borromean-Rings topological order	25
C. Microscopic construction	28
D. Isomorphism between excitations of microscopic construction and continuum field theories	31
VII. Discussion	34
A. Summary	34
B. Outlook	35
Acknowledgments	36
A. Diagrammatics, pentagon and hexagon equations	36
B. Details about basic operators	38
1. Proof of Eq. (30)	39
2. Proof of Eqs. (31), (32) and (33)	39
3. Proof of Eqs. (37), (38) and (39)	40
4. Proof of Eq. (40)	41
5. The commutation relations between B_p and L_M^c	41
6. The commutation relations between A_v and L_M^c	41
7. Proof of Eqs. (52), (53), (54) and (55)	41
C. Irreducible Representations of Quantum Double	43
D. Details of shrinking rules in \mathbb{D}_3 quantum double model	44
References	46

I. INTRODUCTION

Since the discovery of the fractional quantum Hall effect (FQH), $2d^1$ topological orders characterized by long-range entanglement [1] have attracted sustained attention over the past few decades. The universal topological data of $2d$ topological orders—including fusion rules and braiding statistics—admit a unified description in terms of continuum topological quantum field theories, most notably Chern–Simons field theories. Abelian

FQH states are universally described by multicomponent $U(1)$ Chern–Simons theories characterized by an integer-valued K matrix, which encodes the anyon content, fusion rules, braiding statistics, and quantized Hall response. Non-Abelian FQH states offer a richer topological field-theoretical description, which can be formulated in terms of non-Abelian Chern–Simons theories or, alternatively, chiral conformal field theories via bulk–edge correspondence. Prominent examples include the $\nu = 5/2$ Moore–Read state described by an $SU(2)_2$ (Ising) topological field theory, the $\nu = 12/5$ Read–Rezayi state associated with an $SU(2)_3$ theory, and more general parafermionic and higher-rank Chern–Simons theories [2–11]. In these cases, the bulk topological field theory captures universal properties such as ground-state degeneracy, non-Abelian braiding, and knot and link invariants. These properties, alongside their microscopic wave functions and many-body Hamiltonians with Coulomb interactions, provide a unified description of topological orders across all length scales.

Despite rapid progress, establishing a precise and systematic correspondence between microscopic constructions at short distances and continuum field theories at long distances remains a central challenge². This is particularly challenging for non-Abelian phases, where the underlying topological structure is rich and potentially relevant for topological quantum computation. The main issue is that the field variables (e.g., emergent gauge fields of different differential forms) at long distances are fundamentally different from the microscopic degrees of freedom (e.g., electrons, local spins) at short distances, and the guiding principles for research in the two domains are vastly different. Practically, in contrast to Landau’s Fermi liquid theory for weakly interacting electron gases [17], the field variables of continuum field theories of topological order at long distances are not derived directly from operators of constituents such as electrons via perturbative-renormalization-group analysis, but are instead introduced through general principles, often with phenomenological treatments, such as gauge invariance, topological invariance, and duality from composite fermions/bosons. Without explicit reference to the microscopic Hamiltonian during the construction of continuum field theories of topological phases of matter, the

¹ In this paper, “ $(n+1)D$ ” refers to $(n+1)$ -dimensional spacetime with n -dimensional real space. We avoid using “ nD ” or “ $(n)D$ ” unless otherwise specified. When referring specifically to spatial dimensions, we use “ nd ”, e.g., $3d$ ground state, $3d$ topological order, $3d$ cubic lattice, and $1d$ closed string.

² The term “microscopic construction” refers to model study at short distances that directly describe the constituents (e.g., electrons, local spins) of many-body systems, whether through continuum models or lattice models, depending on the specific system. For example, FQH systems, which have chiral topological order, are typically microscopically interacting electron systems that do not involve a lattice. By contrast, Kitaev’s toric code lattice model microscopically realizes \mathbb{Z}_2 topological order. At long wavelengths, quantum many-body systems are treated as novel quantum liquids (fracton order is an exception, which is a non-liquid state described by unconventional types of field theories [1, 12–16]), described by continuum quantum field variables, with the theories being continuum topological field theories if the systems are topologically ordered.

physical relevance and microscopic realizability of these continuum field theories are often questioned. Therefore, while both domains have been studied individually, bridging them in a systematic and step-by-step manner remains crucial, necessary, and valuable for advancing our understanding of various topological phases of matter across all length scales, fostering collaboration and dialogue between physicists and mathematicians from different fields.

While this challenge is already nontrivial in two dimensions (e.g., theory of FQH plateaus) and has been an active area of research for decades, it becomes even more acute in three dimensions. There, both the structure of topological excitations and the available continuum field-theoretical frameworks are quite different. Concretely, in higher spatial dimensions the landscape of topological order broadens substantially: in 3d and beyond, point particles are restricted to bosons or fermions [18–21], but topological excitations generically include spatially extended objects such as loops [22, 23]. We consider regular unknotted loop in this paper; yet, loops can have complicated structures of knots or links [24–29], and exhibit nontrivial statistics themselves [30–32]. Recently, a powerful field-theoretical framework for 3d topological orders at long distances has been provided by untwisted and twisted $(3 + 1)$ D BF theories [33–35], which also capture gauged symmetry-protected-topological (SPT) responses [25, 36–45]. The action contains a BF term, schematically BdA with B a 2-form and A a 1-form gauge field, supplemented by various allowed twisted terms, e.g., $AAdA$, $AAAA$, AAB , $dAdA$, and BB . These terms give rise to a rich variety of higher-dimensional topological phenomena, including particle-loop braiding [33, 46–49], multi-loop braiding [39, 50–58], particle-loop-loop Borromean-Rings braiding [42], emergent fermionic statistics [40, 44, 59, 60], and nontrivial topological responses [36, 38, 45, 61–65]. Within the field-theoretical framework, fractionalization of global symmetry on loop excitations has been analyzed in Refs. [66–68], where mixed three-loop braiding formed by external symmetry fluxes and internal loop excitations plays a key role in classifying higher-dimensional symmetry-enriched topological (SET) phases. However, not all braiding processes can coexist, as certain combinations of twisted terms violate gauge invariance. By excluding such terms, Ref. [43] enumerates all legitimate combinations of braiding processes.

In addition to braiding, twisted BF theories reveal a new class of topological data absent in 2d topological orders, namely, *shrinking rules*, which describe how spatially extended excitations can be continuously shrunk into lower-dimensional ones. Given an n -dimensional excitation, one may shrink it to several k -dimensional excitations with $k < n$. For instance, a loop in 3d topological order can shrink to a point, yielding a particle excitation. In our previous work [69], such shrinking processes were systematically analyzed within $(3+1)$ D twisted BF theories, demonstrating that certain twisted terms can induce

non-Abelian fusion and shrinking rules even for Abelian gauge groups.

Lifting to 4d topological order, topological excitations include particles, loops, and membranes [70–75]. Within $(4 + 1)$ D twisted BF theories [76, 77] there are two BF structures, CdA and $\tilde{B}dB$, where A is a 1-form, C is a 3-form, and B and \tilde{B} are distinct 2-form gauge fields. Corresponding twisted terms include $AAAAA$, $AAAdA$, $AdAdA$, AAC , $AAAB$, BBA , $AdAB$, $AAdB$, and BC . It was shown in Ref. [77] that BBA , $AAAB$, AAC , $AAAAA$, and $AAAdA$ lead to non-Abelian shrinking. Furthermore, BBA and $AAAB$ produce *hierarchical* shrinking, whereby a membrane can shrink to loops that subsequently shrink to particles.

Importantly, the derivation of fusion and shrinking rules in twisted BF field theories allows one to verify that, in 3d topological orders, shrinking rules are consistent with fusion: fusing first and then shrinking yields the same outcome as shrinking first and then fusing. In 4d topological orders, hierarchical shrinking rules remain consistent with fusion, but in general shrinking and fusion need not commute. These consistency conditions motivate *diagrammatic representations* [78] for hierarchical shrinking and fusion, from which algebraic constraints such as fusion pentagon relations and (hierarchical) shrinking–fusion hexagon relations emerge, pointing toward underlying higher-categorical structures. The diagrammatic representations of fusion and braiding of anyons in 2d topological orders have been well established, see Refs. [8, 11].

While these $(3 + 1)$ D field-theoretical results establish a coherent and predictive continuum framework at long distances, the careful verification at short distances remains largely unexplored. A long-standing and heavily scrutinized question remains whether the aforementioned $(3 + 1)$ D field-theoretical descriptions admit 3d faithful microscopic counterparts equipped with tensor-product local Hilbert spaces and short-range interactions. Resolving this problem requires not only identifying the correct lattice degrees of freedom, but also reproducing the full fusion–shrinking structure and its consistency relations at the lattice operator level. In particular, the following questions (i to vi) lie at the core of the short–long distances correspondence: *First*, by studying equivalence relations among gauge-invariant Wilson operators in continuum field theory, one can identify all topologically distinct excitations, including *particles*, *pure loops*, and *decorated loops*. We ask whether these counting results admit a faithful microscopic realization. Specifically, it is crucial to construct lattice creation operators for all excitations and to establish microscopic equivalence relations in order to enable a direct comparison between continuum field theory and lattice models. *Second*, braiding and fusion processes exhibit novel quantum phenomena associated with loop-like excitations in higher dimensions. A microscopic construction of braiding and fusion using lattice operators is therefore essential for a meaningful comparison with continuum field-

theoretical predictions. *Third*, shrinking rules are unique to higher-dimensional topological orders, where loop- or membrane-like excitations can be reduced to lower-dimensional objects. While continuum field theory identifies the *allowed shrinking channels* during non-Abelian shrinking processes, it remains unclear whether these channels are complete or redundant from the perspective of microscopic lattice constructions, and how individual channels can be selectively controlled at the microscopic level. *Fourth*, motivated by the systematic diagrammatics of fusion and shrinking derived from continuum field theory [69, 77, 78], we ask whether shrinking processes and their associated rules can be microscopically justified in exactly solvable three-dimensional lattice models, and whether the corresponding *fusion–shrinking consistency relations* persist at the microscopic level. *Fifth*, in the diagrammatic representations of higher-dimensional topological orders derived purely from field-theoretical considerations, fusion pentagon relations and shrinking–fusion hexagon relations impose stringent constraints required for anomaly-free topological data. Whether these constraints admit a complete microscopic interpretation remains an open question. *Finally*, the (3+1)D BF field theory with an AAB twist was introduced in Ref. [42] in connection with Borromean-rings braiding among a particle and two loop excitations. However, a microscopic construction of this field theory and the associated non-Abelian topological order has remained elusive, raising a long-standing skepticism over the past years since the proposal of the field theory in 2018: are such $BF+AAB$ field theories microscopically realizable in lattice models with tensor-product local Hilbert spaces and short-range qubit or qudit interactions?

In this work, we aim to resolve the above issues raised over the past years, especially focusing on particle and loop excitations, together with their fusion and shrinking processes. We derive the corresponding fusion and shrinking rules, and further demonstrate that non-Abelian shrinking channels can be selectively controlled by tuning internal degrees of freedom of loop operators. We show that the lattice shrinking rules are fully consistent with the fusion rules. Furthermore, by establishing an explicit isomorphism between the excitations in the 3d \mathbb{D}_4 quantum double model and those of the (3+1)D BF field theory with an AAB twist and gauge group $G = (\mathbb{Z}_2)^3$ [42], we demonstrate that the former provides a concrete microscopic realization of the latter. Our results establish a direct bridge between topological field theories and exactly solvable lattice models. Concretely, this work is composed of the following parts.

i. *Microscopic construction of excitation creation operators.* In 3d topological orders, topological excitations include both particles and loops, which are represented by Wilson operators (e.g., Wilson loops and Wilson surfaces) in continuum topological field theory [60, 69, 76, 77]. In the microscopic construction—specifically, the 3d quantum double model with a finite group G —the cor-

responding creation operators for excitations are slightly thickened open membrane operators consisting of a direct part and a dual part. Since the type of a topological excitation is invariant under local operations, the corresponding creation operator must carry conserved topological flux and charge. To construct such excitation operators, we introduce four basic operators T_g^\pm and L_g^\pm in Eqs. (17) and (18). The operators T_g^\pm act as projectors on edges, while L_g^\pm modify the group elements on edges. By linearly combining these basic operators, we systematically construct the cylindrical thickened open membrane operators $W_M(C, R; c, j; c', j')$ in Eq. (51), where C is a conjugacy class and R is an irreducible representation of the centralizer of a representative element in C . $c, c' \in C$ are elements in the conjugacy class C and $j, j' = 1, \dots, n_R$ are row and column indices of the representation matrix Γ^R . We choose the thickened open membrane M to be cylindrical as shown in Fig. 13 to incorporate decorated loops. Applying $W_M(C, R; c, j; c', j')$ to a ground state $|\text{GS}\rangle$ yields an excited state $W_M(C, R; c, j; c', j')|\text{GS}\rangle$. In Sec. III C, we verify that the labels C and R remain invariant under local operations, whereas c, j, c' , and j' can be changed by local operations. Therefore, we conclude that the operator $W_M(C, R; c, j; c', j')$ in Eq. (51) serves as the creation operator for a pair of excitation and anti-excitation, which live on the two different boundaries of the cylindrical membrane M . The excitation is characterized by the pair (C, R) , where C and R label the topological flux and charge associated with the excitation respectively, while c, j, c' , and j' are non-topological labels for the internal degrees of freedom of the excitation. In Table VII, we show that the microscopically constructed excitations in the \mathbb{D}_4 quantum double model exactly correspond to the excitations in the BF field theory with an AAB twist and gauge group $G = (\mathbb{Z}_2)^3$. Our explicit lattice operator formalism establishes the foundation for analyzing fusion and shrinking rules in subsequent sections.

ii. *Microscopic construction of fusion rules and quantum dimensions.* In continuum topological field theory, the fusion rules of topological excitations are encoded in correlation functions of the corresponding Wilson operators [60, 69, 77]. In contrast, in the 3d quantum double model, fusion is governed by the representation theory of the underlying quantum double algebra DG . Although the mathematical methods for computing fusion rules differ between the continuum field theory at long distances and the microscopic lattice model at short distance, the physical picture of fusion is the same: both correspond to bringing two excitations together and detecting the results. As

illustrated in Sec. IV A, by exhausting all non-topological degrees of freedom with C and R fixed, we can obtain a set $\{W_M(C, R; c, j; c', j') | \text{GS}\}$ that spans the total Hilbert space $\mathcal{H}_{(C,R)}$ of the pair of excitation and anti-excitation. Under the local operations, the total Hilbert space $\mathcal{H}_{(C,R)}$ can be written as a tensor product of two local Hilbert spaces: $V_{(C,R)} \otimes V_{(\bar{C}, R^*)}$. The excitation denoted by $[C, R]$ and the anti-excitation denoted by $[\bar{C}, R^*]$ are associated with $V_{(C,R)}$ and $V_{(\bar{C}, R^*)}$ respectively. Mathematically, the local Hilbert space $V_{(C,R)}$ and $V_{(\bar{C}, R^*)}$ form two representation spaces of the quantum double algebra DG . When two excitations $[C_1, R_1]$ and $[C_2, R_2]$ are brought together as shown in Fig. 14, their combined local Hilbert space $V_{(C_1, R_1)} \otimes V_{(C_2, R_2)}$ forms a representation space of a tensor-product representation of DG . The fusion rules are thus obtained from the decomposition of this tensor-product representation into irreducible representations, as summarized in Eq. (65). As concrete illustrations, we work out all fusion rules for $G = \mathbb{Z}_N$ (see Eq. (69)) and for $G = \mathbb{D}_3$ (see Table I), the dihedral group of order 6. After deriving fusion rules, we can obtain the quantum dimensions of topological excitations. The quantum dimension d_a of a topological excitation a is defined as the greatest eigenvalue of the matrix N_a , whose elements are given by $(N_a)_{bc} = N_c^{ab}$. For any Abelian group G , the quantum dimensions of excitations are given by $d_a = 1, \forall a$ because all excitations are Abelian and they do not have internal degrees of freedom. In contrast, for a non-Abelian group G , the quantum dimensions of non-Abelian excitations are greater than one. We compute all quantum dimensions as shown in Table II when $G = \mathbb{D}_3$.

iii. *Microscopic construction of shrinking rules and fusion–shrinking consistency.* In continuum topological field theory, the shrinking process of a loop excitation is defined by continuously shrinking the manifold on which the corresponding Wilson operator is supported [69, 77]. By evaluating the correlation function of the Wilson operator after shrinking, one obtains the corresponding shrinking rules. In this work, to realize shrinking processes on a lattice, we consider a *thickened cylindrical membrane operator* that creates a pair of loop excitations on its two boundary loops. The derivation of shrinking rules relies crucially on the connecting rules of membrane operators. By applying Eq. (75), a thickened cylindrical membrane operator associated with a loop excitation can be shrunk to an infinitesimally thin membrane, which effectively becomes a string operator whose endpoints can carry nontrivial charges and thus behave as particle excitations (see Fig. 15). This physical picture of shrinking is the same as that in continuum field

theory at long distance. For non-Abelian G , even a loop excitation with trivial R in (C, R) can produce nontrivial charges upon shrinking, thereby exemplifying non-Abelian shrinking rules. Mathematically, after shrinking, the local Hilbert space $V_{(C,R)}$ associated with $[C, R]$ is mapped to $\mathcal{S}(V_{(C,R)})$. The shrinking rules are then obtained from the decomposition of $\mathcal{S}(V_{(C,R)})$, as summarized in Eq. (79). A particle is denoted by $[C_e, R']$, where C_e is the conjugacy class of the identity e , and R' is an irreducible representation of G . Then this particle appears after shrinking the loop $[C, R]$ if the representation R' restricts to R on the centralizer Z_r , where $r \in C$ is a preselected representative element of C . The shrinking multiplicity is given by Eq. (89). We derive all shrinking rules explicitly for $G = \mathbb{Z}_N$ (see Eq. (93)) and $G = \mathbb{D}_3$ (see Table III). Moreover, by appropriately choosing the internal degrees of freedom of the membrane operator, we demonstrate that the shrinking channel can be controlled to yield a definite particle outcome. In addition, the algebraic structures of fusion and shrinking rules are not independent; rather, they must satisfy fusion–shrinking consistency conditions, given in Eq. (8), which were previously derived within continuum topological field theory [69, 77] and summarized in a diagrammatic formulation [78]. In this work, by explicitly deriving all fusion and shrinking rules within the 3d quantum double model, we verify that these rules, at the microscopic level, rigorously satisfy Eq. (8). This verification not only confirms the algebraic structure predicted by continuum topological field theory but also establishes a concrete microscopic construction of fusion–shrinking consistency in a lattice setting.

iv. *Microscopic construction of the BF field theory with an AAB twist.* The (3 + 1)D BF field theory with an AAB twist, which supports nontrivial Borromean-Rings braiding [42], provides an important example of a non-Abelian topological order, despite the underlying gauge group $(\mathbb{Z}_2)^3$ being Abelian. Gauge invariance constrains which twisted terms may appear in the BF action, implying that Borromean-rings braiding can coexist only with a compatible subset of multi-loop braiding processes [43]. By further analyzing fusion and shrinking processes in this continuum field theory, Ref. [69] derived the corresponding fusion–shrinking consistency conditions. In Sec. VI, we establish a microscopic construction of this continuum field theory by constructing an explicit correspondence with the 3d \mathbb{D}_4 quantum double model. By comparing the fusion and shrinking tables of the two theories, we construct an explicit isomorphism that maps each excitation in the BF field theory with an AAB twist and gauge group $G = (\mathbb{Z}_2)^3$

to a corresponding excitation in the \mathbb{D}_4 quantum double model as shown in Table VII. This isomorphism preserves both fusion and shrinking rules [Eqs. (167) and (168)], thereby conclusively demonstrating that the 3d \mathbb{D}_4 quantum double model provides a concrete microscopic construction of the BF field theory with an AAB twist and gauge group $G = (\mathbb{Z}_2)^3$. In this way, our results bridge the continuum topological field-theoretic description with an exactly solvable microscopic lattice model. Finally, the results successfully validate the fact that $BF + AAB$ field theories are physically relevant and microscopically realizable in lattice models with tensor-product local Hilbert space and short-range qubit/qudit interactions.

This paper is organized as follows. Sec. II reviews fusion and shrinking rules derived from field theory and formulates their consistency, including a summary of the diagrammatic representations that encode these processes in Sec. II B. Sec. III is devoted to constructing the operators for excitations in the microscopic model. We first introduce the 3d quantum double model, construct the ground states on the three-torus, and compute the ground-state degeneracy (GSD) in Sec. III A. Then, we define four basic operators and assemble excitation operators for particles and loops in Sec. III B and Sec. III C respectively. Sec. IV derives the fusion rules, where fusing two excitations amounts to taking the tensor product of irreducible representations of DG , the quantum double of the group G . The general discussion of fusion is shown in Sec. IV A, followed by two examples when $G = \mathbb{Z}_N$ and $G = \mathbb{D}_3$ in Sec. IV B and Sec. IV C respectively. In Sec. V, we construct lattice shrinking processes and derive the corresponding shrinking rules. A general method for computing the shrinking coefficients is shown in Sec. V A. Then we take $G = \mathbb{Z}_N$ and $G = \mathbb{D}_3$ as examples in Sec. V B and Sec. V C respectively. By selecting specific internal degrees of freedom in the operator in Eq. (51), we demonstrate control over shrinking channels in Sec. V D. We further confirm that all shrinking rules are consistent with the fusion rules in Sec. V E. Sec. VI shows that the 3d \mathbb{D}_4 quantum double model provides a microscopic construction of the BF field theory with an AAB twist and gauge group $G = (\mathbb{Z}_2)^3$. We briefly review the Wilson operators for excitations, fusion rules, and shrinking rules in the BF field theory with an AAB twist and gauge group $G = (\mathbb{Z}_2)^3$ in Sec. VI B first. In the subsequent Sec. VI C, all corresponding data in the \mathbb{D}_4 quantum double model are obtained. By comparing the fusion and shrinking tables of these two theories, we establish an isomorphism between their excitations in Sec. VI D. This isomorphism bridges two complementary approaches to topological order. Finally, Sec. VII provides a brief summary and outlook. In Appendix A, a more advanced discussion of diagrammatics is presented. In Appendix B, we prove several equations about the basic operators introduced in Sec. III. In Appendix C, we briefly review the irreducible representations of the quan-

tum double algebra. Some technical details about calculating shrinking rules in the \mathbb{D}_3 quantum double model are shown in Appendix D.

II. FIELD-THEORETICAL CONSISTENCY CONDITIONS AND DIAGRAMMATICS OF FUSION AND SHRINKING RULES

In this section, we first briefly review the consistency conditions between the fusion and shrinking rules that were obtained from the field-theoretical framework in our previous series of works. Next, we review the construction of diagrammatic representations in which fusion and shrinking processes satisfy stringent consistency conditions. The consistency between the fusion and shrinking will be verified in the microscopic lattice model in Sec. V. Furthermore, different unitary symbols can be defined to transform one diagram into another, as shown in Appendix A. These transformations ultimately yield a set of algebraic constraints of higher-dimensional topological orders. Violation of these constraints signals quantum anomalies, offering a diagnostic tool for identifying anomalies in theoretical models.

A. Consistent fusion and shrinking rules

Fusion rules serve as the most fundamental topological data of a topologically ordered phase. Two excitations collectively behave as another excitation when they are brought to the same spatial region and their total topological charge and flux are measured, which is a process referred to as *fusion*. In general, a fusion rule takes the form

$$a \otimes b = \bigoplus_c N_c^{ab} c, \quad (1)$$

where a , b , and c denote topological excitations, and N_c^{ab} is a non-negative integer called the *fusion coefficient*. The value of N_c^{ab} counts the number of topologically distinct *fusion channels* into c . If $N_c^{ab} = 0$, the fusion channel to c is forbidden. A fusion process with exactly one allowed channel is called *Abelian*, whereas one with multiple possible fusion channels is *non-Abelian*.

In 3d topological orders, the presence of loop-like excitations introduces new types of topological data known as *shrinking rules* [69, 77, 78], which determine how extended excitations can be continuously shrunk into lower-dimensional ones, typically particles. The general form of a shrinking rule reads

$$\mathcal{S}(a) = \bigoplus_b S_b^a b, \quad (2)$$

where \mathcal{S} denotes the shrinking operator, b labels particle excitations, and \bigoplus_b enumerates all possible outcomes. The non-negative integer S_b^a is the *shrinking coefficient*,

counting the number of distinct shrinking channels into \mathbf{b} . If \mathbf{a} is already a particle, the shrinking process acts trivially, i.e., $\mathcal{S}(\mathbf{a}) = \mathbf{a}$. Similar to the fusion, a single shrinking channel corresponds to an Abelian shrinking process, while multiple channels indicate a non-Abelian one.

In our previous works [69, 77], fusion and shrinking rules were systematically analyzed using continuum topological field theory (A brief review of this formalism is provided in the Section 2 of Ref. [78]). As an illustrative example, consider a simple untwisted BF theory with the gauge group $G = \prod_i \mathbb{Z}_{N_i}$. The topological action is

$$S = \int \sum_i \frac{N_i}{2\pi} B^i dA^i, \quad (3)$$

where A^i and B^i are 1- and 2-form $U(1)$ gauge fields, respectively. The gauge transformations are given by $A^i \rightarrow A^i + d\chi^i$ and $B^i \rightarrow B^i + dV^i$, where χ^i and V^i are 0- and 1-form gauge parameters satisfying $\int d\chi^i \in 2\pi\mathbb{Z}$ and $\int dV^i \in 2\pi\mathbb{Z}$. An excitation \mathbf{a} in our field theory is represented by a gauge invariant Wilson operator $\mathcal{O}_{\mathbf{a}}$. If \mathbf{a} is a particle carrying n_i units of gauge charge that is minimally coupled to the A^i field, the Wilson operator $\mathcal{O}_{\mathbf{a}}$ is written as $\mathcal{O}_{\mathbf{a}} = \exp\left(i \int_{\gamma} n_i A^i\right)$, where $\gamma = S^1$ denotes the closed one-dimensional world-line of the particle \mathbf{a} in (3+1)D spacetime. If \mathbf{b} is a loop carrying m_j units of gauge flux that is minimally coupled to the B^j field, we have $\mathcal{O}_{\mathbf{b}} = \exp\left(i \int_{\sigma} m_j B^j\right)$, where $\sigma = S^1 \times S^1$ denotes the closed two-dimensional world-sheet of the loop.

In the continuum topological field theory, fusion of two topological excitations \mathbf{a} and \mathbf{b} is defined as dragging two Wilson operators $\mathcal{O}_{\mathbf{a}}$ and $\mathcal{O}_{\mathbf{b}}$ to the same position. This definition coincides with our microscopic construction of fusion on lattice model as shown in Sec. IV. The correlation function $\langle \mathbf{a} \otimes \mathbf{b} \rangle$ is expressed as

$$\langle \mathbf{a} \otimes \mathbf{b} \rangle = \frac{1}{\mathcal{Z}} \int \mathcal{D}[AB] \exp(iS) \times (\mathcal{O}_{\mathbf{a}} \times \mathcal{O}_{\mathbf{b}}), \quad (4)$$

where \mathcal{Z} is the partition function, and $\mathcal{D}[AB]$ represents the field configurations. The product of the two operators $\mathcal{O}_{\mathbf{a}}$ and $\mathcal{O}_{\mathbf{b}}$ in the above equation can be decomposed as a sum over other operators:

$$\begin{aligned} \langle \mathbf{a} \otimes \mathbf{b} \rangle &= \frac{1}{\mathcal{Z}} \int \mathcal{D}[AB] \exp(iS) \times \left(\sum_c N_c^{\mathbf{ab}} \mathcal{O}_c \right) \\ &= \left\langle \bigoplus_c N_c^{\mathbf{ab}} \right\rangle. \end{aligned} \quad (5)$$

This result is the manifestation of the fusion rule Eq. (1) in the framework of continuum topological field theory.

In the continuum topological field theory formalism, shrinking of the excitation \mathbf{a} is defined as contracting only the spatial components of the manifold supporting the Wilson operator $\mathcal{O}_{\mathbf{a}}$, thereby reducing its spatial dimension while keeping the temporal evolution intact. For example, this operation contracts the two-dimensional

world-sheet $T^2 = S^1 \times S^1$ of a loop to a one-dimensional world-line S^1 . In Sec. V, we will see that our microscopic construction of shrinking in lattice model coincides with this continuum field theory definition. The correlation function of this process denoted by $\langle \mathcal{S}(\mathbf{a}) \rangle$ is written as

$$\langle \mathcal{S}(\mathbf{a}) \rangle = \left\langle \lim_{X_1 \rightarrow X_2} \mathcal{O}_{\mathbf{a}} \right\rangle = \lim_{X_1 \rightarrow X_2} \frac{1}{\mathcal{Z}} \int \mathcal{D}[AB] \exp(iS) \mathcal{O}_{\mathbf{a}}, \quad (6)$$

where X_1 and $X_2 \subset X_1$ are the spacetime trajectories of the excitation \mathbf{a} before and after the shrinking process (e.g., $X_1 = S^1 \times S^1$ and $X_2 = S^1$ for a loop). Crucially, the Wilson operator $\mathcal{O}_{\mathbf{a}}$ generally consists of terms involving integration over the entire X_1 as well as over its proper submanifolds. Since some of these terms are supported on X_1 but cannot be supported on X_2 , they do not survive the shrinking process. Only the terms whose support is restricted to the submanifold X_2 remain. These remaining terms can be decomposed as a sum of Wilson operators for lower-dimensional excitations such as particles. Consequently, Eq. (6) can be written as

$$\begin{aligned} \langle \mathcal{S}(\mathbf{a}) \rangle &= \sum_{\mathbf{b}} \frac{1}{\mathcal{Z}} \int \mathcal{D}[AB] \exp(iS) S_{\mathbf{b}}^{\mathbf{a}} \mathcal{O}_{\mathbf{b}} \\ &= \left\langle \bigoplus_{\mathbf{b}} S_{\mathbf{b}}^{\mathbf{a}} \right\rangle, \end{aligned} \quad (7)$$

where $\bigoplus_{\mathbf{b}}$ only enumerates lower-dimensional excitations (particles in 3d). This result serves as the manifestation of the shrinking rule Eq. (2) in the framework of continuum topological field theory.

A systematic analysis shows that for anomaly-free topological orders, fusion and shrinking must satisfy a *consistency condition*. Specifically, in 3d topological order, the condition reads

$$\mathcal{S}(\mathbf{a}) \otimes \mathcal{S}(\mathbf{b}) = \mathcal{S}(\mathbf{a} \otimes \mathbf{b}), \quad (8)$$

meaning that performing fusion before shrinking yields the same result as shrinking first and then fusing. In the language of category, this implies that the shrinking operator is a *tensor functor* that preserves the fusion structure. We will verify that this condition still holds in the lattice model in Sec. V.

If we further lift the spatial dimension to 4d, topological excitations include not only particles and loops but also membrane-like objects. A membrane excitation can undergo a *hierarchical shrinking process*, in which it first shrinks into loops then the loops further shrink into particles. Correspondingly, the consistency condition in 3d (8) is generalized to

$$\mathcal{S}^2(\mathbf{a}) \otimes \mathcal{S}^2(\mathbf{b}) = \mathcal{S}^2(\mathbf{a} \otimes \mathbf{b}), \quad (9)$$

where \mathcal{S}^2 denotes applying the shrinking operation twice in a hierarchical shrinking process.

In this paper, we focus on the consistent fusion and shrinking rules in 3d topological orders. Starting from

the consistency condition (8), we can further derive algebraic constraints between the fusion coefficients N_c^{ab} and the shrinking coefficients S_b^a . Using Eqs. (1) and (2), one finds

$$\begin{aligned} \mathcal{S}(a \otimes b) &= \mathcal{S}\left(\bigoplus_i N_i^{ab}\right) = \bigoplus_i N_i^{ab} \mathcal{S}(i) \\ &= \bigoplus_i N_i^{ab} \left(\bigoplus_c S_c^i\right) \\ &= \bigoplus_c \left(\sum_i S_c^i N_i^{ab}\right) c, \end{aligned} \quad (10)$$

and

$$\begin{aligned} \mathcal{S}(a) \otimes \mathcal{S}(b) &= \left(\bigoplus_i S_i^a\right) \otimes \left(\bigoplus_j S_j^b\right) \\ &= \bigoplus_i \bigoplus_j [S_i^a S_j^b (i \otimes j)] \\ &= \bigoplus_i \bigoplus_j \left[S_i^a S_j^b \left(\bigoplus_c N_c^{ij}\right)\right] \\ &= \bigoplus_c \left(\sum_{i,j} S_i^a S_j^b N_c^{ij}\right) c. \end{aligned} \quad (11)$$

Comparing both equations above, we can find that the consistency between fusion and shrinking rules enforces a key constraint

$$\sum_i S_c^i N_i^{ab} = \sum_{i,j} S_i^a S_j^b N_c^{ij}, \quad (12)$$

where a, b, c, i, j label all possible excitations. Eq. (12) encodes the algebraic backbone of consistent fusion–shrinking relations and can also be understood through our diagrammatic formulation as shown in Eq. (A6) of Appendix A.

B. Diagrammatics

The consistency conditions Eqs. (8) and (9) in 3d and 4d topological orders inspire the diagrammatic representations of consistent fusion and shrinking rules [78]. We can define elementary diagrams for fusion and shrinking processes and treat them as vectors in the fusion and shrinking spaces respectively. By combining these elementary diagrams, we can build more complex diagrams, and use a series of unitary operations to transform between them. The legitimate forms of these unitary operations are strongly constrained by pentagon equations and (hierarchical) shrinking–fusion hexagon equations, which reveal the algebraic structure of the consistent fusion and shrinking rules. In this section, we briefly review the diagrammatic representations of fusion and shrinking rules

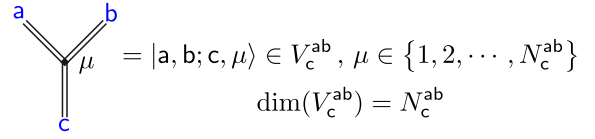


FIG. 1. Elementary fusion diagrams in 3d. a , b and c denote excitations and we highlight them in blue. $\mu = \{1, 2, \dots, N_c^{ab}\}$ labels different fusion channels with the same fusion output c . Double-lines indicate that $a, b, c \in \Phi_0^{3+1}$. If we want to draw a fusion diagram that represents fusion in the set Φ_1^{3+1} , we only need to replace all the double-lines with single-lines.

in 3d. Details about the transformation between different complex diagrams and the derivation of algebraic constraints are collected in Appendix A.

We need to first introduce some notations. We assume that there are only a finite number of topologically distinct excitations in a topological order, and we collect all of them in a set denoted as $\Phi_0^{\mathcal{D}}$, where the superscript \mathcal{D} denotes the spacetime dimension. In this paper, we mainly focus on 3d topological orders and thus $\mathcal{D} = 3+1$. If we perform a shrinking operation on all excitations in Φ_0^{3+1} , all the possible shrinking results form a subset of Φ_0^{3+1} , denoted by Φ_1^{3+1} . We can view the shrinking process as a mapping from the set Φ_0^{3+1} to its subset Φ_1^{3+1} ,

$$\mathcal{S}: \Phi_0^{3+1} \rightarrow \Phi_1^{3+1}. \quad (13)$$

The excitations in the set Φ_i^{3+1} have closed fusion rules, i.e., all possible fusion results of fusing two excitations from the set Φ_i^{3+1} still form the set Φ_i^{3+1} itself. This is a consequence of the finite number of topological excitations and has been verified in (3+1)D twisted BF theories [69, 77]. Thus, we can also treat a fusion process as a mapping,

$$\otimes: \Phi_i^{3+1} \times \Phi_i^{3+1} \rightarrow \Phi_i^{3+1}, \quad i = 0, 1. \quad (14)$$

To build a general diagrammatic framework, we allow for fusion and shrinking multiplicities. In this section, Latin and Greek letters denote excitations and fusion/shrinking channels, respectively.

Now we can construct the diagrammatics for 3d topological orders. The basic diagram in our 3d diagrammatics is defined as follows. Suppose that the fusion process $a \otimes b$ has a fusion channel to c , we can represent the fusion channel diagrammatically in Fig. 1. The solid lines are understood as the spacetime trajectories of the excitations, and here we use double-lines to indicate that $a, b, c \in \Phi_0^{3+1}$. One can simply replace the double-lines with single-lines to obtain a fusion diagram that represents the fusion process in the set Φ_1^{3+1} . In Fig. 1, we use $\mu = \{1, 2, \dots, N_c^{ab}\}$ to label different fusion channels to c , and the fusion diagram can be defined as a vector $|a, b; c, \mu\rangle$. The set of orthogonal vectors $\{|a, b; c, \mu\rangle, \mu = 1, 2, \dots, N_c^{ab}\}$ spans a fusion space V_c^{ab} with $\dim(V_c^{ab}) = N_c^{ab}$.

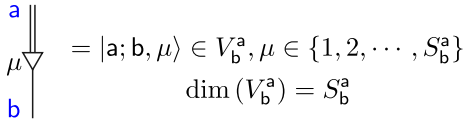


FIG. 2. Shrinking diagram in 3d. The double-line and single-line represent excitations from Φ_0^{3+1} and Φ_1^{3+1} respectively. Since a and b are the input and output of the shrinking process respectively, a can be a loop or a particle while b can only be a particle. We use a triangle to represent the shrinking operation. This diagram can be defined as a vector and the orthogonal set $\{|a; b, \mu\rangle, \mu = 1, 2, \dots, S_b^a\}$ spans the shrinking space V_b^a with $\dim(V_b^a) = S_b^a$.

The basic shrinking diagram is defined as follows. Suppose that $a \in \Phi_0^{3+1}$ and the shrinking process $\mathcal{S}(a)$ has a shrinking channel to $b \in \Phi_1^{3+1}$, then we define the corresponding shrinking diagram in Fig. 2. We use a triangle to represent the shrinking operation. Note that in a specific diagram, a double-line and a single-line may actually represent the same particle. However, they carry distinct meanings: the double-line means that this particle from Φ_0^{3+1} is treated as the input of the shrinking process, while the single-line means that this particle from Φ_1^{3+1} is the output. We define the shrinking diagram in Fig. 2 as a vector $|a; b, \mu\rangle$, where different μ label different orthogonal vectors. The set $\{|a; b, \mu\rangle, \mu = 1, 2, \dots, S_b^a\}$ spans a shrinking space denoted by V_b^a , whose dimension is given by $\dim(V_b^a) = S_b^a$.

We can stack these basic diagrams to construct more complicated diagrams that describe more complicated processes. For example, by stacking two basic fusion diagrams shown in Fig. 1, we construct a fusion diagram that involve three excitations. Consider fusing three excitations $(a \otimes b) \otimes c$ and there exist legitimate fusion channels to d , we can draw this process in Fig. 3, which is defined as a vector $|{(a, b)}; e, \mu\rangle \otimes |e, c; d, \nu\rangle$, where \otimes means tensor product. The corresponding space is denoted as V_d^{abc} , whose dimension is given by

$$\dim(V_d^{abc}) = \sum_e N_e^{ab} N_d^{ec}, \quad (15)$$

because V_d^{abc} is isomorphic to $\oplus_e V_e^{ab} \otimes V_d^{ec}$. We can use a similar tensor product construction to incorporate both fusion and shrinking processes in a diagram. Consider $\mathcal{S}(a) \otimes \mathcal{S}(b)$, the corresponding diagrams are shown in Fig. 4. This diagram is understood as the vector $|d, e; c, \lambda\rangle \otimes |b; e, \nu\rangle \otimes |a; d, \mu\rangle$, where different d, e, μ, ν , and λ label different orthogonal vectors. The diagram shown in Fig. 4 describes the process that a and b shrink to d and e in the μ and ν channels respectively first, then d and e fuse to c in the λ channel. This set of orthogonal vectors spans the space denoted as $V_c^{\mathcal{S}(a) \otimes \mathcal{S}(b)}$, which is isomorphic to $\oplus_{d,e} V_c^{de} \otimes V_e^b \otimes V_d^a$ due to our tensor product construction. Thus, we have

$$\dim(V_c^{\mathcal{S}(a) \otimes \mathcal{S}(b)}) = \sum_{d,e} N_c^{de} S_e^b S_d^a. \quad (16)$$

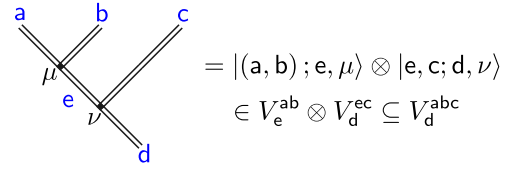


FIG. 3. Fusing three excitations in 3d. a, b , and c are ultimately fuse into d . The bracket “ (a, b) ” is only used to emphasize that a and b fuse together first in the whole three-excitation fusion process and it does not change the vectors. The set of vectors $\{|(a, b); e, \mu\rangle \otimes |e, c; d, \nu\rangle\}$ span the whole space V_d^{abc} , where different μ, ν and e label different orthogonal vectors. The space V_d^{abc} is isomorphic to $\oplus_e (V_e^{ab} \otimes V_d^{ec})$. The dimension of V_d^{abc} is given by $\dim(V_d^{abc}) = \sum_e N_e^{ab} N_d^{ec}$. Here we only draw the fusion diagram for fusion process in the set Φ_0^{3+1} . One can obtain the diagram for subset Φ_1^{3+1} by simply replacing all double-lines with single-lines.

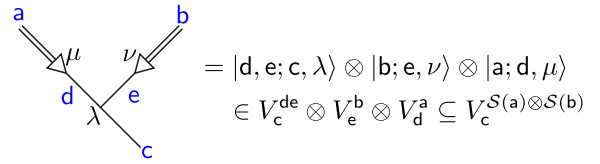


FIG. 4. Incorporating both fusion and shrinking processes in 3d. We stack two basic shrinking diagrams and a basic fusion diagram to describe the process $\mathcal{S}(a) \otimes \mathcal{S}(b)$.

The consistency condition Eq. (8) allows us to introduce a series of unitary operations to transform these complicated diagrams. We can derive important algebraic constraints on these unitary operations known as the pentagon equation and shrinking-fusion hexagon equation. Details of these unitary operations and algebraic constraints are shown in Appendix A.

III. EXCITATION CREATION

To establish a connection between continuum field theory and microscopic lattice constructions, we need a microscopic model for 3d topological order. The 3d quantum double model serves as an ideal platform. In this section, we consider the 3d quantum double lattice model and design the operators to create topological excitations. We note that topological excitations in 3d differ essentially from their 2d counterparts. While 2d topological orders host point-like anyons that exhibit fractional statistics, point-like particles in 3d are constrained to be either bosons or fermions. Furthermore, spatially extended excitations, i.e., loops, appear in 3d and support nontrivial processes such as fusion and shrinking. Investigating these particles and loops, along with their fusion and shrinking rules, reveals structures that extend beyond those found in 2d topological orders. These excitations are the cornerstones of the study of fusion and shrinking rules on lattice in Secs. IV and V.

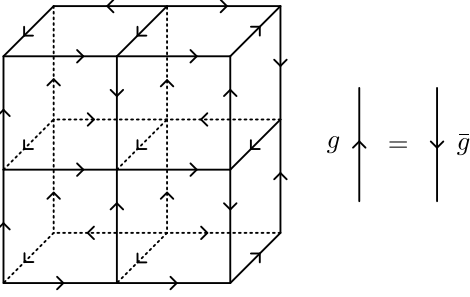


FIG. 5. Local Hilbert space on a cubic lattice. Each edge is assigned with an arrow and a group element $g \in G$. Reversing the arrow of an edge changes the group element g to its inverse \bar{g} .

A. Hamiltonian on a lattice

Consider the 3d quantum double model defined on the cubic lattice with periodic boundary condition. The underlying degrees of freedom are the group elements $g \in G$ on the edges of the cubic lattice. Each edge is assigned with an orientation (an arrow, see Fig. 5) that can be chosen arbitrarily. Reversing the orientation of an edge changes g on the edge to its inverse, \bar{g} . The local state on an edge is denoted as $|g\rangle$ and we set $\langle g|h\rangle = \delta_{g,h}$. The local Hilbert space is spanned by the basis $\{|g\rangle | g \in G\}$ and its dimension is $|G|$, the number of elements in G . A configuration on the whole lattice is written as $|g_1\rangle \otimes |g_2\rangle \otimes \cdots \otimes |g_N\rangle$, where \otimes means tensor product and g_i labels the group element on the i -th edge, $i = 1, 2, \dots, N$. All possible configurations span the total Hilbert space whose dimension is $|G|^N$.

With the local Hilbert space on the edges introduced, we define four basic operators that act on the Hilbert space of an edge. We will see later that the linear combinations of these basic operators give rise to topological excitations. The basic operators (dubbed “ T -operators” and “ L -operators” hereafter) are

$$T_g^+ = |g\rangle \langle g|, \quad T_g^- = |\bar{g}\rangle \langle \bar{g}|, \quad (17)$$

$$L_g^+ = \sum_{k \in G} |gk\rangle \langle k|, \quad L_g^- = \sum_{k \in G} |k\bar{g}\rangle \langle k|. \quad (18)$$

The operator T_g^+ (T_g^-) acts on $|h\rangle$ as a test for whether the group element on the edge equals g (\bar{g}), being a projection operator selecting $h = g$ ($h = \bar{g}$). The operator L_g^+ acts on $|h\rangle$ as a “left-multiplication” operator, $L_g^+ |h\rangle = |gh\rangle$, where the group element on the edge is left-multiplied by g . In contrast, the operator L_g^- acts on $|h\rangle$ as $L_g^- |h\rangle = |h\bar{g}\rangle$, where the group element on the edge is right-multiplied by \bar{g} . We can verify that the basic

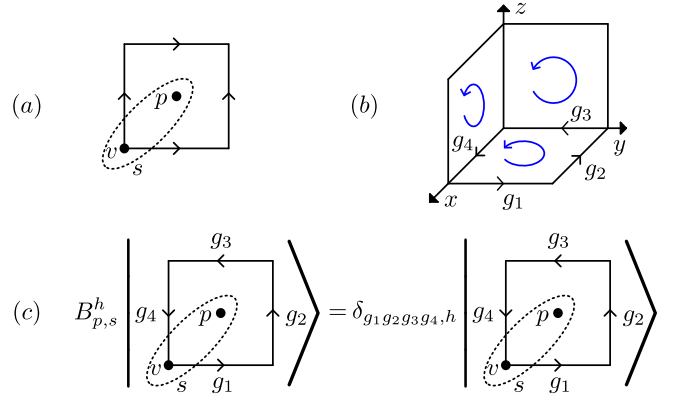


FIG. 6. Action of the plaquette operator $B_{p,s}^h$. (a) A site $s = (v, p)$ is a combination of a vertex v and a plaquette p . (b) The blue arrows denote the product order of the group elements on the edges of the plaquette. (c) $B_{p,s}^h$ projects the ordered product of all group elements on the edges around p , $g_1 g_2 g_3 g_4$, to $h \in G$. Notice that the ordered product depends on the choice of the site $s = (v, p)$, i.e., the choice of vertex v . When $h = e$, $g_1 g_2 g_3 g_4 = e$ implies $g_4 g_1 g_2 g_3 = g_3 g_4 g_1 g_2 = \cdots = e$. But for a general h , $g_1 g_2 g_3 g_4 = h$ does not guarantee other ordered product like $g_4 g_1 g_2 g_3$ is h .

operators satisfy the following properties

$$\begin{aligned} T_g^\pm T_h^\pm &= \delta_{g,h} T_h^\pm, & L_g^\pm L_h^\pm &= L_{gh}^\pm, \\ T_g^+ L_h^+ &= L_h^+ T_{\bar{h}g}^+, & T_g^+ L_h^- &= L_h^- T_{gh}^+, \\ T_g^- L_h^+ &= L_h^+ T_{g\bar{h}}^-, & T_g^- L_h^- &= L_h^- T_{\bar{h}g}^-, \\ (T_g^\pm)^\dagger &= T_g^\pm, & (L_g^\pm)^\dagger &= (L_g^\pm)^{-1} = L_{\bar{g}}^\pm, \\ [L_g^\pm, L_h^\mp] &= 0, & \sum_g T_g^\pm &= L_e^\pm = 1. \end{aligned} \quad (19)$$

Before presenting the Hamiltonian of the 3d quantum double model, we first introduce the plaquette operator $B_{p,s}^h$ acting on the plaquette p and the vertex operator A_v acting on the vertex v .

As shown in Fig. 6, the action of $B_{p,s}^h$ is to measure whether the ordered product of group elements on the edges around the plaquette p equals h . If yes, the state remains intact, otherwise it is annihilated. The site $s = (v, p)$ defined in Fig. 6(a) determines the order of multiplication in the product, which is important because the group elements are generally non-commutative. Specifically, for a plaquette on the xy -plane, we set its normal direction as the $+z$ direction and set the arrows of the edges to form a counterclockwise loop with respect to the normal direction. Then, starting from the vertex v , we multiply the group elements along the loop direction. For other plaquettes on xz - and yz -planes, we set their normal directions as the $+y$ and $+x$ directions, the orientations of the arrows of the edges are shown in Fig. 6(b). A plaquette operator $B_{p,s}^h$ can always be constructed from the basic operators shown in Eq. (17). For

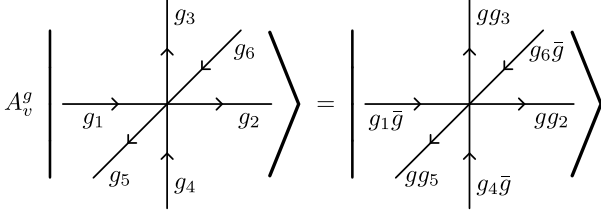


FIG. 7. The action of A_v^g term. $A_v^g |g_i\rangle = |gg_i\rangle$ if the arrow points away from v , $A_v^g |g_i\rangle = |g_i\bar{g}\rangle$ if the arrow points towards v .

example, $B_{p,s}^h$ in Fig. 6(c) can be written as

$$B_{p,s}^h = \sum_{g_1, g_2, g_3 \in G} T_{\bar{g}_3 \bar{g}_2 \bar{g}_1 h}^+ T_{g_3}^+ T_{g_2}^+ T_{g_1}^+, \quad (20)$$

where $T_{g_1}^+$, $T_{g_2}^+$, $T_{g_3}^+$, and $T_{\bar{g}_3 \bar{g}_2 \bar{g}_1 h}^+$ act on the edges labeled by g_1 , g_2 , g_3 , and g_4 respectively. If we take h as the identity element e , the action of $B_{p,s}^h$ is independent of the choice of s . We denote $B_{p,s}^e$ as \bar{B}_p for simplicity. The B_p term can be understood as the zero flux condition. But for a general $h \in G$, the action of $B_{p,s}^h$ depends on the choice of the site. If we choose a different vertex v in $s = (v, p)$, $B_{p,s}^h$ may project the product $g_1 g_2 g_3 g_4$ to another element in the conjugacy class C_h containing h .

The vertex operator A_v^g acts on all edges that are attached to the vertex v . If the arrow of the edge points away from the vertex v , the group element on the edge is multiplied by g on the left. Otherwise, the element on the edge is multiplied by \bar{g} on the right, as shown in Fig. 7. Similar to the plaquette operator, a vertex operator A_v^g can also be written as a product of the basic operators shown in Eq. (18). As an example, we write the vertex operator A_v^g in Fig. 7 as

$$A_v^g = L_g^- L_g^+ L_g^+ L_g^- L_g^+ L_g^-, \quad (21)$$

where the three L_g^+ operators act on the edges labeled by g_2 , g_3 , and g_5 , respectively, while the three L_g^- operators act on the edges labeled by g_1 , g_4 , and g_6 , respectively.

The Hamiltonian is given by

$$H = - \sum_v A_v - \sum_p B_p, \quad (22)$$

where $A_v = \frac{1}{|G|} \sum_{g \in G} A_v^g$. The definition of the B_p term is given after Eq. (20). By means of T - and L - operators shown in Eqs. (17) and (18) as well as the properties shown in Eq. (19), we can verify that A_v 's and B_p 's satisfy

$$A_v^g A_v^h = A_v^{gh}, \quad (23)$$

$$A_v A_v = A_v, \quad (24)$$

$$B_p B_p = B_p, \quad (25)$$

$$[A_v^g, A_v^h] = [B_p, B_{p'}] = [A_v, B_p] = 0. \quad (26)$$

which guarantees the exact solvability of the Hamiltonian.

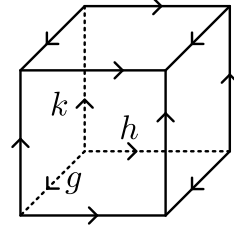


FIG. 8. The simplest 3d lattice on a 3-torus manifold. There are only three independent edges, three independent plaquettes, and one independent vertex. The configuration on this lattice is written as $|g, h, k\rangle$.

Any ground state of the Hamiltonian is a state where all A_v 's and B_p 's have eigenvalues $+1$. From the viewpoint of gauge theory, $A_v = 1$ encodes the gauge invariance and $B_p = 1$ enforces the zero flux condition. The ground state can be obtained as follows. Starting from a product state $|\phi\rangle$ that satisfies the zero flux condition (B_p term has eigenvalue $+1$) everywhere, i.e., $B_p |\phi\rangle = |\phi\rangle$, $\forall p$, then acting the projector $\prod_v A_v$ on $|\phi\rangle$ gives us a ground state $|\text{GS}\rangle = \prod_v A_v |\phi\rangle$. Using Eq. (24) and Eq. (26), we verify that $A_v |\text{GS}\rangle = B_p |\text{GS}\rangle = |\text{GS}\rangle$.

To compute the GSD, we consider the simplest non-trivial case in which the Hamiltonian is defined on a 3-torus T^3 . The 3-torus can be represented by a single cube with periodic boundary condition as shown in Fig. 8. A state satisfying the zero-flux condition can be written as $|g, h, k\rangle$, where the commuting group elements g , h , and k denote the three independent group elements on the single cube. The other condition for a ground state is $A_v |\text{GS}\rangle = |\text{GS}\rangle$. Since there is only one vertex in this cube, we have

$$\begin{aligned} |\text{GS}_{g,h,k}\rangle &= A_v |g, h, k\rangle = \frac{1}{|G|} \sum_{g_0} A_v^{g_0} |g, h, k\rangle \\ &= \frac{1}{|G|} \sum_{g_0} |g_0 g \bar{g}_0, g_0 h \bar{g}_0, g_0 k \bar{g}_0\rangle. \end{aligned} \quad (27)$$

We can also choose states labeled by other commuting elements $|g', h', k'\rangle$ to construct other ground states $|\text{GS}_{g',h',k'}\rangle$. The group theory ensures that $|\text{GS}_{g,h,k}\rangle$ and $|\text{GS}_{g',h',k'}\rangle$ are either the same or orthogonal to each other. By using the Burnside's lemma, the GSD is derived as

$$\text{GSD} = \frac{1}{|G|} \sum_{g_0 \in G} \sum_{\{g,h,k\}} \delta_{g, g_0 g \bar{g}_0} \delta_{h, g_0 h \bar{g}_0} \delta_{k, g_0 k \bar{g}_0}, \quad (28)$$

where $\{g, h, k\}$ is the triplet of commuting group elements. Here, we give the GSD on a 3-torus for some simple groups. For an Abelian group G , the GSD is $|G|^3$. For $G = \mathbb{D}_3$ and $G = \mathbb{D}_4$, the GSD are 21 and 92, respectively. Note that the BF theory with an AAB twist and gauge group $(\mathbb{Z}_2)^3$ also has GSD = 92 on T^3 [69]. In Sec. VI, we further conclude that the fusion and shrinking rules of the 3d $G = \mathbb{D}_4$ quantum double model and

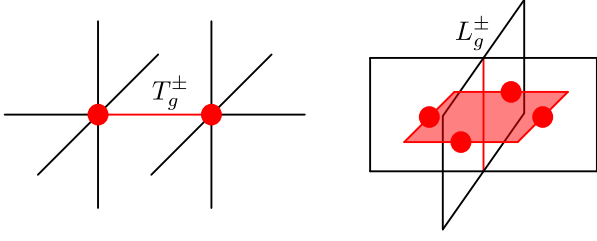


FIG. 9. Acting T - and L -operators [Eq. (18)] on a ground state. These basic operators generally do not commute with the vertex terms or plaquette terms in the Hamiltonian. Thus, a T_g^\pm creates a pair of excited vertices while an L_g^\pm creates a loop-like excited state.

the BF theory with an AAB twist and gauge group $(\mathbb{Z}_2)^3$ are isomorphic, which leads to an exact correspondence between the continuum topological field theory and the microscopic lattice construction.

B. Particle excitations

In Sec. III A, we have introduced the basics of the 3d quantum double model and obtained its ground states. Here, we proceed to create excitations and investigate their properties. Recall that a vertex term A_v and a plaquette term B_p can be constructed by using several L_g^\pm terms and T_g^\pm terms respectively. The ground state condition is $A_v = B_p = 1$, $\forall v, p$. From Eq. (19) we can see that T_g^\pm generally does not commute with L_g^\pm , which means that a T_g^\pm does not commute with the two vertex terms on the endpoints of an edge, and an L_g^\pm does not commute with the four plaquette terms around the edge. Thus, as shown in Fig. 9, acting a T_g^\pm on the ground state creates two excited vertices (i.e., violates the condition $A_v = 1$) on the endpoints of an edge, and acting a L_g^\pm creates four excited plaquettes (i.e., violates the condition $B_p = 1$) whose centers live on a closed loop in the dual lattice. In this sense, the topological excitations in the 3d quantum double model can be particles or loops. In Sec. III B and III C, we illustrate how to construct the operators for particles (Eq. (34)) and loops (51) by using T_g^\pm and L_g^\pm in our 3d quantum double model. For simplicity, we say that an operator violates vertex terms or plaquette terms when this operator does not commute with them in the following discussion.

We first consider the operators for particles. T_L^g is defined as an operator that acts on an oriented string L . If the string L can be obtained by connecting two shorter strings L_1 and L_2 , we define the connecting rule of $T_{L=L_1 \cup L_2}^g$ as

$$T_{L=L_1 \cup L_2}^g = \sum_h T_{L_2}^{\bar{h}g} T_{L_1}^h. \quad (29)$$

When L_i is a single edge, then $T_{L_i}^g = T_g^+$ if the arrow of the edge aligns with the orientation of L_i , otherwise

$T_{L_i}^g = T_g^-$. Note that the operator $T_{L_1}^h$ in Eq. (29) acts first, we demand that the end of L_1 is also the start of L_2 . In the following discussion, we use $\partial_0 L$ and $\partial_1 L$ to denote the start and end of an oriented string L respectively, and we have $\partial_1 L_1 = \partial_0 L_2$. The operator T_L^g projects onto the state in which the ordered product of group elements along L equals g .

When we consider connecting more strings as shown in Fig. 10, we expect that the order of connection is irrelevant, i.e.,

$$T_{L_1 \cup (L_2 \cup L_3)}^g = T_{(L_1 \cup L_2) \cup L_3}^g, \quad (30)$$

where the bracket in $L_1 \cup (L_2 \cup L_3)$ emphasizes that we connect L_2 and L_3 first. Similarly, the bracket in $(L_1 \cup L_2) \cup L_3$ emphasizes that we connect L_1 and L_2 first. We provide the proof of Eq. (30) in Appendix B 1.

Another important property of T_L^g is that it commutes with B_p 's and A_v 's, except those A_v 's at the endpoints of L . We denote a string by $L = (v_0, v_1, \dots, v_n)$ that starts at the vertex v_0 and ends at v_n , where an edge is denoted by $v_i v_{i+1}$. Since this operator does not change the group elements on edges (T_L^g consists of T_g^+ and T_g^-), it automatically commutes with all B_p terms in the Hamiltonian. As for A_v terms, in Appendix B 2 we prove that

$$A_{v_i}^k T_L^g = T_L^g A_{v_i}^k, \quad (31)$$

where $k \in G$ and $i \neq 0, n$. Since $A_{v_i} = \frac{1}{|G|} \sum_{k \in G} A_{v_i}^k$, we conclude that $[A_{v_i}, T_L^g] = 0$ as long as v_i is a vertex inside the string L . However, T_L^g does not commute with the vertex terms at the endpoints of L . In Appendix B 2, we derive the commutation relations between $A_{v_0}^k$, $A_{v_n}^k$, and T_L^g as:

$$A_{v_0=\partial_0 L}^k T_L^g = T_L^{kg} A_{v_0=\partial_0 L}^k, \quad (32)$$

$$A_{v_n=\partial_1 L}^k T_L^g = T_L^{gk} A_{v_n=\partial_1 L}^k, \quad (33)$$

which means that the operator T_L^g violates the A_{v_0} and A_{v_n} term. Therefore, the operator T_L^g creates excited vertices at the endpoints of L , as shown in Fig. 10.

We construct a string operator for particles by linearly combining T_L^g :

$$W_L(R; i, j) = \sum_g [\Gamma_{ij}^R(g)]^* T_L^g = \sum_g \Gamma_{ij}^{R*}(g) T_L^g, \quad (34)$$

where R labels the irreducible representation (irrep) of G , Γ denotes the matrix of the irrep, i, j are row and column indices, $*$ and R^* denote complex conjugate and complex conjugate representation. In Eq. (34), the particle type is characterized by the irrep R . The indices i and j label some internal degrees of freedom that can be changed by a local action as shown in Eqs. (37), (38) and (39). For a particle living on the vertex v , an arbitrary local action on this particle can be generated by the local operators $B_{p,s}^h$ and A_v^g as

$$\sum_{h,g \in G} n_{h,g} B_{p,s}^h A_v^g, \quad (35)$$

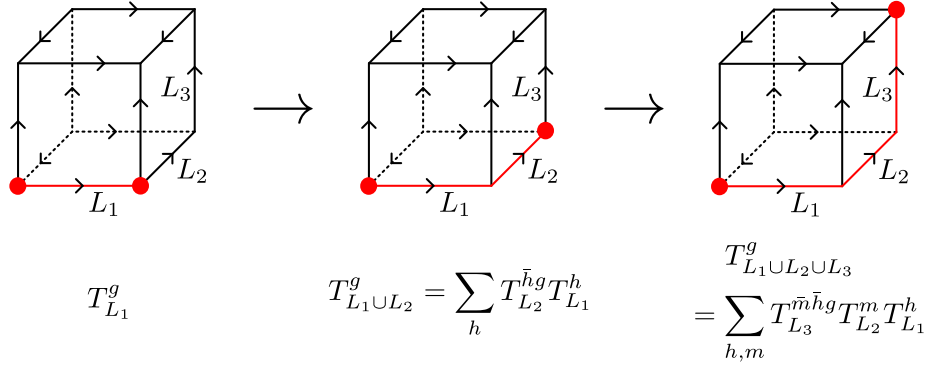


FIG. 10. Connecting three string operators step by step. The red lines and dots denote the string and the excited vertices respectively. This connecting rule allow us to freely move particles.

where $v \in s$, $n_{h,g}$ is a coefficient. Mathematically, Eq. (35) can be viewed as an element of the quantum double algebra DG with basis $\{D_{(h,g)} \equiv B_{p,s}^h A_v^g\}$ on a site s , see Appendix C.

Now we illustrate how the local operators change the internal degrees of freedom i and j in Eq. (34). We label the excited state with two particles as

$$|R; i, j\rangle = W_L(R; i, j) |\text{GS}\rangle. \quad (36)$$

Acting the local operators A_v^g and $B_{p,s}^h$ on the excited state gives

$$A_{v=\partial_0 L}^g |R; i, j\rangle = \sum_k \Gamma_{ki}^R(g) |R; k, j\rangle, \quad (37)$$

$$A_{v=\partial_1 L}^g |R; i, j\rangle = \sum_k \Gamma_{kj}^{R*}(g) |R; i, k\rangle, \quad (38)$$

$$B_{p,s}^h |R; i, j\rangle = \delta_{h,e} |R; i, j\rangle, \quad \forall (p, s), \quad (39)$$

where the derivations are collected in Appendix B3. The local operator A_v^g changes the row (column) indices of Γ^R when acting on the starting (end) point of the string L . Crucially, the particle label R is invariant under the action of the local operators. Thus, we conclude that the indices i and j are related to the internal degrees of freedom of the particles on $\partial_0 L$ and $\partial_1 L$ respectively.

Finally, we give the connecting rule of the string operator $W_{L=L_1 \cup L_2}(R; i, j)$ for the particle as

$$W_{L_1 \cup L_2}(R; i, j) = \sum_k W_{L_2}(R; k, j) W_{L_1}(R; i, k). \quad (40)$$

Since the particles live on the endpoints of the string, the operator $W_{L_1}(R; i, k)$ creates a pair of particles on vertex $v_0 = \partial_0 L_1$ and $v_1 = \partial_1 L_1$ respectively. This connecting rule allows us to move the particle from $v_1 = \partial_1 L_1$ to $v_2 = \partial_1 L_2$. We can similarly move the particle on $v_0 = \partial_0 L_1$ as well. The proof of Eq. (40) is provided in Appendix B4.

C. Loop excitations

In this section, we proceed to construct membrane operators for loops. Unlike the one-dimensional ribbon op-

erators used for anyons in 2d topological orders, the operator that creates a loop excitation in 3d must be a two-dimensional thickened membrane that consists of a dual part and a direct part. The dual part is formed by dual plaquettes and the boundary of the dual part is related to the flux of the loop. Besides nontrivial flux, a loop can also carry some charge decorations. These charge decorations can freely travel along the boundary of the direct part that is formed by direct plaquettes.

We start by considering the simplest thickened membrane as shown in Fig. 11. The red plaquette is the dual part and cuts the edge vv' , the blue vertex v serves as the direct part and can be understood as an infinitesimal direct plaquette $vv_1v_2v_3$, where $v = v_1 = v_2 = v_3$. Now we consider the action of $L_{vv'}^h$ on the edge vv' defined as (see Fig. 11)

$$L_{vv'}^h = \begin{cases} L_h^+, & \text{if } v \rightarrow v' \\ L_h^-, & \text{if } v \leftarrow v' \end{cases}. \quad (41)$$

That means, if the arrow of vv' points from the direct part to the dual part, i.e., from v to v' , we define $L_{vv'}^h$ as L_h^+ to change the group element on vv' . Otherwise, we define $L_{vv'}^h$ as L_h^- . Since acting $L_{vv'}^h$ violates B_p terms around vv' , we conclude that there exists a loop-like excited state living on the boundary the thickened membrane. To create a spatially larger loop excitation, we need to consider connecting several $L_{vv'}^h$ terms.

As shown in Fig. 12, consider creating a loop-like excited state on the boundary of an open thickened membrane M_α , whose dual part cuts α edges. We set the arrows of edges to point from the direct part to the dual part, and we start by acting $L_{v_0v'_0}^h$ on $v_0v'_0$. We construct the operator $L_{M_\alpha}^h$ by using a recursive procedure as follows. The $L_{M_1}^h$ only acts on one edge $v_0v'_0$ and is given by

$$L_{M_1}^h = L_{v_0v'_0}^h. \quad (42)$$

Note that the operator $L_{M_2}^h$ can not be constructed by simply acting another $L_{v_1v'_1}^h$ term on the edge $v_1v'_1$ because the center of the plaquette $p = v'_0v_0v_1v'_1$ does not

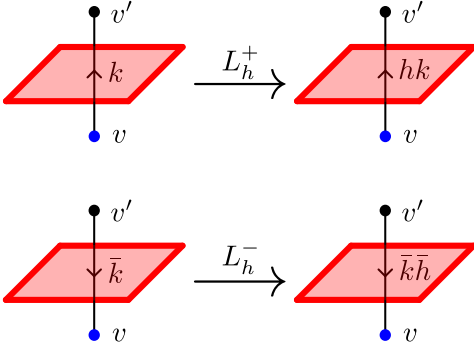


FIG. 11. The action of $L_{vv'}^h$ on the edge vv' is defined in Eq. (41). The red and blue denote the dual part and the direct part of the thickened membrane respectively. Since $L_{vv'}^h$ involves only the single edge vv' , its dual part is uniquely determined as the dual plaquette intersecting vv' . For illustration, we choose the direct part as an infinitesimal direct plaquette $vvvv$ here. However, the choice of the direct part is not unique. Any direct plaquette p (of finite or infinitesimal area) that contains vertex v can serve as the direct part without altering the form of the thickened membrane operator.

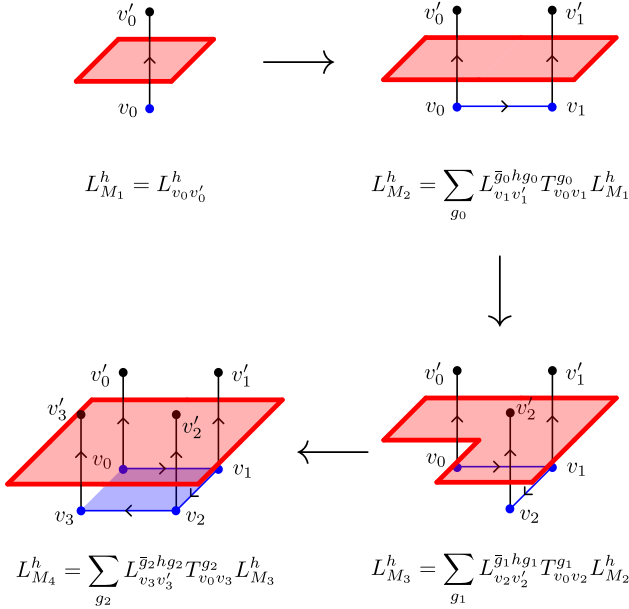


FIG. 12. Constructing the operator $L_{M_\alpha}^h$. We use red and blue to denote the dual part and the direct part respectively. Note that the choice of direct parts has some arbitrariness because we only demand that v_i lives on the direct part. Different choices of the direct part do not change the form of the operator $L_{M_\alpha}^h$. Here, we choose infinitesimal direct plaquettes $v_0v_0v_0v_0$, $v_0v_0v_1v_1$, and $v_1v_1v_2v_2$ as the direct parts of M_1 , $M_2 \setminus M_1$, and $M_3 \setminus M_2$. The direct part of $M_4 \setminus M_3$ is the plaquette $v_0v_1v_2v_3$, which has finite area. The loop-like excited state lives on the boundary of the thickened membrane M_α , where α indicates that the dual part cut α edges. $L_{M_\alpha}^h$ is obtained by using a recursive construction.

live on the boundary of M_2 , which means that the plaquette term $B_{p=v'_0v_0v_1v'_1}$ must be preserved. To obtain the correct form of the operator $L_{M_2}^h$, we need to connect $L_{M_1}^h$ and $L_{v_1v'_1}^{\bar{g}_0h g_0}$ as

$$L_{M_2}^h = \sum_{g_0} L_{v_1v'_1}^{\bar{g}_0h g_0} T_{v_0v_1}^{g_0} L_{M_1}^h = \sum_{g_0} L_{v_1v'_1}^{\bar{g}_0h g_0} T_{v_0v_1}^{g_0} L_{v_0v'_0}^h. \quad (43)$$

The $T_{v_0v_1}^{g_0}$ term and the sum over g_0 are introduced to ensure that the $L_{M_2}^h$ does not violate the plaquette term $B_{p=v'_0v_0v_1v'_1}$, as shown in Appendix B 5. Following the same idea, by connecting $L_{M_2}^h$ and $L_{v_2v'_2}^{\bar{g}_1h g_1}$, we construct the operator $L_{M_3}^h$ as

$$L_{M_3}^h = \sum_{g_1} L_{v_2v'_2}^{\bar{g}_1h g_1} T_{v_0v_2}^{g_1} L_{M_2}^h = \sum_{g_0, g_1} L_{v_2v'_2}^{\bar{g}_1h g_1} T_{v_1v_2}^{\bar{g}_0g_1} L_{v_1v'_1}^{\bar{g}_0h g_0} T_{v_0v_1}^{g_0} L_{v_0v'_0}^h, \quad (44)$$

where $T_{v_0v_2}^{g_1}$ acts on an arbitrary string whose endpoints are denoted by v_0 and v_2 . We choose the string to be (v_0, v_1, v_2) and use the connecting rule Eq. (29) of T_L^g to obtain the second line in the above equation. We can keep constructing operators that involve more edges.

Generally, the connecting rule of $L_{M_\alpha}^h$ is given by

$$L_{M_\alpha}^h = \sum_g L_{v_p v'_p}^{\bar{g} h g} T_{v_0 v_p}^g L_{M_{\alpha-1}}^h, \quad (45)$$

where M_α is obtained by cutting one more edge $v_p v'_p$ than $M_{\alpha-1}$ and $T_{v_0 v_p}^g$ acts on an arbitrary string with endpoints v_0 and v_p . The vertices v_0 and v_p live on the direct part, and the vertex v'_p lives on the dual part. If $v_0 = v_p$, then the term $T_{v_0 v_p}^g$ is defined as $\delta_{g,e}$, which means that Eq. (45) now becomes

$$L_{M_\alpha}^h = \sum_g L_{v_p v'_p}^{\bar{g} h g} \delta_{g,e} L_{M_{\alpha-1}}^h = L_{v_p v'_p}^h L_{M_{\alpha-1}}^h. \quad (46)$$

We further provide the connecting rule of two operators L_M^h and $L_{M'}^{\bar{g} h g}$ from Eq. (45):

$$L_{M \cup M'}^h = \sum_g L_{M'}^{\bar{g} h g} T_{v_0 v_p}^g L_M^h, \quad (47)$$

where M and M' are two membranes whose direct parts start at v_0 and v_p respectively. The direct parts of the two membranes have no overlap, but the boundaries of dual parts have overlap. That is the case that the dual parts of M and M' do not cut the same edges. The direct parts of M and M' can always be chosen to satisfy that they share the common boundary and do not overlap in a finite area, see Fig. 12 as an example. To construct L_M^h and $L_{M'}^h$, we start by acting L_h^\pm on $v_0 v'_0$ and $v_p v'_p$ respectively.

By using Eq. (47), we can create any open membrane operator that violates all plaquette terms along

the boundary of the dual part of M . Besides the disk-like operator shown in Fig. 12, we can also construct a cylindrical operator as shown in Fig. 13. We consider four disk-like thickened membranes and label them as M_{0123} , M_{0345} , M_{4567} , and M_{1267} , where the subscripts imply which vertices are on the direct part. For example, M_{0123} means that the vertices v_0, v_1, v_2 , and v_3 are on the direct part and we construct the corresponding disk-like operators by acting L_h^\pm on the edge that contains the vertex v_0 first. By using Eqs. (46) and (47), we connect operators $L_{M_{0123}}^h$ and $L_{M_{0345}}^h$ as

$$L_{M_{0123} \cup M_{0345}}^h = \sum_g L_{M_{0345}}^{\bar{g}hg} \delta_{g,e} L_{M_{0123}}^h = L_{M_{0345}}^h L_{M_{0123}}^h, \quad (48)$$

where both $L_{M_{0123}}$ and $L_{M_{0345}}$ start at the edge that contains vertex v_0 , thus we have $T_{v_0 v_p}^g = \delta_{g,e}$. Continuing to connect the remaining operators, we have:

$$\begin{aligned} L_{M_{0123} \cup M_{0345} \cup M_{4567}}^h &= \sum_g L_{M_{4567}}^{\bar{g}hg} T_{v_0 v_4}^g L_{M_{0123} \cup M_{0345}}^h \\ &= \sum_g L_{M_{4567}}^{\bar{g}hg} T_{v_0 v_4}^g L_{M_{0123}}^h L_{M_{0345}}^h. \end{aligned} \quad (49)$$

Finally, we derive the cylindrical operator

$$\begin{aligned} L_{M_{\text{cylindrical}}}^h &= \sum_k L_{M_{1267}}^{\bar{k}hk} T_{v_0 v_1}^k L_{M_{0123} \cup M_{0345} \cup M_{4567}}^h \\ &= \sum_{g,k} L_{M_{1267}}^{\bar{k}hk} T_{v_0 v_1}^k L_{M_{4567}}^{\bar{g}hg} T_{v_0 v_4}^g L_{M_{0345}}^h L_{M_{0123}}^h, \end{aligned} \quad (50)$$

where $M_{\text{cylindrical}}$ is defined as $M_{\text{cylindrical}} = M_{0123} \cup M_{0345} \cup M_{4567} \cup M_{1267}$. The plaquette terms are violated along the two boundaries of the dual part of the cylinder.

As shown in Appendix B 5, the connecting rule Eq. (45) ensures that the plaquette terms that live in the bulk of M are not violated by L_M^h . We also show in Appendix B 6 that, among the vertex terms, A_{v_0} does not commute with L_M^h , if and only if h is not in the center $Z(G) = \{z \in G \mid zg = gz, \forall g \in G\}$ of G . All other vertex terms commute with L_M^h .

Having derived the connecting rule for the L -operators, we are ready to construct the membrane operators for loop excitations. In the quantum double model, loops are characterized by a pair of data (C, R) , where C is the conjugacy class and R is the irrep of the centralizer of C . We write a membrane operator for loops as

$$W_M(C, R; c, j; c', j') = \sum_{g \in Z_r} \Gamma_{jj'}^{R^*}(g) L_M^c T_P^{g c g \bar{c}'}, \quad (51)$$

where M is the thickened membrane, R^* denotes complex conjugate representation, $c \in C$, Z_r is the centralizer of the representative r of the conjugacy class

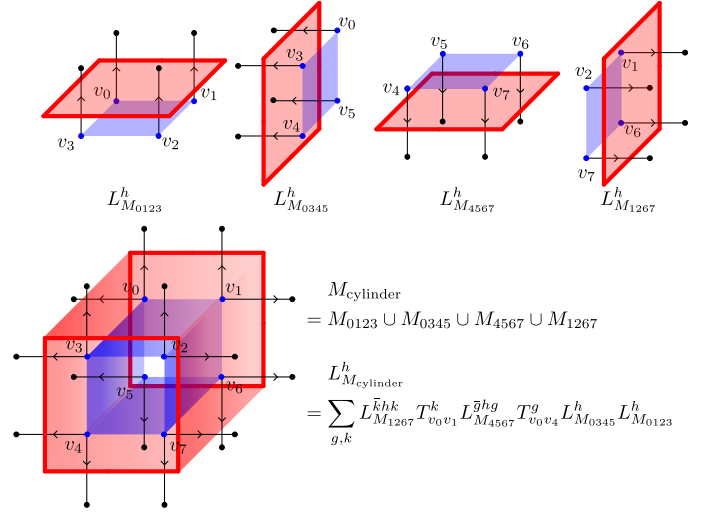


FIG. 13. Constructing the operator $L_{M_{\text{cylindrical}}}^h$. We use red and blue to denote the dual part and the direct part respectively. We connect four disk-like operators to form a cylindrical operator. For a disk-like membrane, the subscript implies which vertices are on the direct part, and the first number in the subscript implies the starting position of the corresponding operator.

$C = \{q_c r \bar{q}_c \mid q_c \in G\}$. Given a fixed $r \in C$, for an arbitrary element $c \in C$, there are generally different choices of q_c satisfying $c = q_c r \bar{q}_c$. Thus, we need to preselect r and q_c for given C and c . Different choices of r and q_c do not affect physics. j and j' are row and column indices of the matrix $\Gamma^{R^*}(g)$. In the later discussion, we will see that c, c', j and j' are just some local degrees of freedom and they can be changed by local operators. P is an arbitrary open string that lives on the direct part of the thickened membrane M . Besides, P ends on the boundary of the direct part of M . For example, consider the membrane M_4 shown in the Fig. 12, where we use blue color to denote the direct part. The boundary of the direct part of M is a closed path $(v_0, v_1, v_2, v_3, v_0)$, so choices such as $P = (v_0, v_1)$, $P = (v_1, v_0, v_3)$, $P = (v_0, v_1, v_2, v_3)$, etc, are all legitimate. If we consider a cylindrical membrane shown in the Fig. 13, the boundaries of the direct part consist of two closed paths $(v_0, v_1, v_6, v_5, v_0)$ and $(v_2, v_3, v_4, v_7, v_2)$. We are allowed to choose $P = (v_0, v_3)$, or $P = (v_0, v_3, v_2)$, or $P = (v_3, v_2, v_7, v_6)$, etc, as long as the two endpoints of P are on the two closed paths respectively.

The conjugacy class C is viewed as the flux of the loop and it is related to the L_M^c term in Eq. (51). The irrep R is viewed as the charge decoration of the loop and it is related to the $T_P^{g c g \bar{c}'}$ term in Eq. (51). Physically, the charge decoration is allowed to freely travel along the loop excitation. Thus, if we consider the thickened membrane M in Eq. (51) to be a disk-like membrane similar to those in Fig. 12, there will be a pair of charge and anti-charge decorations on a loop excitation. We can move the decorations and annihilate them, which results in a pure

loop (i.e., without charge decorations). To encompass the decorated loops, we need to consider the M to be a cylindrical membrane as shown in Fig. 13, and let the two endpoints of the string P live on the two boundaries of the direct part of the cylindrical membrane. In this case, we create a pair of loop and anti-loop, and they carry the charge decoration and the anti-charge decoration respectively. Besides, the operator Eq. (51) automatically becomes a string operator Eq. (34) for a pair of particle and anti-particle when we set $c = e$. In the following discussion, we only consider M to be a cylindrical membrane.

Finally, we illustrate how local degrees of freedom in Eq. (51) are changed by the local operators. For the operator $W_M(C, R; c, j; c', j')$, we denote the two boundaries of M as $\partial_0 M$ and $\partial_1 M$. Without loss of generality, we consider that the L_M^c term acts on the edge $v_0 v'_0 \ni p_0$ first, and the last edge acted on by the L_M^c term is denoted by $v_1 v'_1 \ni p_1$, where plaquettes p_0 and p_1 are violated. We set $\partial_0 P = v_0$, $\partial_1 P = v_1$, and demand that v_0 and p_0 form a site $s_0 = (v_0, p_0)$, v_1 and p_1 form a site $s_1 = (v_1, p_1)$. A state for a pair of loops is written as $W_M(C, R; c, j; c', j') |GS\rangle$. As shown in Appendix B 7, all local actions on the boundary $\partial_0 M$ ($\partial_1 M$) can be derived by considering the actions of $A_{v_0}^g$ ($A_{v_1}^g$) and B_{p_0, s_0}^h (B_{p_1, s_1}^h) on the site s_0 (s_1). On the site $s_0 \in \partial_0 M$, the actions of local operators are given by

$$A_{v_0}^g W_M(C, R; c, j; c', j') |GS\rangle = \sum_i \Gamma_{ij}^R (\bar{q} g c \bar{g} g q c) W_M(C, R; g c \bar{g}, i; c', j') |GS\rangle, \quad (52)$$

$$B_{p_0, s_0}^h W_M(C, R; c, j; c', j') |GS\rangle = \delta_{c, h} W_M(C, R; c, j; c', j') |GS\rangle. \quad (53)$$

On the site $s_1 \in \partial_1 M$, we have

$$A_{v_1}^g W_M(C, R; c, j; c', j') |GS\rangle = \sum_i \Gamma_{ij'}^{R*} (\bar{q} g c' \bar{g} g q c') W_M(C, R; c, j; g c' \bar{g}, i) |GS\rangle, \quad (54)$$

$$B_{p_1, s_1}^h W_M(C, R; c, j; c', j') |GS\rangle = \delta_{c', h} W_M(C, R; c, j; c', j') |GS\rangle. \quad (55)$$

The label (C, R) is conserved under the actions of local operators, which justifies the statement: a topological excitation is characterized by a pair of data (C, R) . The local degrees of freedom c (c') and j (j') can be changed by the local operators on the site s_0 (s_1), leading to the conclusion that c (c') and j (j') label the internal degrees of freedom of the loop living on the boundary $\partial_0 M$ ($\partial_1 M$).

IV. FUSION RULES AND QUANTUM DIMENSIONS

In Sec. III, by linearly combining basic T - and L -operators, we explicitly construct the operator Eq. (51)

for topological excitations and obtain the corresponding connecting rules, which allow us to create, move, and deform excitations. To encompass both pure loops and decorated loops, we choose the thickened membrane M in Eq. (51) to be cylindrical. In this section, we proceed to consider the process of fusing topological excitations in the microscopic model. We will first illustrate the general fusion rules in Sec. IV A and then take 3d $G = \mathbb{Z}_N$ and $G = \mathbb{D}_3$ quantum double model as examples in Sec. IV B and Sec. IV C respectively.

A. General consideration

As mentioned in Sec. III C, acting Eq. (51) on a ground state creates a pair of loops living on the two boundaries of the cylindrical membrane M . We write such a state as $W_M(C, R; c, j; c', j') |GS\rangle$. Fixing (C, R) and exhausting c, j, c', j' , we obtain a set of basis states

$$\{W_M(C, R; c, j; c', j') |GS\rangle \mid c, c' \in C; j, j' = 1, \dots, n_R\}, \quad (56)$$

where C denotes a conjugacy class of G , R denotes an irrep of the centralizer subgroup of the representative $r \in C$, n_R is the dimension of the irrep R . This set spans the Hilbert space $\mathcal{H}_{(C, R)}$ of the two loops. From Eqs. (52), (53), (54) and (55), it follows that for any vector $|w\rangle \in \mathcal{H}_{(C, R)}$, we have $(\sum_{h, g \in G} n_{h, g} B_{p, s}^h A_v^g) |w\rangle \in \mathcal{H}_{(C, R)}$. Thus, we call $\mathcal{H}_{(C, R)}$ an invariant space under the local actions Eq. (35). Each loop denoted by $[C, R]$ corresponds to such an invariant space $\mathcal{H}_{(C, R)}$, whose dimension is given by $|C|^2 \dim(R)^2$. If we consider all possible choices of (C, R) , the total dimension of the space $\oplus_{(C, R)} \mathcal{H}_{(C, R)}$ becomes

$$\sum_{C, R} |C|^2 \dim(R)^2 = \sum_C |C|^2 \frac{|G|}{|C|} = |G| \sum_C |C| = |G|^2. \quad (57)$$

It follows that for $\oplus_{(C, R)} \mathcal{H}_{(C, R)}$, a factor of $|G|$ in the total dimension is carried by the two boundaries of M .

Eqs. (52) and (53) (Eqs. (54) and (55)) show that local operators on the boundaries $\partial_0 M$ ($\partial_1 M$) only change the labels c and j (c' and j'). Thus, under the local actions, the Hilbert space $\mathcal{H}_{(C, R)}$ can be written as

$$\mathcal{H}_{(C, R)} = V_{(C, R)} \otimes V_{(\bar{C}, R^*)}, \quad (58)$$

where \otimes means tensor product, $\bar{C} = \{g \bar{c} \bar{g} \mid g \in G\}$, R^* denotes the complex conjugate representation. $V_{(C, R)}$ and $V_{(\bar{C}, R^*)}$ are local spaces of the loop $[C, R]$ and the anti-loop $[\bar{C}, R^*]$ living on $\partial_0 M$ and $\partial_1 M$ respectively. When we focus on the area near the boundary $\partial_0 M$, we denote the state $W_M(C, R; c, j; c', j') |GS\rangle$ in this area as $|c, j\rangle_{(C, R)}$ because c' and j' are invariant under the local actions. $|c, j\rangle_{(C, R)}$ only labels

the local internal degrees of freedom c and j of the loop $[C, R]$ living on $\partial_0 M$. Thus, by exhausting all c and j with fixed c' and j' , we obtain a set of basis $\{|c, j\rangle_{(C, R)} \mid c \in C, j = 1, \dots, n_R\}$, which spans the local space $V_{(C, R)}$ of the loop $[C, R]$. The local space $V_{(C, R)}$ is invariant under the local actions near the boundary $\partial_0 M$. Similarly, the invariant local space $V_{(\bar{C}, R^*)}$ is spanned by $\{|c', j'\rangle_{(\bar{C}, R^*)} \mid c' \in C, j' = 1, \dots, n_R\}$, where $|c', j'\rangle_{(\bar{C}, R^*)}$ labels the local internal degrees of freedom c', j' of the anti-loop $[\bar{C}, R^*]$ living on $\partial_1 M$ and is understood as the state $W_M(C, R; c, j; c', j') |GS\rangle$ in the area near the boundary $\partial_1 M$.

The notations above also apply to the particles because Eq. (51) automatically becomes a string operator Eq. (34) for a pair of particle and anti-particle when we set $c = e$. In this case, $|c, j\rangle_{(C, R)}$ and $|c', j'\rangle_{(\bar{C}, R^*)}$ are simplified as $|j\rangle_{(R)}$ and $|j'\rangle_{(R^*)}$ and they label the internal degrees of freedom on vertices $\partial_0 P$ and $\partial_1 P$.

Consider a site $s = (v_0, p_0)$ on the boundary $\partial_0 M$ and we demand that the string P starts at v_0 , then all possible local actions on excitation $[C, R]$ are given by Eq. (35), which form the quantum double algebra DG with basis $\{D_{(h, g)} = B_{p, s}^h A_v^g\}$. An irrep of the quantum double DG is also characterized by the pair (C, R) , and the action of DG on the corresponding representation space is given by Eqs. (C13) and (C14). By comparing Eqs. (52), (53) and Eqs. (C14), (C13), we can see that the local space $V_{(C, R)}$ of the excitation $[C, R]$ can be regarded as the representation space of the irrep. The action of DG on $V_{(C, R)}$ is given by

$$\begin{aligned} & \Pi^{(C, R)}(D_{(h, g)}) |c, j\rangle_{(C, R)} \\ &= \sum_i \Gamma_{ij}^R (\bar{q}_{gc\bar{g}} g q c) \delta_{h, gc\bar{g}} |gc\bar{g}, i\rangle_{(C, R)}, \end{aligned} \quad (59)$$

where $\Pi^{(C, R)}$ is the irrep of DG . Details about the irreps of DG are shown in Appendix C. For $V_{(\bar{C}, R^*)}$, one can similarly regard it as the representation space of the irrep of DG labeled by (\bar{C}, R^*) . In the following discussion, we only need to focus on the local space $V_{(C, R)}$ of the excitation $[C, R]$ because mathematically, $V_{(\bar{C}, R^*)}$ is just the dual space of $V_{(C, R)}$. The fusion and shrinking rules derived from $V_{(\bar{C}, R^*)}$ are consistent with those derived from $V_{(C, R)}$.

In our 3d quantum double model, we move two excitations $[C_1, R_1]$ and $[C_2, R_2]$ to the same position $\partial_0 M_1 = \partial_0 M_2$ as shown in Fig. 14 to implement a fusion process. This physical picture of fusion in the lattice model coincides with that in the continuum field theory as shown in Sec. II A. When the two excitations are brought together at $\partial_0 M_1$, we denote the state given by

$$W_{M_1}(C_1, R_1; c_1, j_1; c'_1, j'_1) W_{M_2}(C_2, R_2; c_2, j_2; c'_2, j'_2) |GS\rangle \quad (60)$$

as the local state

$$|c_1, j_1\rangle_{(C_1, R_1)} \otimes |c_2, j_2\rangle_{(C_2, R_2)} \quad (61)$$

in the area near the boundary $\partial_0 M_1$ because $c'_1, j'_1, c'_2,$ and j'_2 are invariant under the local actions. The local action of $D_{(h, g)} = B_{p_0, s_0}^h A_{v_0}^g$ on the state in Eq. (60) is given by

$$\begin{aligned} & B_{p_0, s_0}^h A_{v_0}^g W_{M_1}(C_1, R_1; c_1, j_1; c'_1, j'_1) \\ & \times W_{M_2}(C_2, R_2; c_2, j_2; c'_2, j'_2) |GS\rangle \\ &= \sum_{i_1} \Gamma_{i_1 j_1}^{R_1} (\bar{q}_{gc_1 \bar{g}} g q c_1) W_{M_1}(C_1, R_1; gc_1 \bar{g}, i_1; c'_1, j'_1) \\ & \times B_{p_0, s_0}^{g \bar{c}_1 \bar{g} h} A_{v_0}^g W_{M_2}(C_2, R_2; c_2, j_2; c'_2, j'_2) |GS\rangle \\ &= \sum_{i_1} \Gamma_{i_1 j_1}^{R_1} (\bar{q}_{gc_1 \bar{g}} g q c_1) W_{M_1}(C_1, R_1; gc_1 \bar{g}, i_1; c'_1, j'_1) \\ & \times \sum_{i_2} \Gamma_{i_2 j_2}^{R_2} (\bar{q}_{gc_2 \bar{g}} g q c_2) W_{M_2}(C_2, R_2; gc_2 \bar{g}, i_2; c'_2, j'_2) \\ & \times B_{p_0, s_0}^{g \bar{c}_2 \bar{c}_1 \bar{g} h} A_{v_0}^g |GS\rangle. \end{aligned} \quad (62)$$

Note that

$$\begin{aligned} & B_{p_0, s_0}^{g \bar{c}_2 \bar{c}_1 \bar{g} h} A_{v_0}^g |GS\rangle = \delta_{h, gc_1 c_2 \bar{g}} |GS\rangle \\ &= \sum_{k \in G} \delta_{h \bar{k}, gc_1 \bar{g}} \delta_{k, gc_2 \bar{g}} |GS\rangle. \end{aligned} \quad (63)$$

Thus, by using Eq. (59), we conclude that the wave function in Eq. (62) corresponds to the local state given by

$$\begin{aligned} & \sum_{k \in G} \Pi^{(C_1, R_1)}(D_{(h \bar{k}, g)}) |c_1, j_1\rangle_{(C_1, R_1)} \\ & \otimes \Pi^{(C_2, R_2)}(D_{(k, g)}) |c_2, j_2\rangle_{(C_2, R_2)}. \end{aligned} \quad (64)$$

From Eq. (64), we can see that the local Hilbert space on the boundary $\partial_0 M_1$ spanned by $\{|c_1, j_1\rangle_{(C_1, R_1)} \otimes |c_2, j_2\rangle_{(C_2, R_2)}\}$ can be written as $V_{(C_1, R_1)} \otimes V_{(C_2, R_2)}$, which forms a representation space of a tensor product representation $\Pi^{(C_1, R_1)} \otimes \Pi^{(C_2, R_2)}$. Generally, the tensor product representation decomposes as

$$\begin{aligned} & \Pi^{(C_1, R_1)} \otimes \Pi^{(C_2, R_2)} = \bigoplus_{(C, R)} N_{(C, R)}^{(C_1, R_1)(C_2, R_2)} \Pi^{(C, R)}, \\ & V_{(C_1, R_1)} \otimes V_{(C_2, R_2)} = \bigoplus_{(C, R)} N_{(C, R)}^{(C_1, R_1)(C_2, R_2)} V_{(C, R)}, \end{aligned} \quad (65)$$

where \bigoplus is the direct sum that exhausts all possible choices of (C, R) . Since each excitation corresponds to an invariant space $V_{(C, R)}$ and the tensor product space $V_{(C_1, R_1)} \otimes V_{(C_2, R_2)}$ decomposes as a direct sum of several invariant spaces, Eq. (65) is deemed as the fusion rules Eq. (1) of the quantum double, with the fusion coefficient

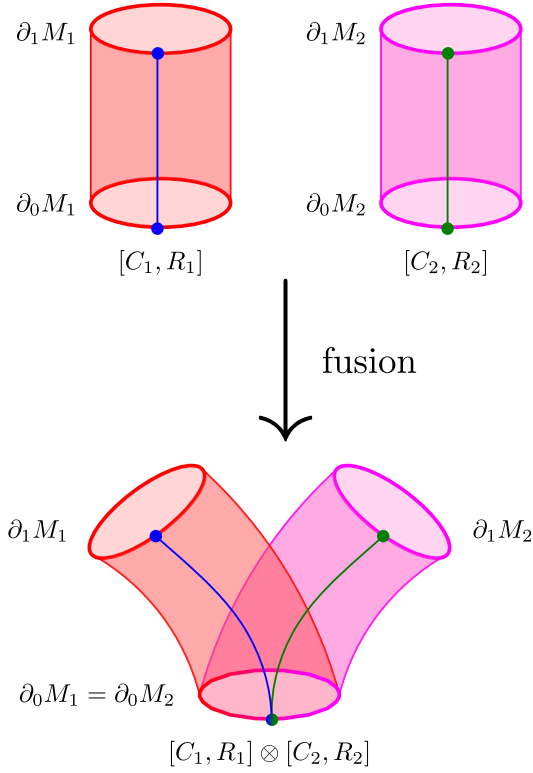


FIG. 14. Fusing two excitations. As shown on the top, we consider the excitations $[C_1, R_1]$ and $[C_2, R_2]$ living on the two boundaries $\partial_0 M_1$ and $\partial_0 M_2$ respectively. The red and purple denote the operators $L_{M_1}^{c_1 \in C_1}$ and $L_{M_2}^{c_2 \in C_2}$ in Eq. (51) respectively and the blue and green denote the operators $T_{P_1}^{q_{c_1} g \bar{q}_{c_1}}$ and $T_{P_2}^{q_{c_2} g \bar{q}_{c_2}}$ in Eq. (51) respectively. We bring $[C_1, R_1]$ and $[C_2, R_2]$ to a common position $\partial_0 M_1 = \partial_0 M_2$ to implement the fusion process. This microscopic realization of fusion corresponds directly to the fusion in the continuum field theory, where two Wilson operators are brought together at the same location.

$N_{(C,R)}^{(C_1,R_1)(C_2,R_2)}$ given by

$$\begin{aligned} & N_{(C,R)}^{(C_1,R_1)(C_2,R_2)} \\ &= \frac{1}{|G|} \sum_{h,g} \text{tr} \left[\Pi^{(C_1,R_1)} \otimes \Pi^{(C_2,R_2)} \left(\Delta \left(D_{(h,g)} \right) \right) \right] \\ & \quad \times \left\{ \text{tr} \left[\Pi^{(C,R)} \left(D_{(h,g)} \right) \right] \right\}^* , \end{aligned} \quad (66)$$

where $*$ means complex conjugate and we define

$$\Delta \left(D_{(h,g)} \right) = \sum_{k \in G} D_{(h\bar{k},g)} \otimes D_{(k,g)} . \quad (67)$$

If $N_{(C,R)}^{(C_1,R_1)(C_2,R_2)}$ does not vanish, then there are $N_{(C,R)}^{(C_1,R_1)(C_2,R_2)}$ channels to fuse $[C_1, R_1]$ and $[C_2, R_2]$ to $[C, R]$. We use the fusion diagram shown in Fig. 1 to represent these fusion channels.

B. Abelian fusion rules

Here, we provide an example of Abelian fusion rules in the 3d quantum double model. Consider an Abelian group $G = \mathbb{Z}_N$ and denote the generator of \mathbb{Z}_N by g . A group element can be written as g^α , and g^α itself forms a conjugacy class. Since the corresponding centralizer is $Z_{g^\alpha} = G$, and G has $|G|$ one-dimensional irreps, we find $|G| \times |G|$ excitations labeled by $[g^\alpha, R^{(\beta)}]$, where $\alpha, \beta = 0, 1, 2, \dots, |G| - 1$ and $R^{(\beta)}$ labels an irrep. We write $\Gamma^{R^{(\beta)}}(g^\alpha) = \omega^{\alpha\beta}$ with $\omega = \exp(2\pi i/N)$. Since G is an Abelian group, the tensor product representation is directly given by

$$\begin{aligned} & \Pi^{(g^{\alpha_1}, R^{(\beta_1)})} \otimes \Pi^{(g^{\alpha_2}, R^{(\beta_2)})} \\ &= \Pi^{(g^{(\alpha_1 + \alpha_2 \bmod N)}, R^{(\beta_1 + \beta_2 \bmod N)})} , \end{aligned} \quad (68)$$

which leads to the fusion rules:

$$\begin{aligned} & \left[g^{\alpha_1}, R^{(\beta_1)} \right] \otimes \left[g^{\alpha_2}, R^{(\beta_2)} \right] \\ &= \left[g^{(\alpha_1 + \alpha_2 \bmod N)}, R^{(\beta_1 + \beta_2 \bmod N)} \right] . \end{aligned} \quad (69)$$

The corresponding fusion diagram can be obtained by writing **a**, **b**, and **c** as $[g^{\alpha_1}, R^{(\beta_1)}]$, $[g^{\alpha_2}, R^{(\beta_2)}]$, and $[g^{(\alpha_1 + \alpha_2 \bmod N)}, R^{(\beta_1 + \beta_2 \bmod N)}]$ respectively, and writing $\mu = 1$ in Fig. 1.

C. Non-Abelian fusion rules

From Eq. (59) we see that when the group G is Abelian, the irrep of the quantum double DG is one-dimensional, which indicates that there are only Abelian fusion rules. To obtain non-Abelian fusion rules, we need to consider a non-Abelian group. Here, we take the simplest non-Abelian group $G = \mathbb{D}_3$ as an example. The \mathbb{D}_3 group has two generators r and t , which satisfy $r^3 = t^2 = e$, $rt = tr^2$. We label the three conjugacy classes in \mathbb{D}_3 as

$$C_e = \{e\} , \quad C_r = \{r, r^2\} , \quad C_t = \{t, tr, tr^2\} , \quad (70)$$

where e , r , and t serve as the representatives of the classes C_e , C_r , and C_t respectively. Their corresponding centralizers are

$$Z_e = \mathbb{D}_3 , \quad Z_r = \{e, r, r^2\} \simeq \mathbb{Z}_3 , \quad Z_t = \{e, t\} \simeq \mathbb{Z}_2 , \quad (71)$$

where \simeq denotes isomorphism. To choose a set of q_c in Eq. (51), we need to consider $Q_g = G/Z_g$ as follows

$$Q_e = \{e\} , \quad Q_r = \{e, t\} , \quad Q_t = \{e, r, r^2\} . \quad (72)$$

A natural choice for \mathbb{D}_3 is $q_e = q_r = q_t = e$, $q_{r^2} = t$, $q_{tr} = r$, and $q_{tr^2} = r^2$. Thus, there are eight topological excitations and we label them as

$$\begin{aligned} & [Id] , \quad [A] , \quad [B] , \quad [C_r, Id] , \\ & [C_r, \omega] , \quad [C_r, \omega^2] , \quad [C_t, Id] , \quad [C_t, -] , \end{aligned} \quad (73)$$

where we write the particles $[C_e, Id]$, $[C_e, A]$, and $[C_e, B]$ as $[Id]$, $[A]$, and $[B]$ respectively for simplicity. Id is the 1d trivial representation, A and B are the nontrivial 1d and 2d representations of \mathbb{D}_3 respectively. ω and ω^2 are two nontrivial 1d representations of \mathbb{Z}_3 respectively. $-$ is the nontrivial 1d representation of \mathbb{Z}_2 . We choose the representation matrices of the generators of \mathbb{D}_3 to be

$$\begin{aligned} \Gamma^A(t^n r^m) &= (-1)^n, & \Gamma^-(t) &= -1, \\ \Gamma^B(t) &= \begin{pmatrix} 0 & 1 \\ 1 & 0 \end{pmatrix}, & \Gamma^B(r) &= \begin{pmatrix} \omega & 0 \\ 0 & \omega^2 \end{pmatrix}, \\ \Gamma^\omega(r^m) &= \omega^m, & \Gamma^{\omega^2}(r^m) &= \omega^{2m}, \end{aligned} \quad (74)$$

where $\omega = \exp(2\pi i/3)$. By using Eq. (66), we derive all fusion rules as shown in Table I. For an excitation \mathbf{a} , we can define a matrix $N_{\mathbf{a}}$ with matrix elements $(N_{\mathbf{a}})_{\mathbf{bc}} = N_{\mathbf{c}}^{\mathbf{ab}}$. The greatest eigenvalue $d_{\mathbf{a}}$ of the matrix $N_{\mathbf{a}}$ is called the quantum dimension of \mathbf{a} . All quantum dimensions of excitations in the $G = \mathbb{D}_3$ quantum double model are shown in Table II.

V. SHRINKING RULES AND FUSION-SHRINKING CONSISTENCY

The presence of the loop excitations in the 3d topological orders leads to nontrivial shrinking rules, which determine how loops are shrunk into particles. The field-theoretical description of this shrinking process has been established, as reviewed in Sec. II A. In this section, we explicitly construct the shrinking process and calculate the shrinking rules in the microscopic model. We begin by presenting the general formulation of shrinking rules in Sec. V A, followed by concrete examples for the 3d $G = \mathbb{Z}_N$ and $G = \mathbb{D}_3$ quantum double models in Sec. V B and Sec. V C respectively. Furthermore, by appropriately choosing the internal degrees of freedom in the loop operators, we can control the shrinking channels as demonstrated in Sec. V D. Finally, in Sec. V E, we verify that the consistency condition Eq. (8) between fusion and shrinking rules derived from continuum field theory also holds in our microscopic lattice model.

A. General consideration

Consider a cylindrical membrane M that creates a pair of loop and anti-loop as shown in Fig. 15. The red membrane supports the L_M^c operator and the blue string supports the $T_P^{q_c g \bar{q}_{c'}}$ operators. Recall the connecting rule Eq. (47), since the operator L_c^\pm has the inverse $L_{\bar{c}}^\pm$, we can shrink a membrane $M \cup M'$ to a smaller one M (by smaller we mean M cuts fewer edges) as

$$L_M^c = L_{M'}^{g \bar{c} g} L_{M \cup M'}^c. \quad (75)$$

When the dual parts of M' and $M \cup M'$ cut the same edges, Eq. (75) allows us to shrink a cylindrical membrane to an infinitesimal thin one, which behaves as a

string operator. In Fig. 15, this shrinking process shrinks the flux of the loop to the vacuum, but the blue string is not affected. The microscopic realization of shrinking corresponds to the shrinking in the continuum field theory, as shown in Sec. II A. Even if we consider a loop without any charge decoration, after such a shrinking process, the end of the blue string may still behave as nontrivial particles. To be more specific, after the shrinking process, the operator in Eq. (51) becomes

$$\begin{aligned} \mathcal{S}(W_M(C, R; c, j; c', j')) &= \mathcal{S} \left(\sum_{g \in Z_r} \Gamma_{jj'}^{R*}(g) L_M^c T_P^{q_c g \bar{q}_{c'}} \right) \\ &= \sum_{g \in Z_r} \Gamma_{jj'}^{R*}(g) T_P^{q_c g \bar{q}_{c'}}. \end{aligned} \quad (76)$$

If we choose the irrep R to be the trivial representation which corresponds to zero charge decoration, the operator on the right hand side is

$$\sum_{g \in Z_r} \Gamma^{Id}(g) T_P^{q_c g \bar{q}_{c'}} = \sum_{g \in Z_r} T_P^{q_c g \bar{q}_{c'}}, \quad (77)$$

where $Id^* = Id$. This operator generally does not commute with the vertex terms $A_{v_0 = \partial_0 P}$ and $A_{v_1 = \partial_1 P}$. Thus, acting this operator on the ground state creates excited vertices $v_0 = \partial_0 P$ and $v_1 = \partial_1 P$.

In Sec. IV, we have shown that the set of basis $\{W_M(C, R; c, j; c', j') | \text{GS}\}$ spans the Hilbert space $\mathcal{H}_{(C, R)}$ of a pair of excitations on the two boundaries $\partial_0 M$ and $\partial_1 M$ of the cylindrical membrane M . After the shrinking process, the set of basis becomes $\{\mathcal{S}(W_M(C, R; c, j; c', j')) | \text{GS}\}$, where $c, c' \in C$ and $j, j' = 1, \dots, n_R$. This set of basis spans the Hilbert space

$$\mathcal{S}(\mathcal{H}_{(C, R)}) = \mathcal{S}(V_{(C, R)}) \otimes \mathcal{S}(V_{(\bar{C}, R^*)}). \quad (78)$$

On the boundary $\partial_0 M$, the local space denoted by $\mathcal{S}(V_{(C, R)})$ is spanned by $\{\mathcal{S}(|c, j\rangle_{(C, R)})\}$, where $c \in C$ and $j = 1 \dots, n_R$. Under the action of the quantum double DG (i.e., the local action Eq. (35)), the space $\mathcal{S}(V_{(C, R)})$ decomposes as a direct sum of its invariant subspaces:

$$\mathcal{S}(V_{(C, R)}) = \bigoplus_{R'} S_{(C_e, R')}^{(C, R)} V_{(C_e, R')}, \quad (79)$$

where $S_{(C_e, R')}^{(C, R)}$ is the shrinking coefficient, $C_e = \{e\}$, R' denotes an irrep of G . The equation above is understood as the shrinking rules Eq. (2). Each allowed invariant subspace $V_{(C_e, R')}$ corresponds to a particle $[R']$ (we write $[C_e, R']$ as $[R']$ for simplicity) and the coefficient $S_{(C_e, R')}^{(C, R)}$ counts the shrinking channels into $[R']$.

To derive the explicit form of the shrinking coefficient, we express the membrane operator

TABLE I. Fusion table for the \mathbb{D}_3 quantum double model. There are eight excitations in the \mathbb{D}_3 quantum double model. $[Id]$ and $[A]$ are Abelian particles. $[B]$ is a non-Abelian particle. $[C_r, Id]$, $[C_r, \omega]$, $[C_r, \omega^2]$, $[C_t, Id]$, and $[C_t, -]$ are non-Abelian loops.

\otimes	$[Id]$	$[A]$	$[B]$	$[C_r, Id]$	$[C_r, \omega]$	$[C_r, \omega^2]$	$[C_t, Id]$	$[C_t, -]$
$[Id]$	$[Id]$	$[A]$	$[B]$	$[C_r, Id]$	$[C_r, \omega]$	$[C_r, \omega^2]$	$[C_t, Id]$	$[C_t, -]$
$[A]$	$[A]$	$[Id]$	$[B]$	$[C_r, Id]$	$[C_r, \omega]$	$[C_r, \omega^2]$	$[C_t, -]$	$[C_t, Id]$
$[B]$	$[B]$	$[B]$	$\begin{matrix} [Id] \\ \oplus [A] \\ \oplus [B] \end{matrix}$	$\begin{matrix} [C_r, \omega] \\ \oplus [C_r, \omega^2] \end{matrix}$	$\begin{matrix} [C_r, Id] \\ \oplus [C_r, \omega^2] \end{matrix}$	$\begin{matrix} [C_r, Id] \\ \oplus [C_r, \omega] \end{matrix}$	$\begin{matrix} [C_t, Id] \\ \oplus [C_t, -] \end{matrix}$	$\begin{matrix} [C_t, Id] \\ \oplus [C_t, -] \end{matrix}$
$[C_r, Id]$	$[C_r, Id]$	$[C_r, Id]$	$\begin{matrix} [C_r, \omega] \\ \oplus [C_r, \omega^2] \end{matrix}$	$\begin{matrix} [C_r, Id] \\ \oplus [A] \\ \oplus [Id] \end{matrix}$	$\begin{matrix} [C_r, \omega^2] \\ \oplus [B] \end{matrix}$	$\begin{matrix} [C_r, \omega] \\ \oplus [B] \end{matrix}$	$\begin{matrix} [C_t, Id] \\ \oplus [C_t, -] \end{matrix}$	$\begin{matrix} [C_t, Id] \\ \oplus [C_t, -] \end{matrix}$
$[C_r, \omega]$	$[C_r, \omega]$	$[C_r, \omega]$	$\begin{matrix} [C_r, Id] \\ \oplus [C_r, \omega^2] \end{matrix}$	$\begin{matrix} [C_r, \omega^2] \\ \oplus [B] \end{matrix}$	$\begin{matrix} [C_r, \omega] \\ \oplus [A] \\ \oplus [Id] \end{matrix}$	$\begin{matrix} [C_r, Id] \\ \oplus [B] \end{matrix}$	$\begin{matrix} [C_t, Id] \\ \oplus [C_t, -] \end{matrix}$	$\begin{matrix} [C_t, Id] \\ \oplus [C_t, -] \end{matrix}$
$[C_r, \omega^2]$	$[C_r, \omega^2]$	$[C_r, \omega^2]$	$\begin{matrix} [C_r, Id] \\ \oplus [C_r, \omega] \end{matrix}$	$\begin{matrix} [C_r, \omega] \\ \oplus [B] \end{matrix}$	$\begin{matrix} [C_r, Id] \\ \oplus [B] \end{matrix}$	$\begin{matrix} [C_r, \omega^2] \\ \oplus [A] \\ \oplus [Id] \end{matrix}$	$\begin{matrix} [C_t, Id] \\ \oplus [C_t, -] \end{matrix}$	$\begin{matrix} [C_t, Id] \\ \oplus [C_t, -] \end{matrix}$
$[C_t, Id]$	$[C_t, Id]$	$[C_t, -]$	$\begin{matrix} [C_t, Id] \\ \oplus [C_t, -] \end{matrix}$	$\begin{matrix} [C_t, Id] \\ \oplus [C_t, -] \end{matrix}$	$\begin{matrix} [C_t, Id] \\ \oplus [C_t, -] \end{matrix}$	$\begin{matrix} [C_t, Id] \\ \oplus [C_t, -] \end{matrix}$	$\begin{matrix} [Id] \\ \oplus [B] \\ \oplus [C_r, Id] \\ \oplus [C_r, \omega] \\ \oplus [C_r, \omega^2] \end{matrix}$	$\begin{matrix} [A] \\ \oplus [B] \\ \oplus [C_r, Id] \\ \oplus [C_r, \omega] \\ \oplus [C_r, \omega^2] \end{matrix}$
$[C_t, -]$	$[C_t, -]$	$[C_t, Id]$	$\begin{matrix} [C_t, Id] \\ \oplus [C_t, -] \end{matrix}$	$\begin{matrix} [C_t, Id] \\ \oplus [C_t, -] \end{matrix}$	$\begin{matrix} [C_t, Id] \\ \oplus [C_t, -] \end{matrix}$	$\begin{matrix} [C_t, Id] \\ \oplus [C_t, -] \end{matrix}$	$\begin{matrix} [A] \\ \oplus [B] \\ \oplus [C_r, Id] \\ \oplus [C_r, \omega] \\ \oplus [C_r, \omega^2] \end{matrix}$	$\begin{matrix} [Id] \\ \oplus [B] \\ \oplus [C_r, Id] \\ \oplus [C_r, \omega] \\ \oplus [C_r, \omega^2] \end{matrix}$

TABLE II. Quantum dimension table for the \mathbb{D}_3 quantum double model. The quantum dimension of \mathbf{a} is defined as the greatest eigenvalue of the matrix $N_{\mathbf{a}}$, whose elements are given by $(N_{\mathbf{a}})_{bc} = N_c^{ab}$. We can obtain all the fusion coefficients in Table I.

Excitation	$[Id]$	$[A]$	$[B]$	$[C_r, Id]$	$[C_r, \omega]$	$[C_r, \omega^2]$	$[C_t, Id]$	$[C_t, -]$
Quantum dimension	1	1	2	2	2	2	3	3

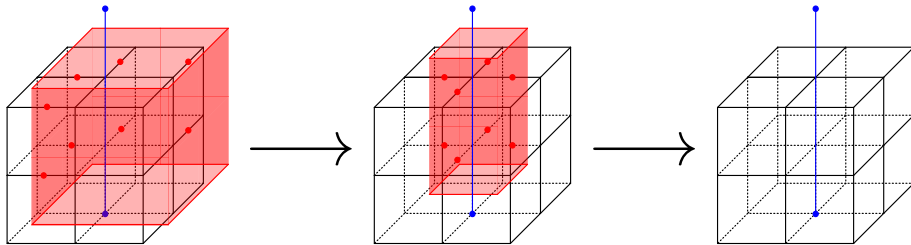


FIG. 15. The red denotes the dual part of M and all edges cut by the dual part are acted by operator L_M^c . We omit the direct part and only draw the blue string to represent the action of $T_P^{q_c g \bar{q}_{c'}}$ because other edges on the direct part will not be acted by $T_P^{q_c g \bar{q}_{c'}}$. The flux of the loop lives on the boundaries of the direct part (red membrane) and we can shrink it to the vacuum. Yet, the blue string cannot be shrunk. After such a shrinking process, the end of the blue string generally behaves as a superposition of particles.

$\mathcal{S}(W_M(C, R; c, j; c', j'))$ as a linear combination of the operators for particles:

$$\mathcal{S}(W_M(C, R; c, j; c', j')) = \sum_{R, i, i'} x(R', i, i') W_P(R; i, i'), \quad (80)$$

where $x(R', i, i')$ is the undetermined coefficient, and R and R' denote irreps of the centralizer Z_r and the full group G , respectively. Substituting the explicit forms of W_M and W_P yields

$$\sum_{h \in Z_r} \Gamma_{jj'}^{R*}(h) T_P^{qc h \bar{q}c'} = \sum_{R', i, i'} x(R', i, i') \sum_{g \in G} \Gamma_{ii'}^{R'*}(g) T_P^g. \quad (81)$$

Substituting $h = \bar{q}_c g q_{c'}$ into the left-hand side of the above equation, we obtain

$$\sum_{g \in q_c Z_r \bar{q}_{c'}} \Gamma_{jj'}^{R*}(\bar{q}_c g q_{c'}) T_P^g = \sum_{R', i, i'} x(R', i, i') \sum_{g \in G} \Gamma_{ii'}^{R'*}(g) T_P^g. \quad (82)$$

By comparing the coefficients in the front of T_P^g operator, we obtain the equation

$$\delta_{g \in q_c Z_r \bar{q}_{c'}} \Gamma_{jj'}^{R*}(\bar{q}_c g q_{c'}) = \sum_{R', i, i'} x(R', i, i') \Gamma_{ii'}^{R'*}(g), \quad (83)$$

where $\delta_{g \in q_c Z_r \bar{q}_{c'}}$ is defined to be 1 if $g \in q_c Z_r \bar{q}_{c'}$ and 0 otherwise. Using the Schur orthogonality:

$$\frac{1}{|G|} \sum_g \Gamma_{ii'}^{R'*}(g) \Gamma_{jj'}^{R''}(g) = \frac{1}{\dim(R')} \delta_{R', R''} \delta_{ij} \delta_{i'j'}, \quad (84)$$

we find the expression of $x(R', i, i')$ as

$$\begin{aligned} & \sum_{g \in G} \sum_{R'', j, j'} x(R'', j, j') \Gamma_{jj'}^{R''*}(g) \Gamma_{ii'}^{R'}(g) \\ &= \sum_{R'', j, j'} x(R'', j, j') \frac{|G| \delta_{R'', R'} \delta_{ij} \delta_{i'j'}}{\dim(R')} \\ &= \frac{|G|}{\dim(R')} x(R', i, i'). \end{aligned} \quad (85)$$

Using Eqs. (83) and (85), we have

$$\begin{aligned} x(R', i, i') &= \frac{\dim(R')}{|G|} \sum_{g \in G} \delta_{g \in q_c Z_r \bar{q}_{c'}} \Gamma_{jj'}^{R*}(\bar{q}_c g q_{c'}) \Gamma_{ii'}^{R'}(g) \\ &= \frac{\dim(R')}{|G|} \sum_{h \in Z_r} \Gamma_{jj'}^{R*}(h) \Gamma_{ii'}^{R'}(q_c h \bar{q}_{c'}), \end{aligned} \quad (86)$$

where we have used $h = \bar{q}_c g q_{c'}$ to obtain the second line. By decomposing $\Gamma_{ii'}^{R'}(q_c h \bar{q}_{c'})$ as $\sum_{k, l} \Gamma_{ik}^{R'}(q_c) \Gamma_{kl}^{R'}(h) \Gamma_{li'}^{R'}(\bar{q}_{c'})$, we finally obtain the explicit form of $x(R', i, i')$:

$$\begin{aligned} & x(R', i, i') \\ &= \frac{\dim(R')}{|G|} \sum_{k, l} \Gamma_{ik}^{R'}(q_c) \Gamma_{li'}^{R'}(\bar{q}_{c'}) \sum_{h \in Z_r} \Gamma_{jj'}^{R*}(h) \Gamma_{kl}^{R'}(h). \end{aligned} \quad (87)$$

This gives the unique solution for the coefficient in the shrinking rule Eq. (80).

Let us now examine which particle excitation $R' \in \text{Rep}(G)$ can appear after shrinking a loop excitation $[C, R]$ in Eq. (80), where C is a conjugacy class of G and $R \in \text{Rep}(Z_r)$. The shrinking of a loop excitation forgets the conjugacy class C that labels its flux. Therefore, we need to understand how a representation $R \in \text{Rep}(Z_r)$ decomposes into representations $R' \in \text{Rep}(G)$. In other words, we should view representation R of the subgroup Z_r as representation R' of the full group G .

A natural candidate is the *induction functor* $\text{Ind}_{Z_r}^G$, which maps an irrep R of the subgroup Z_r to a direct sum of irreps R' of G . The induction functor is adjoint to the *restriction functor* $\text{Res}_{Z_r}^G$. It implies that a particle excitation R' appears after shrinking the loop excitation $[C, R]$ if the representation R' of G restricts to R on the subgroup Z_r .

This is indeed confirmed by the last summation $\sum_{h \in Z_r} \Gamma_{jj'}^{R*}(h) \Gamma_{kl}^{R'}(h)$ in Eq. (87). We can first decompose $R' \in \text{Rep}(G)$ into irreps of Z_r ; applying Eq. (84) then yields a delta function. We therefore conclude that $x(R', i, i')$ vanishes unless R is contained in $\text{Res}_{Z_r}^G(R')$. Consequently, the loop excitation $[C, R]$ can shrink to the particle excitation R' if and only if R is a subrepresentation of $\text{Red}_{Z_r}^G(R')$, or equivalently, by Frobenius reciprocity, if R' is a subrepresentation of $\text{Ind}_{Z_r}^G(R)$.

This result yields the direct sum decomposition of the space $\mathcal{S}(V_{(C, R)})$ into the particle excitations $[C_e, R']$, where the irrep R' of G appears with the multiplicity given by its occurrence in the induced representation $\text{Ind}_{Z_r}^G(R)$. Explicitly, we have

$$\mathcal{S}(V_{(C, R)}) = \bigoplus_{R' \in \text{Irr}(G)} m_R(R') \cdot V_{(C_e, R')}, \quad (88)$$

where the non-negative integral multiplicity $m_R(R')$ can be calculated from the inner product of the corresponding characters:

$$m_R(R') = \langle \chi_{R'}, \text{Ind}_{Z_r}^G(\chi_R) \rangle_G = \langle \text{Res}_{Z_r}^G(\chi_{R'}), \chi_R \rangle_{Z_r}. \quad (89)$$

This decomposition corresponds to the shrinking rule

$$\mathcal{S}([C, R]) = \bigoplus_{R' \in \text{Irr}(G)} m_R(R') \cdot [C_e, R']. \quad (90)$$

B. Abelian shrinking rules

To illustrate the shrinking rules more specifically, we take $G = \mathbb{Z}_N$ and $G = \mathbb{D}_3$ as two examples. We first consider $G = \mathbb{Z}_N$. As mentioned in Sec. IV B, an excitation can be labeled by $[g^\alpha, R^{(\beta)}]$, where g is the generator of the group $G = \mathbb{Z}_N$, $\alpha, \beta = 0, 1, 2, \dots, |G| - 1$ and $R^{(\beta)}$ labels an irrep of $G = \mathbb{Z}_N$. The representation matrix

is given by $\Gamma^{R^{(\beta)}}(g^\alpha) = \omega^{\alpha\beta}$, where $\omega = \exp(2\pi i/N)$. Thus, the operator for excitation $[g^\alpha, R^{(\beta)}]$ is given by

$$\begin{aligned} W_M(g^\alpha, R^{(\beta)}) &= \sum_{\gamma=0}^{N-1} \omega^{-\beta\gamma} L_M^{g^\alpha} T_P^{g^\gamma} \\ &= \sum_{\gamma=0}^{N-1} \exp\left(\frac{-i2\pi\beta\gamma}{N}\right) L_M^{g^\alpha} T_P^{g^\gamma}. \end{aligned} \quad (91)$$

Since c, j, c', j' only have one possible choice, we omit these labels and simply write $W_M(g^\alpha, R^{(\beta)}; g^\alpha, 1; g^\alpha, 1)$ as $W_M(g^\alpha, R^{(\beta)})$ in the above equation. We use the procedure shown in Fig. 15 to shrink the flux part of $[g^\alpha, R^{(\beta)}]$ and we obtain

$$\begin{aligned} \mathcal{S}\left(W_M(g^\alpha, R^{(\beta)})\right) &= \sum_{\gamma=0}^{N-1} \exp\left(\frac{-i2\pi\beta\gamma}{N}\right) T_P^{g^\gamma} \\ &= W_M(e, R^{(\beta)}), \end{aligned} \quad (92)$$

where $W_M(e, R^{(\beta)})$ is exactly the operator for the particle $[e, R^{(\beta)}]$. From the above equation, we directly conclude that all shrinking rules in the 3d $G = \mathbb{Z}_N$ quantum double model are Abelian and take the form

$$\mathcal{S}\left([g^\alpha, R^{(\beta)}]\right) = [e, R^{(\beta)}]. \quad (93)$$

The corresponding shrinking diagram is obtained by writing **a** and **b** as $[g^\alpha, R^{(\beta)}]$ and $[e, R^{(\beta)}]$ respectively, and writing $\mu = 1$ in Fig. 2.

C. Non-Abelian shrinking rules

Now we consider the shrinking rules when $G = \mathbb{D}_3$. Unlike the Abelian case, some excitations in the 3d $G = \mathbb{D}_3$ quantum double model are non-Abelian, which means that there are some internal degrees of freedom in the corresponding operator. For example, according to Eq. (51) and the data about \mathbb{D}_3 shown in Sec. IV C, the operators with different degrees of freedom for a pure loop (i.e., without charge decoration) $[C_r, Id]$ are given by

$$\begin{aligned} W_M(C_r, Id; r; r) &= \sum_{g \in Z_r} \Gamma^{Id}(g) L_M^r T_P^g \\ &= L_M^r T_P^e + L_M^r T_P^r + L_M^r T_P^{r^2}, \end{aligned} \quad (94)$$

$$\begin{aligned} W_M(C_r, Id; r^2; r) &= \sum_{g \in Z_r} \Gamma^{Id}(g) L_M^{r^2} T_P^{tg} \\ &= L_M^{r^2} T_P^t + L_M^{r^2} T_P^{tr} + L_M^{r^2} T_P^{tr^2}, \end{aligned} \quad (95)$$

$$\begin{aligned} W_M(C_r, Id; r^2; r^2) &= \sum_{g \in Z_r} \Gamma^{Id}(g) L_M^{r^2} T_P^{gt} \\ &= L_M^{r^2} T_P^e + L_M^{r^2} T_P^{r^2} + L_M^{r^2} T_P^r, \end{aligned} \quad (96)$$

$$\begin{aligned} W_M(C_r, Id; r; r^2) &= \sum_{g \in Z_r} \Gamma^{Id}(g) L_M^r T_P^{gt} \\ &= L_M^r T_P^t + L_M^r T_P^{tr^2} + L_M^r T_P^{tr}, \end{aligned} \quad (97)$$

where we omit the row and column indices $j = j' = 1$ of the one-dimensional matrix. The internal degrees of freedom of the operator are labeled by the elements in the conjugacy class $C_r = \{r, r^2\}$.

Although $[C_r, Id]$ does not carry any charge decoration, after the shrinking process, the remaining operator may still violate the vertex terms at the two ends of the string P . Focus on the local space on $\partial_0 M$, we fix $c' = r$ and exhaust $c \in C_r$ to obtain a set of basis in $V_{(C_r, Id)}$. When $c = r$, after the shrinking process as shown in Fig. 15, the flux part of $[C_r, Id]$ vanishes and the operator shown in Eq. (94) becomes

$$\mathcal{S}(W_M(C_r, Id; r, r)) = T_P^e + T_P^r + T_P^{r^2}. \quad (98)$$

Notice that the operators for particles $[Id]$ and $[A]$ are given by

$$W_P(Id) = T_P^e + T_P^r + T_P^{r^2} + T_P^t + T_P^{tr} + T_P^{tr^2}, \quad (99)$$

$$W_P(A) = T_P^e + T_P^r + T_P^{r^2} - T_P^t - T_P^{tr} - T_P^{tr^2}, \quad (100)$$

where $W_M(Id)$ and $W_M(A)$ are the simplified notations of $W_M(C_e, Id; e, 1; e, 1)$ and $W_M(C_e, A; e, 1; e, 1)$. Comparing the above equations, we have

$$\mathcal{S}(W_M(C_r, Id; r, r)) = \frac{1}{2} [W_P(Id) + W_P(A)]. \quad (101)$$

On the other hand, when $c = r^2$, after the shrinking process, the operator shown in Eq. (95) is given by

$$\mathcal{S}(W_M(C_r, Id; r^2, r)) = \frac{1}{2} [W_P(Id) - W_P(A)]. \quad (102)$$

To interpret these results as shrinking rules, we note that before the shrinking process, the space $V_{(C_r, Id)}$ of $[C_r, Id]$ is spanned by $\{|r\rangle_{(C_r, Id)}, |r^2\rangle_{(C_r, Id)}\}$, where we omit $j = j' = 1$. According to the discussion in Sec. IV, $|r\rangle_{(C_r, Id)}$ and $|r^2\rangle_{(C_r, Id)}$ correspond to the states $W_M(C_r, Id; r, r) |GS\rangle$ and $W_M(C_r, Id; r^2, r) |GS\rangle$ near $\partial_0 M$. Eqs. (101) and (102) indicate that after the shrinking process, the set of basis transforms as $\mathcal{S}(|r\rangle_{(C_r, Id)}) = \frac{1}{2} [|1\rangle_{(Id)} + |1\rangle_{(A)}]$ and $\mathcal{S}(|r^2\rangle_{(C_r, Id)}) = \frac{1}{2} [|1\rangle_{(Id)} - |1\rangle_{(A)}]$, where we omit $c = e$ and C_e for simplicity, $|1\rangle_{(Id)}$ and $|1\rangle_{(A)}$ correspond to the states $W_P(Id) |GS\rangle$ and $W_P(A) |GS\rangle$ near $\partial_0 M$. Now the space $V_{(C_r, Id)}$ becomes $\mathcal{S}(V_{(C_r, Id)})$, which is spanned by $\left\{ \frac{1}{2} [|1\rangle_{(Id)} + |1\rangle_{(A)}], \frac{1}{2} [|1\rangle_{(Id)} - |1\rangle_{(A)}] \right\}$. Since the sets of basis $\{|1\rangle_{(Id)}\}$ and $\{|1\rangle_{(A)}\}$ span one-dimensional local spaces $V_{(Id)}$ and $V_{(A)}$ that are invariant under the action of the quantum double DG , the space $\mathcal{S}(V_{(C_r, Id)})$ decomposes as $\mathcal{S}(V_{(C_r, Id)}) = V_{(Id)} \oplus V_{(A)}$, which gives the shrinking rule

$$\mathcal{S}([C_r, Id]) = [Id] \oplus [A]. \quad (103)$$

TABLE III. Shrinking table for the 3d \mathbb{D}_3 quantum double model. One can also use Eq. (90) to directly obtain these results.

Loop	$[C_r, Id]$	$[C_r, \omega]$	$[C_r, \omega^2]$	$[C_t, Id]$	$[C_t, -]$
$S(\text{Loop})$	$[Id] \oplus [A]$	$[B]$	$[B]$	$[Id] \oplus [B]$	$[A] \oplus [B]$

This result is consistent with Eq. (90) since $\text{Ind}_{Z_r}^{\mathbb{D}_3}(Id)$ can be decomposed as $\text{Ind}_{Z_r}^{\mathbb{D}_3}(Id) = Id \oplus A$.

One can also fix $c' = r^2$ and exhaust $c \in C_r$ to obtain the basis in $V_{(C_r, Id)}$, i.e., consider the operators shown in Eqs. (96) and (97), because physically the local actions near $\partial_0 M$ cannot distinguish $W_M(C, R; c, j; c', j')$ and $W_M(C, R; c, j; c'', j'')$. By using the same method, we will derive the same shrinking rule Eq. (103).

Similarly, we can derive all the shrinking rules in the 3d \mathbb{D}_3 quantum double model as shown in Appendix D. All the shrinking rules are collected in Table III. Although the five loops in the \mathbb{D}_3 quantum double model are all non-Abelian excitations, only $[C_r, Id]$, $[C_t, Id]$, and $[C_t, -]$ have non-Abelian shrinking rules, while $[C_r, \omega]$ and $[C_r, \omega^2]$ have Abelian shrinking rules.

D. Controlling non-Abelian shrinking channels

In the continuum field theory [69, 77], non-Abelian shrinking rules obtained by computing the correlation functions only generally show us what shrinking channels are legitimate. However, in our microscopic lattice model, we can not only derive general shrinking rules as in Table III, but also further investigate how to determine which channels are selected in a specific shrinking process. In this section, by tuning the internal degrees of freedom in Eq. (51), we demonstrate control over these non-Abelian shrinking channels.

Consider a general loop $[C, R]$ in the quantum double model with a finite group G . In Sec. IV A, we have mentioned that $[C, R]$ is associated with a local Hilbert space $V_{(C, R)}$ spanned by $\{|c, j\rangle_{(C, R)}\}$, where $|c, j\rangle_{(C, R)}$ labels the local degrees of freedom in the state $W_M(C, R; c, j; c', j')|GS\rangle$ near the boundary $\partial_0 M$. Since all the operators $W_M(C, R; c, j; c', j')$ and the corresponding basis states $|c, j\rangle_{(C, R)}$ carry conserved labels (C, R) , an arbitrary linear combination of these operators

$$\sum_{m(c, j)} m(c, j) W_M(C, R; c, j; c', j') \quad (104)$$

and the corresponding linear combination of the basis states

$$|\Psi\rangle_{(C, R)} = \sum_{m(c, j)} m(c, j) |c, j\rangle_{(C, R)} \quad (105)$$

also carry the conserved labels (C, R) , where $m(c, j)$ is a coefficient. Thus, the creation operator for the

loop $[C, R]$ does not necessarily take the form of $W_M(C, R; c, j; c', j')$ but rather is generally given by Eq. (104). Correspondingly, the general state for the loop $[C, R]$ is given by Eq. (105). Changing the set of coefficients from $\{m(c, j)\}$ to $\{m'(c, j)\}$ in Eq. (104) is equivalent to rotating the vector $|\Psi\rangle_{(C, R)}$ in the space $V_{(C, R)}$ to $|\Psi'\rangle_{(C, R)}$:

$$|\Psi'\rangle_{(C, R)} = \sum_{m'(c, j)} m'(c, j) |c, j\rangle_{(C, R)} \in V_{(C, R)}. \quad (106)$$

Suppose the basis state $|c, j\rangle_{(C, R)}$ is shrunk to a linear combination of particle states

$$\mathcal{S}\left(|c, j\rangle_{(C, R)}\right) = \sum_{i, R'} n(i, R') |i\rangle_{(R')}, \quad (107)$$

where R' is an irrep of G , $i = 1, \dots, n_{R'}$, $n(i, R')$ is a coefficient. For a non-Abelian loop, if we perform the shrinking operation on the states $|\Psi\rangle_{(C, R)}$ and $|\Psi'\rangle_{(C, R)}$, we obtain

$$\begin{aligned} \mathcal{S}\left(|\Psi\rangle_{(C, R)}\right) &= \sum_{m(c, j)} m(c, j) \mathcal{S}\left(|c, j\rangle_{(C, R)}\right) \\ &= \sum_{m(c, j)} \sum_{i, R'} m(c, j) n(i, R') |i\rangle_{(R')} \end{aligned} \quad (108)$$

and

$$\begin{aligned} \mathcal{S}\left(|\Psi'\rangle_{(C, R)}\right) &= \sum_{m'(c, j)} m'(c, j) \mathcal{S}\left(|c, j\rangle_{(C, R)}\right) \\ &= \sum_{m'(c, j)} \sum_{i, R'} m'(c, j) n(i, R') |i\rangle_{(R')} \end{aligned} \quad (109)$$

respectively. The resulting states in Eqs. (108) and (109) may live in different local Hilbert spaces for particles. By choosing the coefficients $\{m(c, j)\}$ in Eq. (104) properly, we have $\mathcal{S}\left(|\Psi\rangle_{(C, R)}\right) \in V_{(R')}$, which means that the loop picks a determined shrinking channel leading to the particle $[R']$ in a shrinking process.

To better illustrate the control over non-Abelian shrinking channels, we take the \mathbb{D}_3 quantum double model as an example. According to Table III, the three non-Abelian loops in the \mathbb{D}_3 quantum double model, i.e., $[C_r, Id]$, $[C_t, Id]$ and $[C_t, -]$, have non-Abelian shrinking rules. We start by considering the loop $[C_r, Id]$. By linearly combining the two operators $W_M(C_r, Id; r, r)$ and $W_M(C_r, Id; r^2, r)$ as

$$\begin{aligned} & [W_M(C_r, Id; r, r) \pm W_M(C_r, Id; r^2, r)] \\ &= \left[\sum_{g \in Z_r} \Gamma^{Id}(g) L_M^r T_P^g \pm \sum_{g \in Z_r} \Gamma^{Id}(g) L_M^r T_P^{tg} \right] \\ &= L_M^r T_P^e + L_M^r T_P^r + L_M^r T_P^{r^2} \pm L_M^{r^2} T_P^t \pm L_M^{r^2} T_P^{tr} \\ & \quad \pm L_M^{r^2} T_P^{tr^2} \end{aligned} \quad (110)$$

and then acting it on a ground state, we obtain a vector $|r\rangle_{(C_r, Id)} \pm |r^2\rangle_{(C_r, Id)} \in V_{(C_r, Id)}$. Thus, the operator given by Eq. (110) is a legitimate operator for excitation $[C_r, Id]$. The shrinking process will remove the flux part, i.e.,

$$\begin{aligned} & \mathcal{S} \left([W_M(C_r, Id; r, r) \pm W_M(C_r, Id; r^2, r)] \right) \quad (111) \\ & = T_P^e + T_P^r + T_P^{r^2} \pm T_P^t \pm T_P^{tr} \pm T_P^{tr^2} = \begin{cases} W_P(Id) & + \\ W_P(A) & - \end{cases}. \end{aligned}$$

Thus, we have

$$\mathcal{S} \left(|r\rangle_{(C_r, Id)} \pm |r^2\rangle_{(C_r, Id)} \right) = \begin{cases} |1\rangle_{(Id)} \in V_{(Id)} & + \\ |1\rangle_{(A)} \in V_{(A)} & - \end{cases}. \quad (112)$$

The result above means that by choosing certain degrees of freedom, we can choose the shrinking channel to $[Id]$ or $[A]$. We can use the shrinking diagram shown in Fig. 2 to describe these different channels. When we choose $+$ in Eq. (110), we write a and b as $[C_r, Id]$ and $[Id]$ respectively in Fig. 2. When we choose $-$ in Eq. (110), we write a and b as $[C_r, Id]$ and $[A]$ respectively in Fig. 2.

Similarly, we illustrate how to control other non-Abelian shrinking channels. We can write the corresponding sets of operators for $[C_t, Id]$ and $[C_t, -]$ as $\{W_M(C_t, Id; t, t), W_M(C_t, Id; tr, t), W_M(C_t, Id; tr^2, t)\}$ and $\{W_M(C_t, -; t, t), W_M(C_t, -; tr, t), W_M(C_t, -; tr^2, t)\}$ respectively. The explicit forms of the operators above can be found in Appendix D. For $[C_t, Id]$, by linearly combining the operators as

$$W_M(C_t, Id; t, t) + W_M(C_t, Id; tr, t) + W_M(C_t, Id; tr^2, t), \quad (113)$$

and

$$W_M(C_t, Id; t, t) - W_M(C_t, Id; tr, t), \quad (114)$$

we can control the shrinking channel to $[Id]$ and $[B]$ respectively. One can verify that after the shrinking process, the remaining T -operators in Eqs. (113) and (114) can be written as linear combinations of the operators for $[Id]$ and $[B]$ respectively. Likewise, for $[C_t, -]$, by linearly combining the operators as

$$W_M(C_t, -; t, t) + W_M(C_t, -; tr, t) + W_M(C_t, -; tr^2, t), \quad (115)$$

and

$$W_M(C_t, -; t, t) - W_M(C_t, -; tr, t), \quad (116)$$

we can control the shrinking channel to $[A]$ and $[B]$ respectively.

E. Consistency relations between fusion and shrinking

A systematic check using the fusion Table I and the shrinking Table III demonstrates that all fusion and shrinking processes satisfy the consistency condition Eq. (8) derived from the continuum topological field theory. For example, as shown in Fig. 16, if we consider shrinking two excitations $[C_r, Id]$ and $[C_t, -]$ followed by fusion in the \mathbb{D}_3 quantum double model, we have

$$\begin{aligned} \mathcal{S}([C_r, Id]) \otimes \mathcal{S}([C_t, -]) &= ([Id] \oplus [A]) \otimes ([A] \oplus [B]) \\ &= [Id] \oplus [A] \oplus 2 \cdot [B]. \quad (117) \end{aligned}$$

If we first fuse $[C_r, Id]$ and $[C_t, -]$, and then perform the shrinking process, we have

$$\begin{aligned} \mathcal{S}([C_r, Id] \otimes [C_t, -]) &= \mathcal{S}([C_t, Id] \oplus [C_t, -]) \\ &= [Id] \oplus [A] \oplus 2 \cdot [B] \\ &= \mathcal{S}([C_r, Id]) \otimes \mathcal{S}([C_t, -]). \quad (118) \end{aligned}$$

We can similarly verify the consistency condition for other excitations. We conclude that Eq. (8) applies to the 3d quantum double model with arbitrary finite group G .

Another important property of the shrinking rules obtained from the continuum topological field theory is that the shrinking process preserves the quantum dimensions of the excitations, i.e.,

$$d_a = \sum_b S_b^a d_b, \quad (119)$$

where d_a and d_b are quantum dimensions of excitations a and b respectively. By using Tables II and III, we verify that Eq. (119) holds in our 3d quantum double model. As an illustration, consider the excitation $[C_r, Id]$ in the \mathbb{D}_3 quantum double model, which has $d_{[C_r, Id]} = 2$. Its shrinking rule yields $[Id] \oplus [A]$, where $d_{[Id]} = d_{[A]} = 1$, thus satisfying Eq. (119).

VI. MICROSCOPIC CONSTRUCTION OF THE BF FIELD THEORY WITH AN AAB TWIST

A. Overview

Within the framework of continuum field theory, the (3+1)D BF field theory with an AAB twist unveils a hidden layer of quantum statistical behavior in 3d topological phases. Unlike conventional particle-loop braiding, where a phase arises from the direct winding of a particle around a loop, this theory supports braiding processes in which a particle moves around two unlinked loops without winding around either [42]. The resulting trajectory, together with the loops, forms intricate Brunnian structures such as the Borromean rings, i.e., a configuration in which all three components are pairwise unlinked yet collectively linked. Remarkably, the nontrivial Borromean

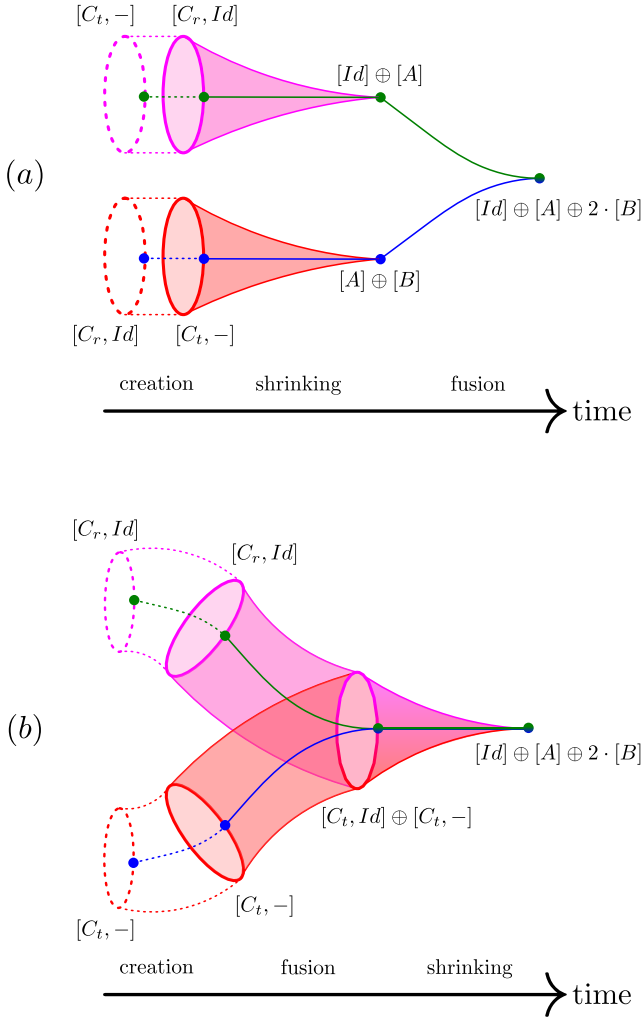


FIG. 16. Consistency relations between the fusion and shrinking rules. We create two pairs of loops by applying the cylindrical membrane operators in Eq. (51). In the \mathbb{D}_3 quantum double model, any excitation is self-dual, i.e., the corresponding anti-excitation is itself. After creating the two pairs of loops, we can use the connecting rules Eqs. (40) and (47) to move or deform the loops. (a) First, we obtain $[Id] \oplus [A]$ and $[A] \oplus [B]$ by shrinking two excitations $[C_r, Id]$ and $[C_t, -]$ respectively. Then we obtain $[Id] \oplus [A] \oplus 2 \cdot [B]$ by fusing $[Id] \oplus [A]$ and $[A] \oplus [B]$. (b) First, we obtain $[C_r, Id] \otimes [C_t, -]$ by fusing two excitations $[C_r, Id]$ and $[C_t, -]$. Then, we obtain $[Id] \oplus [A] \oplus 2 \cdot [B]$ by shrinking $[C_r, Id] \otimes [C_t, -]$. These two processes shown in (a) and (b) produce the same results.

rings braiding indicates that this theory exhibits non-Abelian topological order, despite the underlying gauge group $G = \prod_i \mathbb{Z}_{N_i}$ being Abelian. It is important to note that Borromean rings braiding is not compatible with all multi-loop braiding processes, because a legitimate topological action cannot be written down to describe certain combinations of these processes [43]. This incompatibility stems from the requirement that the action for the twisted BF theory must be gauge invariant. Building on these results, Ref. [69] systematically com-

putes all fusion and shrinking rules in the BF theory with an AAB twist and confirm the presence of non-Abelian fusion and shrinking rules. Moreover, these rules are shown to satisfy the consistency condition Eq. (8), which strongly constrains the associated fusion and shrinking coefficients.

In this section, we present the 3d \mathbb{D}_4 quantum double model as a microscopic construction of the BF theory with an AAB twist. The fact that all nontrivial fusion and shrinking rules in the BF theory with an AAB twist are captured by the \mathbb{D}_4 quantum double model allows us to establish a concrete correspondence between these two theories. This result not only confirms the data derived from the continuum field theory but also demonstrates how these data are encoded in the microscopic lattice model.

B. BF field theory with AAB twisted term as a Borromean-Rings topological order

Here, we briefly review the BF field theory with an AAB twist. We will discuss how to label topological excitations by Wilson operators and calculate fusion and shrinking rules from correlation functions.

Given a gauge group $G = \prod_{i=1}^3 \mathbb{Z}_{N_i}$, this theory describes three 3d \mathbb{Z}_{N_i} toric codes coupled in a nontrivial way, via the topological action

$$S_{\text{BR}} = \int \sum_{i=1}^3 \frac{N_i}{2\pi} B^i dA^i + q A^1 A^2 B^3, \quad (120)$$

where A^i and B^i are 1- and 2-form $U(1)$ gauge fields respectively. Here, the BF terms serve as the effective description of the \mathbb{Z}_{N_i} toric codes, and the AAB twist encodes the coupling among them. As we will show in the following main text, With the simplest $G = (\mathbb{Z}_2)^3$, this theory shares same topological data as the 3d \mathbb{D}_4 quantum double model.

The coefficient $q = \frac{p N_1 N_2 N_3}{(2\pi)^2 N_{123}}$ is quantized due to the large gauge invariance, where $p \in \mathbb{Z}_{N_{123}}$, N_{123} is the greatest common divisor of N_1 , N_2 and N_3 . Lagrange multipliers B^1 , B^2 , and A^3 enforce the flat-connection conditions: $dA^1 = 0$, $dA^2 = 0$, and $dB^3 = 0$. The gauge

transformations are given by

$$\begin{aligned}
A^1 &\rightarrow A^1 + d\chi^1, \\
A^2 &\rightarrow A^2 + d\chi^2, \\
B^3 &\rightarrow B^3 + dV^3, \\
A^3 &\rightarrow A^3 + d\chi^3 \\
&\quad + \frac{2\pi q}{N_3} \left(\chi^2 A^1 - \chi^1 A^2 + \frac{1}{2} \chi^2 d\chi^1 - \frac{1}{2} \chi^1 d\chi^2 \right), \\
B^1 &\rightarrow B^1 + dV^1 \\
&\quad - \frac{2\pi q}{N_1} (\chi^2 B^3 - A^2 V^3 + \chi^2 dV^3), \\
B^2 &\rightarrow B^2 + dV^2 \\
&\quad + \frac{2\pi q}{N_2} (\chi^1 B^3 - A^1 V^3 + \chi^1 dV^3), \tag{121}
\end{aligned}$$

where χ^i and V^i are 0- and 1-form gauge parameters with $\int d\chi^i \in 2\pi\mathbb{Z}$ and $\int dV^i \in 2\pi\mathbb{Z}$.

The topological excitations in this continuum field theory are represented by gauge invariant Wilson operators. We denote a particle excitation by $\mathbf{P}_{n_1 n_2 n_3}$; in the case of $G = (\mathbb{Z}_2)^3$, $n_1, n_2, n_3 = 0, 1$, corresponding to n_1, n_2 , and n_3 units of $\mathbb{Z}_{N_1}, \mathbb{Z}_{N_2}$, and \mathbb{Z}_{N_3} gauge charge. The gauge charges are minimally coupled to 1-form fields A^i . For example, \mathbf{P}_{100} denotes a particle carrying only one unit of \mathbb{Z}_{N_1} gauge charge, and it corresponds to a Wilson operator

$$\mathcal{O}_{\mathbf{P}_{100}} = \exp \left(i \int_{\gamma} A^1 \right), \tag{122}$$

where the $\gamma = S^1$ is the world-line of the particle. \mathbf{P}_{100} is an Abelian particle excitation. A typical non-Abelian particle in this continuum field theory is \mathbf{P}_{001} , whose gauge invariant Wilson operator is

$$\begin{aligned}
\mathcal{O}_{\mathbf{P}_{001}} &= 2 \exp \left[i \int_{\gamma} A^3 + \frac{1}{2} \frac{2\pi q}{N_3} (d^{-1} A^1 A^2 - d^{-1} A^2 A^1) \right] \\
&\quad \times \delta \left(\int_{\gamma} A^1 \right) \delta \left(\int_{\gamma} A^2 \right), \tag{123}
\end{aligned}$$

where the normalization factor 2 in the front of $\mathcal{O}_{\mathbf{P}_{001}}$ ensures that all fusion and shrinking coefficients are integers. One can verify that the total part in the exponent is gauge invariant, while $e^{i \int_{\gamma} A^3}$ alone is not. Here, $d^{-1} A^1$ and $d^{-1} A^2$ are defined through auxiliary fields, $d^{-1} A^1 = \alpha^1$ and $d^{-1} A^2 = \alpha^2$, such that $d\alpha^1 = A^1$ and $d\alpha^2 = A^2$. Since on the closed manifold γ one has $\int_{\gamma} d\alpha^{1,2} = 0$, we need to introduce two delta functions,

$$\delta \left(\int_{\gamma} A^1 \right) = \begin{cases} 1, & \int_{\gamma} A^1 = 0 \pmod{2\pi} \\ 0, & \text{else} \end{cases} \tag{124}$$

$$\delta \left(\int_{\gamma} A^2 \right) = \begin{cases} 1, & \int_{\gamma} A^2 = 0 \pmod{2\pi} \\ 0, & \text{else} \end{cases} \tag{125}$$

to ensure the gauge invariance.

A loop excitation can carry gauge fluxes that are minimally coupled to 2-form fields B^i and decorated by gauge charges that are minimally coupled to 1-form fields A^i . We use $\mathbf{L}_{n_1 n_2 n_3}^{m_1 m_2 m_3}$ to represent a loop, where $n_i, m_i = 0, 1$. The subscript $n_1 n_2 n_3$ denotes n_1, n_2 , and n_3 units of $\mathbb{Z}_{N_1}, \mathbb{Z}_{N_2}$, and \mathbb{Z}_{N_3} gauge flux. The superscript $m_1 m_2 m_3$ denotes m_1, m_2 , and m_3 units of $\mathbb{Z}_{N_1}, \mathbb{Z}_{N_2}$, and \mathbb{Z}_{N_3} gauge charge decoration. For example, the gauge invariant Wilson operator for the Abelian loop \mathbf{L}_{001}^{000} is

$$\mathcal{O}_{\mathbf{L}_{001}^{000}} = \exp \left(i \int_{\sigma} B^3 \right), \tag{126}$$

where \mathbf{L}_{001} is the abbreviation for \mathbf{L}_{001}^{000} . $\sigma = S^1 \times S^1$ is the world-sheet of the loop. Analogous to the non-Abelian particle \mathbf{P}_{001} , the gauge invariant Wilson operator for a non-Abelian loop must contain additional nontrivial terms and delta function constraints. For instance, the Wilson operator for non-Abelian decorated loop \mathbf{L}_{100}^{001} is given by

$$\begin{aligned}
\mathcal{O}_{\mathbf{L}_{100}^{001}} &= 2 \exp \left[i \int_{\sigma} B^1 + \frac{1}{2} \frac{2\pi q}{N_1} (d^{-1} A^2 B^3 + d^{-1} B^3 A^2) \right. \\
&\quad \left. + i \int_{\gamma} A^3 + \frac{1}{2} \frac{2\pi q}{N_3} (d^{-1} A^1 A^2 - d^{-1} A^2 A^1) \right] \\
&\quad \times \delta \left(\int_{\gamma} A^2 \right) \delta \left(\int_{\sigma} B^3 - \int_{\gamma} A^1 \right), \tag{127}
\end{aligned}$$

where the normalization factor 2 ensures that all fusion and shrinking coefficients are integers. $d^{-1} B^3$ is defined as $d^{-1} B^3 = \beta^3$ such that $d\beta^3 = B^3$. In Ref. [69], the delta function constraints in Eq. (127) are originally written as $\delta \left(\int_{\gamma} A^2 \right) \delta \left(\int_{\sigma} B^3 \right) \delta \left(\int_{\gamma} A^1 \right)$. This set of conditions, however, is stronger than necessary and can be relaxed to $\delta \left(\int_{\gamma} A^2 \right) \delta \left(\int_{\sigma} B^3 - \int_{\gamma} A^1 \right)$ while preserving the gauge invariance of Eq. (127). The delta function $\delta \left(\int_{\sigma} B^3 - \int_{\gamma} A^1 \right)$ is defined as

$$\delta \left(\int_{\sigma} B^3 - \int_{\gamma} A^1 \right) = \begin{cases} 1, & \int_{\sigma} B^3 - \int_{\gamma} A^1 = 0 \pmod{2\pi} \\ 0, & \text{else} \end{cases} \tag{128}$$

The delta functions leads to possible equivalence relations between Wilson operators, which is vital in the identification of all topological excitations of this theory. We say two Wilson operators \mathcal{O}_a and \mathcal{O}_b are equivalent if the correlation function $\langle \mathcal{O}_a \mathcal{Q} \rangle = \langle \mathcal{O}_b \mathcal{Q} \rangle$ holds for an arbitrary operator \mathcal{Q} . In this case, the excitations **a** and **b** should be considered as the same excitation because no operator can distinguish them. When computing fusion and shrinking rules, we only need to consider distinct Wilson operators. Take the particle \mathbf{P}_{101} as an example.

The gauge invariant Wilson operator is given by

$$\begin{aligned} \mathcal{O}_{P_{101}} = & 2 \exp \left[i \int_{\gamma} A^1 + i \int_{\gamma} A^3 \right. \\ & \left. + \frac{1}{2} \frac{2\pi q}{N_3} (d^{-1} A^1 A^2 - d^{-1} A^2 A^1) \right] \\ & \times \delta \left(\int_{\gamma} A^1 \right) \delta \left(\int_{\gamma} A^2 \right). \end{aligned} \quad (129)$$

Since the delta function $\delta \left(\int_{\gamma} A^1 \right)$ enforces that $\int_{\gamma} A^1 = 0 \pmod{2\pi}$, the term $\int_{\gamma} A^1$ does not contribute to any correlation function $\langle \mathcal{O}_{P_{101}} \mathcal{Q} \rangle$ and we can simply drop it. Thus, we have $\langle \mathcal{O}_{P_{101}} \mathcal{Q} \rangle = \langle \mathcal{O}_{P_{001}} \mathcal{Q} \rangle$ and P_{101} is equivalent to P_{001} . Similarly, the delta function $\delta \left(\int_{\gamma} A^2 \right)$ also leads to equivalence relation. We conclude that $P_{001} = P_{101} = P_{011} = P_{111}$, where $=$ indicates equivalence. These four notations form an equivalence class, and they all represent the same excitation. In the following discussion, we select P_{001} as the representative of this equivalence class.

Our analysis, based on gauge invariance and a careful treatment of delta functions, reveals that S_{BR} with a gauge group $G = (\mathbb{Z}_2)^3$ admits 22 distinct Wilson operators for excitations. This count differs from the 19 excitations originally reported in Ref. [69]. The discrepancy arises because the delta function constraints in the Wilson operators for the loops L_{100}^{001} , L_{010}^{001} , and L_{110}^{001} were overly restrictive. By relaxing these constraints as demonstrated for L_{100}^{001} in Eq. (127), we obtain the 22 excitations.

Having identified the complete set, we then compute their correlation functions as in Eqs. (5) and (7) to derive all fusion and shrinking rules. Here we present some typical examples.

First, we consider the fusion rules. Particles P_{100} and P_{010} are all Abelian excitations, where the Wilson operator for P_{010} is obtained by simply replacing A^1 with A^2 in Eq. (122). The fusion of P_{100} and P_{010} produces another Abelian particle P_{110} , whose gauge charges are the combination of the gauge charges carried by P_{100} and P_{010} . This result is also indicated by the Wilson operator: $\mathcal{O}_{P_{110}} = \exp \left(i \int_{\gamma} A^1 + A^2 \right)$.

For a non-Abelian excitation, the corresponding Wilson operator carries delta functions, which enforce some integrals to be trivial. A typical example is the particle P_{001} , whose Wilson operator (see Eq. (123)) carries two delta functions $\delta \left(\int_{\gamma} A^1 \right)$ and $\delta \left(\int_{\gamma} A^2 \right)$. Thus, the fusion processes $P_{001} \otimes P_{100}$ and $P_{001} \otimes P_{010}$ are given by

$$P_{001} \otimes P_{100} = P_{001} \otimes P_{010} = P_{001} \quad (130)$$

because $\int_{\gamma} A^1$ and $\int_{\gamma} A^2$ do not contribute to the correlation functions. When we bring the particles P_{001} and P_{100} (P_{010}) together, the gauge charge carried by P_{100} (P_{010}) becomes trivial.

The fusion rules mentioned above are Abelian fusion rules because they have a single fusion channel. We can obtain a non-Abelian fusion rule by fusing a non-Abelian pure loop L_{100} and a non-Abelian particle P_{001} , where the Wilson operator for L_{100} is given by

$$\begin{aligned} \mathcal{O}_{L_{100}} = & 2 \exp \left[i \int_{\sigma} B^1 + \frac{1}{2} \frac{2\pi q}{N_1} (d^{-1} A^2 B^3 + d^{-1} B^3 A^2) \right] \\ & \times \delta \left(\int_{\gamma} A^2 \right) \delta \left(\int_{\sigma} B^3 \right). \end{aligned} \quad (131)$$

Using the Wilson operator for L_{100}^{101} :

$$\begin{aligned} \mathcal{O}_{L_{100}^{101}} = & 2 \exp \left[i \int_{\sigma} B^1 + \frac{1}{2} \frac{2\pi q}{N_1} (d^{-1} A^2 B^3 + d^{-1} B^3 A^2) \right. \\ & \left. + i \int_{\gamma} A^1 + A^3 + \frac{1}{2} \frac{2\pi q}{N_3} (d^{-1} A^1 A^2 - d^{-1} A^2 A^1) \right] \\ & \times \delta \left(\int_{\gamma} A^2 \right) \delta \left(\int_{\sigma} B^3 - \int_{\gamma} A^1 \right), \end{aligned} \quad (132)$$

we compute the correlation function

$$\langle \mathcal{O}_{L_{100}} \times \mathcal{O}_{P_{001}} \rangle = \langle \mathcal{O}_{L_{100}^{001}} + \mathcal{O}_{L_{100}^{101}} \rangle, \quad (133)$$

where the Wilson operators for P_{001} and L_{100}^{001} are shown in Eqs. (123) and (127). Thus, we conclude that the non-Abelian fusion rule is given by $L_{100} \otimes P_{001} = L_{100}^{001} \oplus L_{100}^{101}$. The two fusion channels mean that if we measure the fusion output, there are two possible results corresponding to L_{100}^{001} and L_{100}^{101} .

After deriving all fusion rules, as illustrated in Sec. IV C, we obtain all quantum dimensions of excitations by computing the greatest eigenvalues of the corresponding fusion coefficient matrices. In the BF theory with an AAB twist and the gauge group $(\mathbb{Z}_2)^3$, any Abelian excitation a has quantum dimension $d_a = 1$ and any non-Abelian excitation b has $d_b = 2$.

Now, we present some typical shrinking rules. Consider an Abelian pure loop L_{001} , the shrinking rule is simply $\mathcal{S}(L_{001}) = 1$ because when the manifold σ is shrunk to γ , the integral $\int_{\sigma} B^3$ does not contribute to the correlation function. If we decorate the pure loop with a nontrivial charge, then the shrinking process annihilates the flux while leaving the decoration intact. For example, $\mathcal{S}(L_{001}^{100}) = P_{100}$.

However, for a non-Abelian pure loop such as L_{100} , the shrinking process can lead to a nontrivial gauge charge because the Wilson operator in Eq. (131) carries a delta function $\delta \left(\int_{\gamma} A^2 \right)$. When the manifold σ is shrunk to γ , all integrals over σ in Eq. (131) vanish. Thus, $\langle \mathcal{S}(\mathcal{O}_{L_{100}}) \rangle = \langle 2\delta \left(\int_{\gamma} A^2 \right) \rangle$. Note that when the gauge group is $(\mathbb{Z}_2)^3$, we can expand the delta function as $\delta \left(\int_{\gamma} A^2 \right) = \frac{1}{2} \left[1 + \exp \left(\int_{\gamma} A^2 \right) \right]$, which leads to the shrinking rule

$$\mathcal{S}(L_{001}) = 1 \oplus P_{010}. \quad (134)$$

If we measure the result of shrinking L_{100} , we can obtain either the trivial particle 1 or the nontrivial particle P_{010} . The general shrinking rule Eq. (134) obtained from the continuum field theory only shows all possible shrinking channels. However, we can not determine which channel will be selected in a specific shrinking process. In Sec. VID, we will show that the 3d \mathbb{D}_4 quantum double model is a microscopic construction of the BF theory with an AAB twist and the gauge group $(\mathbb{Z}_2)^3$. In this microscopic model, by tuning the internal degrees of freedom in the operators for loops, we can control which shrinking channel happens in a specific shrinking process, as shown in Sec. VD.

We can verify that the fusion and shrinking rules satisfy the consistency condition shown in Eq. (8). Take L_{100} and P_{001} as examples. Eq. (133) shows that fusing L_{100} and P_{001} first produces $L_{100}^{001} \oplus L_{100}^{101}$. By computing the correlation function Eq (7), we conclude that $\mathcal{S}(L_{100}^{001}) = \mathcal{S}(L_{100}^{101}) = P_{001}$. Thus, fusing L_{100} and P_{001} followed by shrinking is given by

$$\begin{aligned} \mathcal{S}(L_{100} \otimes P_{001}) &= \mathcal{S}(L_{100}^{001} \oplus L_{100}^{101}) = P_{001} \oplus P_{001} \\ &= 2 \cdot P_{001}, \end{aligned} \quad (135)$$

where the result $2 \cdot P_{001}$ means that in the whole process, there are two channels pointing to the excitation P_{001} . On the other hand, shrinking L_{100} and P_{001} followed by fusion is given by

$$\begin{aligned} \mathcal{S}(L_{100}) \otimes \mathcal{S}(P_{001}) &= (1 \oplus P_{010}) \otimes P_{001} = P_{001} \oplus P_{001} \\ &= 2 \cdot P_{001}, \end{aligned} \quad (136)$$

where we have used Eqs. (130) and (134). Thus, fusion followed by shrinking yields the same results as shrinking followed by fusion.

C. Microscopic construction

After reviewing the BF field theory with an AAB twist and the gauge group $(\mathbb{Z}_2)^3$, in this section we present the excitations, fusion rules, and shrinking rules in the \mathbb{D}_4 quantum double model. Denote the two generators of $G = \mathbb{D}_4$ by r and t , then we have $r^4 = t^2 = e$ and $rt = t\bar{r} = tr^3$. We label the five conjugacy classes as

$$\begin{aligned} C_e &= \{e\}, & C_{r^2} &= \{r^2\}, & C_r &= \{r, r^3\}, \\ C_t &= \{t, tr^2\}, & C_{tr} &= \{tr, tr^3\}, \end{aligned} \quad (137)$$

where e, r, t, tr , and r^2 serve as the representative of the classes C_e, C_r, C_t, C_{tr} and C_{r^2} respectively. Their corresponding centralizers are

$$\begin{aligned} Z_e &= Z_{r^2} = \mathbb{D}_4, \\ Z_r &= \{e, r, r^2, r^3\} \simeq \mathbb{Z}_4, \\ Z_t &= \{e, t, r^2, tr^2\} \simeq \mathbb{Z}_2 \times \mathbb{Z}_2, \\ Z_{tr} &= \{e, r^2, tr, tr^3\} \simeq \mathbb{Z}_2 \times \mathbb{Z}_2, \end{aligned} \quad (138)$$

where \simeq denotes isomorphism. Consider $Q_g = G/Z_g$, we have

$$Q_e = Q_{r^2} = \{e\}, \quad Q_r = \{e, t\}, \quad Q_t = Q_{tr} = \{e, r\}. \quad (139)$$

We choose $q_e = q_r = q_t = q_{tr} = q_{r^2} = e$, $q_{r^3} = t$, and $q_{tr^2} = q_{tr^3} = r$. We label the five irreps of \mathbb{D}_4 as $Id, \mathcal{R}, \mathcal{T}, \mathcal{RT}$, and \mathcal{B} , where \mathcal{B} is a $2d$ irrep, others are $1d$ irreps. The representation matrices of the generators are given by

$$\begin{aligned} \Gamma^{Id}(g) &= 1, & \Gamma^{\mathcal{R}}(r) &= -1, \\ \Gamma^{\mathcal{R}}(t) &= 1, & \Gamma^{\mathcal{T}}(r) &= 1, \\ \Gamma^{\mathcal{T}}(t) &= -1, & \Gamma^{\mathcal{RT}}(r) &= \Gamma^{\mathcal{RT}}(t) = -1, \\ \Gamma^{\mathcal{B}}(r) &= \begin{pmatrix} 0 & -1 \\ 1 & 0 \end{pmatrix}, & \Gamma^{\mathcal{B}}(t) &= \begin{pmatrix} 1 & 0 \\ 0 & -1 \end{pmatrix}. \end{aligned} \quad (140)$$

The four $1d$ irreps of $\mathbb{Z}_4 = \{e, r, r^2, r^3\}$ are labeled by Id, ω, ω^2 , and ω^3 . The representation matrices of the generator are given by

$$\Gamma^{Id}(g) = 1, \quad \Gamma^{\omega^n}(r) = \omega^n, \quad (141)$$

where $n = 1, 2, 3$ and $\omega = \exp(\pi i/2) = i$. The four $1d$ irreps of $\mathbb{Z}_2 \times \mathbb{Z}_2 = \{e, a, b, ab\}$ are labeled by Id, a, b , and ab . The representation matrices of the generator are given by

$$\begin{aligned} \Gamma^{Id}(g) &= \Gamma^a(b) = \Gamma^b(a) = 1, \\ \Gamma^a(a) &= \Gamma^b(b) = \Gamma^{ab}(a) = \Gamma^{ab}(b) = -1. \end{aligned} \quad (142)$$

Recall that each excitation is labeled by a pair (C, R) . Thus, we conclude that there are $5 + 5 + 4 + 4 + 4 = 22$ excitations in the \mathbb{D}_4 quantum double model. When $C = C_e$, the five irreps of the group \mathbb{D}_4 correspond to the five particles labeled by

$$[Id], \quad [\mathcal{R}], \quad [\mathcal{T}], \quad [\mathcal{RT}], \quad [\mathcal{B}], \quad (143)$$

where we omit C_e in the notation $[C, R]$. For the nontrivial conjugacy classes C_r, C_t, C_{tr} , and C_{r^2} , the numbers of associated inequivalent irreps are four, four, four, and five respectively. The resulting $4 + 4 + 4 + 5 = 17$ distinct pairs (C, R) correspond to loop excitations, labeled as follows:

$$\begin{aligned} [C_r, Id], & \quad [C_r, \omega], & [C_r, \omega^2], & \quad [C_r, \omega^3], \\ [C_t, Id], & \quad [C_t, a], & [C_t, b], & \quad [C_t, ab], \\ [C_{tr}, Id], & \quad [C_{tr}, a], & [C_{tr}, b], & \quad [C_{tr}, ab], \\ [C_{r^2}, Id], & \quad [C_{r^2}, \mathcal{R}], & [C_{r^2}, \mathcal{T}], & \quad [C_{r^2}, \mathcal{RT}], \\ [C_{r^2}, \mathcal{B}]. & & & \end{aligned} \quad (144)$$

The irrep R encodes the charge decoration carried by the loop. A loop with the trivial irrep Id is a pure loop, whereas a loop with any nontrivial irrep is a decorated loop carrying additional gauge charge.

Using the same strategy illustrated in Sec. IV and Sec. V, we derive some typical fusion and shrinking rules as examples. Consider three particles $[\mathcal{R}]$, $[\mathcal{T}]$, and $[\mathcal{RT}]$. They are associated with three 1d irreps \mathcal{R} , \mathcal{T} , and \mathcal{RT} of the group $G = \mathbb{D}_4$. Recall that the general form of the creation operator for a particle is given by Eq. (34). Thus, the corresponding operators for $[\mathcal{R}]$, $[\mathcal{T}]$ and $[\mathcal{RT}]$ have no internal degrees of freedom, which indicates that they are Abelian particles. According to the discussion in Sec. IV A, a particle labeled by R is associated with a local Hilbert space $V_{(R)}$ spanned by $\{|j\rangle_{(R)} \mid j = 1, \dots, n_R\}$, where n_R denotes the dimension of the irrep R . Thus, the one-dimensional Hilbert spaces for $[\mathcal{R}]$, $[\mathcal{T}]$, and $[\mathcal{RT}]$ are spanned by $\{|1\rangle_{(\mathcal{R})}\}$, $\{|1\rangle_{(\mathcal{T})}\}$, and $\{|1\rangle_{(\mathcal{RT})}\}$. When we bring $[\mathcal{R}]$ and $[\mathcal{T}]$ to a site s and fuse them, the local Hilbert space on the site s is spanned by $\{|1\rangle_{(\mathcal{R})} \otimes |1\rangle_{(\mathcal{T})}\}$. The local operation $D_{(h,g)} \equiv B^h A^g$ (we omit the labels p , s , and v for the plaquette, site, and vertex here for simplicity) acts on the local state $|1\rangle_{(\mathcal{R})} \otimes |1\rangle_{(\mathcal{T})}$ as

$$\begin{aligned} & \sum_{k \in G} D_{(h\bar{k},g)} |1\rangle_{(\mathcal{R})} \otimes D_{(k,g)} |1\rangle_{(\mathcal{T})} \\ &= \delta_{h,e} \Gamma^{\mathcal{R}}(g) |1\rangle_{(\mathcal{R})} \otimes \Gamma^{\mathcal{T}}(g) |1\rangle_{(\mathcal{T})}, \end{aligned} \quad (145)$$

where we have used Eq. (59). From Eq. (140) we conclude that $\Gamma^{\mathcal{R}}(g) \Gamma^{\mathcal{T}}(g) = \Gamma^{\mathcal{RT}}(g)$. Comparing this with the action of $D_{(h,g)}$ on the local state $|1\rangle_{(\mathcal{RT})}$:

$$D_{(h,g)} |1\rangle_{(\mathcal{RT})} = \delta_{h,e} \Gamma^{\mathcal{RT}}(g) |1\rangle_{(\mathcal{RT})}, \quad (146)$$

we conclude that the spaces spanned by $\{|1\rangle_{(\mathcal{R})} \otimes |1\rangle_{(\mathcal{T})}\}$ and $\{|1\rangle_{(\mathcal{RT})}\}$ correspond to equivalent irreps of the quantum double algebra, which leads to the fusion rule

$$[\mathcal{R}] \otimes [\mathcal{T}] = [\mathcal{RT}]. \quad (147)$$

The charge carried by $[\mathcal{RT}]$ is simply the combination of charges carried by $[\mathcal{R}]$ and $[\mathcal{T}]$. This is similar to the case in Sec. VIB, where $\mathsf{P}_{100} \otimes \mathsf{P}_{010} = \mathsf{P}_{110}$.

The particle $[\mathcal{B}]$ in the \mathbb{D}_4 quantum double model is a non-Abelian particle because it is associated with a $2d$ irrep \mathcal{B} of the group $G = \mathbb{D}_4$. From Eq. (34) we can see that the creation operator for $[\mathcal{B}]$ has internal degrees of freedom labeled by the row and column indices of the representation matrix. The corresponding local Hilbert space $V_{(\mathcal{B})}$ is spanned by $\{|j\rangle_{(\mathcal{B})} \mid j = 1, 2\}$, which indicates that the quantum dimension of $[\mathcal{B}]$ is $d_{[\mathcal{B}]} = 2$. If we consider bringing $[\mathcal{B}]$ and $[\mathcal{R}]$ to the same site s , then the local Hilbert space on s is spanned by $\{|1\rangle_{(\mathcal{R})} \otimes |j\rangle_{(\mathcal{B})} \mid j = 1, 2\}$. The local operation $D_{(h,g)} \equiv$

$B^h A^g$ acts on $|1\rangle_{(\mathcal{R})} \otimes |j\rangle_{(\mathcal{B})}$ as

$$\begin{aligned} & \sum_{k \in G} D_{(h\bar{k},g)} |1\rangle_{(\mathcal{R})} \otimes D_{(k,g)} |j\rangle_{(\mathcal{B})} \\ &= \delta_{h,e} \Gamma^{\mathcal{R}}(g) |1\rangle_{(\mathcal{R})} \otimes \sum_{i=1}^2 [\Gamma^{\mathcal{B}}(g)]_{ij} |i\rangle_{(\mathcal{B})} \\ &= \delta_{h,e} \sum_{i=1}^2 [\tilde{\Gamma}^{\mathcal{B}}(g)]_{ij} |1\rangle_{(\mathcal{R})} \otimes |i\rangle_{(\mathcal{B})}, \end{aligned} \quad (148)$$

where we have used Eqs. (59) and (140), $\tilde{\Gamma}^{\mathcal{B}}(g) = U^\dagger \Gamma^{\mathcal{B}}(g) U$, U is a unitary matrix given by $U = \begin{pmatrix} 1 & 0 \\ 0 & -1 \end{pmatrix}$. Comparing Eq. (148) with the action of $D_{(h,g)}$ on the local state $|j\rangle_{(\mathcal{B})}$:

$$D_{(h,g)} |j\rangle_{(\mathcal{B})} = \delta_{h,e} \sum_{i=1}^2 [\Gamma^{\mathcal{B}}(g)]_{ij} |i\rangle_{(\mathcal{B})}, \quad (149)$$

we conclude that the spaces spanned by $\{|1\rangle_{(\mathcal{R})} \otimes |j\rangle_{(\mathcal{B})} \mid j = 1, 2\}$ and $\{|j\rangle_{(\mathcal{B})} \mid j = 1, 2\}$ correspond to equivalent irreps of the quantum double algebra, which leads to the fusion rule

$$[\mathcal{R}] \otimes [\mathcal{B}] = [\mathcal{B}]. \quad (150)$$

Similarly, we have

$$[\mathcal{T}] \otimes [\mathcal{B}] = [\mathcal{B}]. \quad (151)$$

These results show that when we bring $[\mathcal{B}]$ together with either $[\mathcal{R}]$ or $[\mathcal{T}]$, the charge carried by the latter becomes trivial. Comparing with the fusion rules Eq. (130) in Sec. VIB, we can see that $[\mathcal{B}]$ has the same fusion behavior as P_{001} in the BF field theory. In Sec. VID, we will confirm that P_{100} , P_{010} , P_{110} , and P_{001} can be mapped to $[\mathcal{R}]$, $[\mathcal{T}]$, $[\mathcal{RT}]$, and $[\mathcal{B}]$ without altering fusion and shrinking rules.

The fusion rules mentioned above are all Abelian. Now, we consider a typical example of non-Abelian fusion rule. In Sec. VIB, we have obtained a typical non-Abelian fusion rule as $\mathsf{L}_{100} \otimes \mathsf{P}_{001} = \mathsf{L}_{100}^{001} \oplus \mathsf{L}_{100}^{101}$. Its counterpart in the 3d \mathbb{D}_4 quantum double model is given by

$$[C_r, Id] \otimes [\mathcal{B}] = [C_r, \omega] \oplus [C_r, \omega^3], \quad (152)$$

where $[C_r, Id]$ is a non-Abelian pure loop, $[C_r, \omega]$ and $[C_r, \omega^3]$ are non-Abelian decorated loops. These three non-Abelian loops are associated with the conjugacy class C_r , where $|C_r| = 2$. Since the irreps Id , ω , and ω^3 of the centralizer Z_r are one-dimensional, according to Eq. (51), the internal degrees of freedom in the creation operators for these loops are labeled by the elements in conjugacy class C_r . Thus, the local Hilbert spaces corresponding to these three loops are two-dimensional, which indicates that their quantum dimensions are two. For

$[C_r, Id]$, the corresponding local Hilbert space is spanned by $\{|r\rangle_{(C_r, Id)}, |r^3\rangle_{(C_r, Id)}\}$. Fusing $[C_r, Id]$ and $[\mathcal{B}]$ leads to a local Hilbert space $V_{(C_r, Id)} \otimes V_{(\mathcal{B})}$ spanned by $\{|g\rangle_{(C_r, Id)} \otimes |j\rangle_{(\mathcal{B})} \mid g = c, c^3; j = 1, 2\}$. Using Eq. (66), we conclude that $V_{(C_r, Id)} \otimes V_{(\mathcal{B})}$ can be decomposed as $V_{(C_r, Id)} \otimes V_{(\mathcal{B})} = V_{(C_r, \omega)} \oplus V_{(C_r, \omega^3)}$, which leads to the fusion rule Eq. (152). Bringing $[\mathcal{B}]$ and $[C_r, Id]$ together does not produce a definite fusion result but rather two possible channels.

Now, we present some typical shrinking rules. Same as the BF field theory with an AAB twist and the gauge group $(\mathbb{Z}_2)^3$, the \mathbb{D}_4 quantum double model only has one nontrivial Abelian pure loop $[C_{r^2}, Id]$, whose operator is given by $W_M(C_{r^2}, Id) = \sum_{g \in \mathbb{D}_4} L_M^r T_P^g$. Following the discussion in Sec. V, after the shrinking process, the operator becomes $\sum_{g \in \mathbb{D}_4} T_P^g = W_P(Id)$. Thus, we conclude that

$$\mathcal{S}([C_{r^2}, Id]) = [Id]. \quad (153)$$

If we decorate $[C_{r^2}, Id]$ with a charge $[\mathcal{R}]$, we obtain another Abelian decorated loop $[C_{r^2}, \mathcal{R}]$, which is the counterpart of L_{001}^{100} in Sec. VI B. Using Eq. (51), we obtain the operator for $[C_{r^2}, \mathcal{R}]$ as $\sum_{g \in \mathbb{D}_4} \Gamma^{\mathcal{R}}(g) L_M^r T_P^g$. After the shrinking process, the operator becomes $\sum_{g \in \mathbb{D}_4} \Gamma^{\mathcal{R}}(g) T_P^g = W_P(\mathcal{R})$. Thus, we conclude that

$$\mathcal{S}([C_{r^2}, \mathcal{R}]) = [\mathcal{R}]. \quad (154)$$

The charge decoration on the Abelian loop is unaffected by the shrinking process.

Only non-Abelian pure loops can have non-Abelian shrinking rules. Take the counterpart of L_{100} , i.e., $[C_r, Id]$, as an example. The corresponding operators are given by

$$W_M(C_r, Id; r, r) = \sum_{g \in \mathbb{Z}_r} L_M^r T_P^g, \quad (155)$$

$$W_M(C_r, Id; r^3, r) = \sum_{g \in \mathbb{Z}_r} L_M^{r^3} T_P^{tg}. \quad (156)$$

After the shrinking process, the operators become

$$\begin{aligned} \mathcal{S}(W_M(C_r, Id; r, r)) &= \sum_{g \in \mathbb{Z}_r} T_P^g \\ &= \frac{1}{2} [W_P(Id) + W_P(\mathcal{T})], \end{aligned} \quad (157)$$

$$\begin{aligned} \mathcal{S}(W_M(C_r, Id; r^3, r)) &= \sum_{g \in \mathbb{Z}_r} T_P^{tg} \\ &= \frac{1}{2} [W_P(Id) - W_P(\mathcal{T})]. \end{aligned} \quad (158)$$

Thus, the local Hilbert space $\mathcal{S}(V_{(C_r, Id)})$ spanned by

$$\begin{aligned} &\left\{ \mathcal{S}\left(|r\rangle_{(C_r, Id)}\right), \mathcal{S}\left(|r^3\rangle_{(C_r, Id)}\right) \right\} \\ &= \left\{ \frac{1}{2} [|1\rangle_{(Id)} + |1\rangle_{(\mathcal{T})}], \frac{1}{2} [|1\rangle_{(Id)} - |1\rangle_{(\mathcal{T})}] \right\} \end{aligned} \quad (159)$$

can be decomposed as $\mathcal{S}(V_{(C_r, Id)}) = V_{(Id)} \oplus V_{(\mathcal{T})}$, which leads to the shrinking rule

$$\mathcal{S}([C_r, Id]) = [Id] \oplus [\mathcal{T}]. \quad (160)$$

This shrinking rule coincides with Eq. (134). It is possible to observe a nontrivial charge after shrinking the pure loop $[C_r, Id]$.

In the continuum field theory, the shrinking rules like Eq. (134) only shows all possible shrinking channels without containing information about how these channels are selected. One advantage of our microscopic lattice model is that we can control the non-Abelian shrinking channels by tuning the internal degrees of freedom in Eq. (51). Take the pure loop $[C_r, Id]$ as an example. Following the discussion in Sec. V D, we can linearly combine the operators shown in Eqs. (155) and (156) to obtain another legitimate creation operator for $[C_r, Id]$ because this new operator still carries the conserved labels C_r and Id . When we linearly combine the operators in Eqs. (155) and (156) as

$$\begin{aligned} &W_M(C_r, Id; r, r) + W_M(C_r, Id; r^3, r) \\ &= \sum_{g \in \mathbb{Z}_r} L_M^r T_P^g + \sum_{g \in \mathbb{Z}_r} L_M^{r^3} T_P^{tg}, \end{aligned} \quad (161)$$

the shrinking process leads to

$$\begin{aligned} \mathcal{S}\left(\sum_{g \in \mathbb{Z}_r} L_M^r T_P^g + \sum_{g \in \mathbb{Z}_r} L_M^{r^3} T_P^{tg}\right) &= \sum_{g \in \mathbb{D}_4} T_P^g \\ &= W_P(Id). \end{aligned} \quad (162)$$

In this case, shrinking the loop $[C_r, Id]$ produces a definite result $[Id]$. On the other hand, when we linearly combine the operators in Eqs. (155) and (156) as

$$\begin{aligned} &W_M(C_r, Id; r, r) - W_M(C_r, Id; r^3, r) \\ &= \sum_{g \in \mathbb{Z}_r} L_M^r T_P^g - \sum_{g \in \mathbb{Z}_r} L_M^{r^3} T_P^{tg} \\ &= \sum_{g \in \mathbb{Z}_r} \Gamma^{\mathcal{T}}(g) L_M^r T_P^g + \sum_{g \in \mathbb{Z}_r} \Gamma^{\mathcal{T}}(tg) L_M^{r^3} T_P^{tg}, \end{aligned} \quad (163)$$

the shrinking process leads to

$$\begin{aligned} \mathcal{S}\left(\sum_{g \in \mathbb{Z}_r} \Gamma^{\mathcal{T}}(g) L_M^r T_P^g + \sum_{g \in \mathbb{Z}_r} \Gamma^{\mathcal{T}}(tg) L_M^{r^3} T_P^{tg}\right) \\ = \sum_{g \in \mathbb{D}_4} \Gamma^{\mathcal{T}}(g) T_P^g = W_P(\mathcal{T}). \end{aligned} \quad (164)$$

In this case, shrinking the loop $[C_r, Id]$ produces a definite result $[\mathcal{T}]$.

The fusion and shrinking rules obtained from our \mathbb{D}_4 quantum double model satisfy the consistency condition Eq. (8). For example, we can fuse $[C_r, Id]$ and $[\mathcal{B}]$ as

shown in Eq. (152) first. The subsequent shrinking process leads to

$$\begin{aligned} \mathcal{S}([C_r, Id] \otimes [\mathcal{B}]) &= \mathcal{S}([C_r, \omega] \oplus [C_r, \omega^3]) \\ &= [\mathcal{B}] \oplus [\mathcal{B}] = 2 \cdot [\mathcal{B}], \end{aligned} \quad (165)$$

where we have used $\mathcal{S}([C_r, \omega]) = \mathcal{S}([C_r, \omega^3]) = [\mathcal{B}]$. If we shrink $[C_r, Id]$ and $[\mathcal{B}]$ first and then perform fusion, we have

$$\begin{aligned} \mathcal{S}([C_r, Id]) \otimes \mathcal{S}([\mathcal{B}]) &= ([Id] \oplus [\mathcal{T}]) \otimes [\mathcal{B}] \\ &= [\mathcal{B}] \oplus [\mathcal{B}] = 2 \cdot [\mathcal{B}], \end{aligned} \quad (166)$$

which has the same result as fusion followed by shrinking.

Finally, we present all the fusion rules in Tables IV and V as well as all the shrinking rules in Table VI. In Sec. VID, by comparing the fusion and shrinking tables of the 3d \mathbb{D}_4 quantum double model to those of the BF field theory with an AAB twist and gauge group $(\mathbb{Z}_2)^3$, we establish an isomorphism between the excitations in these two theories.

D. Isomorphism between excitations of microscopic construction and continuum field theories

We establish that the \mathbb{D}_4 quantum double model matches the BF field theory with an AAB twist and gauge group $G = (\mathbb{Z}_2)^3$, by constructing an explicit isomorphism between their excitations. A direct comparison of the fusion and shrinking tables of these two theories confirms that the isomorphism $f : \mathbf{a} \mapsto [C, R]$ preserves the fusion and shrinking structures, satisfying

$$f(\mathbf{a}) \otimes f(\mathbf{b}) = f(\mathbf{a} \otimes \mathbf{b}), \quad (167)$$

$$f(\mathcal{S}(\mathbf{a})) = \mathcal{S}(f(\mathbf{a})), \quad (168)$$

where \mathbf{a} and \mathbf{b} denote excitations in the BF field theory with an AAB twist and gauge group $G = (\mathbb{Z}_2)^3$, and $[C, R]$ denotes an excitation in the \mathbb{D}_4 quantum double model. For example, consider mapping the following excitations as

$$\begin{aligned} f(\mathbf{1}) &= [Id], \\ f(\mathbf{P}_{010}) &= [\mathcal{T}], \\ f(\mathbf{L}_{100}) &= [C_r, Id], \\ f(\mathbf{P}_{001}) &= [\mathcal{B}], \\ f(\mathbf{L}_{100}^{001}) &= [C_r, \omega], \\ f(\mathbf{L}_{100}^{101}) &= [C_r, \omega^3]. \end{aligned} \quad (169)$$

By using Eqs. (133) and (152), we can verify that

$$\begin{aligned} f(\mathbf{L}_{100}) \otimes f(\mathbf{P}_{001}) &= [C_r, Id] \otimes [\mathcal{B}] \\ &= [C_r, \omega] \oplus [C_r, \omega^3] \end{aligned} \quad (170)$$

and

$$\begin{aligned} f(\mathbf{L}_{100} \otimes \mathbf{P}_{001}) &= f(\mathbf{L}_{100}^{001} \oplus \mathbf{L}_{100}^{101}) \\ &= [C_r, \omega] \oplus [C_r, \omega^3] \\ &= f(\mathbf{L}_{100}) \otimes f(\mathbf{P}_{001}). \end{aligned} \quad (171)$$

The isomorphism f preserves the fusion rules. As for the shrinking rules, we have

$$f(\mathcal{S}(\mathbf{L}_{100})) = f(\mathbf{1} \oplus \mathbf{P}_{010}) = [Id] \oplus [\mathcal{T}] \quad (172)$$

and

$$\begin{aligned} \mathcal{S}(f(\mathbf{L}_{100})) &= \mathcal{S}([C_r, Id]) = [Id] \oplus [\mathcal{T}] \\ &= f(\mathcal{S}(\mathbf{L}_{100})), \end{aligned} \quad (173)$$

where we have used Eqs. (134) and (160). The isomorphism f preserves the shrinking rules. We present the explicit form of this isomorphism f in Table VII. Under the isomorphism f , the gauge fluxes that are minimally coupled to 2-form fields B^1, B^2 and B^3 are related to the conjugacy classes C_r, C_t and $C_{r,2}$ respectively. The gauge charges that are minimally coupled to 1-form fields A^1, A^2 and A^3 are related to the irreps \mathcal{R}, \mathcal{T} , and \mathcal{B} respectively.

Note that the choice of isomorphism from the BF field theory with an AAB twist and gauge group $G = (\mathbb{Z}_2)^3$ to the \mathbb{D}_4 quantum double model is not unique. An alternative isomorphism $\tilde{f} : \mathbf{a} \mapsto [C, R]$ can be constructed by $\tilde{f} = f \circ F$, where F permutes excitations in the BF field theory with an AAB twist and gauge group $G = (\mathbb{Z}_2)^3$ as

$$\begin{aligned} F(\mathbf{P}_{n_1 n_2 n_3}) &= \mathbf{P}_{n_2 n_1 n_3}, \\ F(\mathbf{L}_{n_1 n_2 n_3}^{m_1 m_2 m_3}) &= \mathbf{L}_{n_2 n_1 n_3}^{m_2 m_1 m_3}. \end{aligned} \quad (174)$$

Under the isomorphism \tilde{f} , the examples shown in Eq. (169) now become

$$\begin{aligned} \tilde{f}(\mathbf{1}) &= f(\mathbf{1}) = [Id], \\ \tilde{f}(\mathbf{P}_{010}) &= f(\mathbf{P}_{100}) = [\mathcal{R}], \\ \tilde{f}(\mathbf{L}_{100}) &= f(\mathbf{L}_{010}) = [C_t, Id], \\ \tilde{f}(\mathbf{P}_{001}) &= f(\mathbf{P}_{001}) = [\mathcal{B}], \\ \tilde{f}(\mathbf{L}_{100}^{001}) &= f(\mathbf{L}_{010}^{001}) = [C_t, a], \\ \tilde{f}(\mathbf{L}_{100}^{101}) &= f(\mathbf{L}_{010}^{101}) = [C_t, ab], \end{aligned} \quad (175)$$

where we have used Table VII for the isomorphism f . From Tables IV and VI, we obtain the following fusion and shrinking rules

$$[C_t, Id] \otimes [\mathcal{B}] = [C_t, a] \oplus [C_t, ab], \quad (176)$$

$$\mathcal{S}([C_t, Id]) = [Id] \oplus [\mathcal{R}]. \quad (177)$$

Thus, we can verify that the isomorphism \tilde{f} still preserves the fusion rules

$$\begin{aligned} \tilde{f}(\mathbf{L}_{100}) \otimes \tilde{f}(\mathbf{P}_{001}) &= [C_t, Id] \otimes [\mathcal{B}] \\ &= [C_t, a] \oplus [C_t, ab], \end{aligned} \quad (178)$$

$$\begin{aligned} \tilde{f}(\mathbf{L}_{100} \otimes \mathbf{P}_{001}) &= \tilde{f}(\mathbf{L}_{100}^{001} \oplus \mathbf{L}_{100}^{101}) \\ &= [C_t, a] \oplus [C_t, ab] \\ &= \tilde{f}(\mathbf{L}_{100}) \otimes \tilde{f}(\mathbf{P}_{001}), \end{aligned} \quad (179)$$

TABLE IV. The first part of fusion table for the \mathbb{D}_4 quantum double model. The complete fusion table is a 22×22 table. This table shows columns 1 to 11 and columns 12 to 22 are shown in Table V.

\otimes	$[Id]$	$[\mathcal{R}]$	$[\mathcal{T}]$	$[\mathcal{RT}]$	$[\mathcal{B}]$	$[C_r, Id]$	$[C_r, \omega]$	$[C_r, \omega^2]$	$[C_r, \omega^3]$	$[C_t, Id]$	$[C_t, a]$
$[Id]$	$[Id]$	$[\mathcal{R}]$	$[\mathcal{T}]$	$[\mathcal{RT}]$	$[\mathcal{B}]$	$[C_r, Id]$	$[C_r, \omega]$	$[C_r, \omega^2]$	$[C_r, \omega^3]$	$[C_t, Id]$	$[C_t, a]$
$[\mathcal{R}]$	$[\mathcal{R}]$	$[Id]$	$[\mathcal{RT}]$	$[\mathcal{T}]$	$[\mathcal{B}]$	$[C_r, \omega^2]$	$[C_r, \omega^3]$	$[C_r, Id]$	$[C_r, \omega]$	$[C_t, Id]$	$[C_t, a]$
$[\mathcal{T}]$	$[\mathcal{T}]$	$[\mathcal{RT}]$	$[Id]$	$[\mathcal{R}]$	$[\mathcal{B}]$	$[C_r, Id]$	$[C_r, \omega]$	$[C_r, \omega^2]$	$[C_r, \omega^3]$	$[C_t, b]$	$[C_t, ab]$
$[\mathcal{RT}]$	$[\mathcal{RT}]$	$[\mathcal{T}]$	$[\mathcal{R}]$	$[Id]$	$[\mathcal{B}]$	$[C_r, \omega^2]$	$[C_r, \omega^3]$	$[C_r, Id]$	$[C_r, \omega]$	$[C_t, b]$	$[C_t, ab]$
$[\mathcal{B}]$	$[\mathcal{B}]$	$[\mathcal{B}]$	$[\mathcal{B}]$	$[\mathcal{B}]$	$[Id]$ $\oplus [\mathcal{R}]$ $\oplus [\mathcal{T}]$ $\oplus [\mathcal{RT}]$	$[C_r, \omega^3]$ $\oplus [C_r, \omega]$	$[C_r, \omega^2]$ $\oplus [C_r, Id]$	$[C_r, \omega^3]$ $\oplus [C_r, \omega]$	$[C_r, \omega^2]$ $\oplus [C_r, Id]$	$[C_t, ab]$ $\oplus [C_t, a]$	$[C_t, Id]$ $\oplus [C_t, b]$
$[C_r, Id]$	$[C_r, Id]$	$[C_r, \omega^2]$	$[C_r, Id]$	$[C_r, \omega^2]$	$[C_r, \omega^3]$ $\oplus [C_r, \omega]$	$[C_{r,2}, Id]$ $\oplus [C_{r,2}, \mathcal{T}]$ $\oplus [\mathcal{T}]$ $\oplus [Id]$	$[C_{r,2}, \mathcal{B}]$ $\oplus [\mathcal{B}]$	$[C_{r,2}, \mathcal{RT}]$ $\oplus [C_{r,2}, \mathcal{R}]$ $\oplus [\mathcal{RT}]$ $\oplus [\mathcal{R}]$	$[C_{r,2}, \mathcal{B}]$ $\oplus [\mathcal{B}]$	$[C_{tr}, Id]$ $\oplus [C_{tr}, b]$	$[C_{tr}, ab]$ $\oplus [C_{tr}, a]$
$[C_r, \omega]$	$[C_r, \omega]$	$[C_r, \omega^3]$	$[C_r, \omega]$	$[C_r, \omega^3]$	$[C_r, \omega^2]$ $\oplus [C_r, Id]$	$[C_{r,2}, \mathcal{B}]$ $\oplus [\mathcal{B}]$	$[C_{r,2}, \mathcal{RT}]$ $\oplus [C_{r,2}, \mathcal{R}]$ $\oplus [\mathcal{T}]$ $\oplus [Id]$	$[C_{r,2}, \mathcal{B}]$ $\oplus [\mathcal{B}]$	$[C_{r,2}, Id]$ $\oplus [C_{r,2}, \mathcal{T}]$ $\oplus [\mathcal{RT}]$ $\oplus [\mathcal{R}]$	$[C_{tr}, ab]$ $\oplus [C_{tr}, a]$	$[C_{tr}, Id]$ $\oplus [C_{tr}, b]$
$[C_r, \omega^2]$	$[C_r, \omega^2]$	$[C_r, Id]$	$[C_r, \omega^2]$	$[C_r, Id]$	$[C_r, \omega^3]$ $\oplus [C_r, \omega]$	$[C_{r,2}, \mathcal{RT}]$ $\oplus [C_{r,2}, \mathcal{R}]$ $\oplus [\mathcal{RT}]$ $\oplus [\mathcal{R}]$	$[C_{r,2}, \mathcal{B}]$ $\oplus [\mathcal{B}]$	$[C_{r,2}, Id]$ $\oplus [C_{r,2}, \mathcal{T}]$ $\oplus [\mathcal{T}]$ $\oplus [Id]$	$[C_{r,2}, \mathcal{B}]$ $\oplus [\mathcal{B}]$	$[C_{tr}, Id]$ $\oplus [C_{tr}, b]$	$[C_{tr}, ab]$ $\oplus [C_{tr}, a]$
$[C_r, \omega^3]$	$[C_r, \omega^3]$	$[C_r, \omega]$	$[C_r, \omega^3]$	$[C_r, \omega]$	$[C_r, \omega^2]$ $\oplus [C_r, Id]$	$[C_{r,2}, \mathcal{B}]$ $\oplus [\mathcal{B}]$	$[C_{r,2}, Id]$ $\oplus [C_{r,2}, \mathcal{T}]$ $\oplus [\mathcal{RT}]$ $\oplus [\mathcal{R}]$	$[C_{r,2}, \mathcal{B}]$ $\oplus [\mathcal{B}]$	$[C_{r,2}, \mathcal{RT}]$ $\oplus [C_{r,2}, \mathcal{R}]$ $\oplus [\mathcal{T}]$ $\oplus [Id]$	$[C_{tr}, ab]$ $\oplus [C_{tr}, a]$	$[C_{tr}, Id]$ $\oplus [C_{tr}, b]$
$[C_t, Id]$	$[C_t, Id]$	$[C_t, Id]$	$[C_t, b]$	$[C_t, b]$	$[C_t, ab]$ $\oplus [C_t, a]$	$[C_{tr}, Id]$ $\oplus [C_{tr}, b]$	$[C_{tr}, ab]$ $\oplus [C_{tr}, a]$	$[C_{tr}, Id]$ $\oplus [C_{tr}, b]$	$[C_{tr}, ab]$ $\oplus [C_{tr}, a]$	$[C_{r,2}, Id]$ $\oplus [C_{r,2}, \mathcal{R}]$ $\oplus [\mathcal{R}]$ $\oplus [Id]$	$[C_{r,2}, \mathcal{B}]$ $\oplus [\mathcal{B}]$
$[C_t, a]$	$[C_t, a]$	$[C_t, a]$	$[C_t, ab]$	$[C_t, ab]$	$[C_t, Id]$ $\oplus [C_t, b]$	$[C_{tr}, ab]$ $\oplus [C_{tr}, a]$	$[C_{tr}, Id]$ $\oplus [C_{tr}, b]$	$[C_{tr}, ab]$ $\oplus [C_{tr}, a]$	$[C_{tr}, Id]$ $\oplus [C_{tr}, b]$	$[C_{r,2}, \mathcal{B}]$ $\oplus [\mathcal{B}]$	$[C_{r,2}, \mathcal{RT}]$ $\oplus [C_{r,2}, \mathcal{T}]$ $\oplus [\mathcal{R}]$ $\oplus [Id]$
$[C_t, b]$	$[C_t, b]$	$[C_t, b]$	$[C_t, Id]$	$[C_t, Id]$	$[C_t, ab]$ $\oplus [C_t, a]$	$[C_{tr}, Id]$ $\oplus [C_{tr}, b]$	$[C_{tr}, ab]$ $\oplus [C_{tr}, a]$	$[C_{tr}, Id]$ $\oplus [C_{tr}, b]$	$[C_{tr}, ab]$ $\oplus [C_{tr}, a]$	$[C_{r,2}, \mathcal{RT}]$ $\oplus [C_{r,2}, \mathcal{T}]$ $\oplus [\mathcal{RT}]$ $\oplus [\mathcal{T}]$	$[C_{r,2}, \mathcal{B}]$ $\oplus [\mathcal{B}]$
$[C_t, ab]$	$[C_t, ab]$	$[C_t, ab]$	$[C_t, a]$	$[C_t, a]$	$[C_t, Id]$ $\oplus [C_t, b]$	$[C_{tr}, ab]$ $\oplus [C_{tr}, a]$	$[C_{tr}, Id]$ $\oplus [C_{tr}, b]$	$[C_{tr}, ab]$ $\oplus [C_{tr}, a]$	$[C_{tr}, Id]$ $\oplus [C_{tr}, b]$	$[C_{r,2}, \mathcal{B}]$ $\oplus [\mathcal{B}]$	$[C_{r,2}, Id]$ $\oplus [C_{r,2}, \mathcal{R}]$ $\oplus [\mathcal{RT}]$ $\oplus [\mathcal{T}]$
$[C_{tr}, Id]$	$[C_{tr}, Id]$	$[C_{tr}, b]$	$[C_{tr}, b]$	$[C_{tr}, Id]$	$[C_{tr}, ab]$ $\oplus [C_{tr}, a]$	$[C_t, Id]$ $\oplus [C_t, b]$	$[C_t, ab]$ $\oplus [C_t, a]$	$[C_t, Id]$ $\oplus [C_t, b]$	$[C_t, ab]$ $\oplus [C_t, a]$	$[C_r, \omega^2]$ $\oplus [C_r, Id]$	$[C_r, \omega^3]$ $\oplus [C_r, \omega]$
$[C_{tr}, a]$	$[C_{tr}, a]$	$[C_{tr}, ab]$	$[C_{tr}, ab]$	$[C_{tr}, a]$	$[C_{tr}, Id]$ $\oplus [C_{tr}, b]$	$[C_t, ab]$ $\oplus [C_t, a]$	$[C_t, Id]$ $\oplus [C_t, b]$	$[C_t, ab]$ $\oplus [C_t, a]$	$[C_t, Id]$ $\oplus [C_t, b]$	$[C_r, \omega^3]$ $\oplus [C_r, \omega]$	$[C_r, \omega^2]$ $\oplus [C_r, Id]$
$[C_{tr}, b]$	$[C_{tr}, b]$	$[C_{tr}, Id]$	$[C_{tr}, Id]$	$[C_{tr}, b]$	$[C_{tr}, ab]$ $\oplus [C_{tr}, a]$	$[C_t, Id]$ $\oplus [C_t, b]$	$[C_t, ab]$ $\oplus [C_t, a]$	$[C_t, Id]$ $\oplus [C_t, b]$	$[C_t, ab]$ $\oplus [C_t, a]$	$[C_r, \omega^2]$ $\oplus [C_r, Id]$	$[C_r, \omega^3]$ $\oplus [C_r, \omega]$
$[C_{tr}, ab]$	$[C_{tr}, ab]$	$[C_{tr}, a]$	$[C_{tr}, a]$	$[C_{tr}, ab]$	$[C_{tr}, Id]$ $\oplus [C_{tr}, b]$	$[C_t, ab]$ $\oplus [C_t, a]$	$[C_t, Id]$ $\oplus [C_t, b]$	$[C_t, ab]$ $\oplus [C_t, a]$	$[C_t, Id]$ $\oplus [C_t, b]$	$[C_r, \omega^3]$ $\oplus [C_r, \omega]$	$[C_r, \omega^2]$ $\oplus [C_r, Id]$
$[C_{r,2}, Id]$	$[C_{r,2}, Id]$	$[C_{r,2}, \mathcal{R}]$	$[C_{r,2}, \mathcal{T}]$	$[C_{r,2}, \mathcal{RT}]$	$[C_{r,2}, \mathcal{B}]$	$[C_r, Id]$	$[C_r, \omega^3]$	$[C_r, \omega^2]$	$[C_r, \omega]$	$[C_t, Id]$	$[C_t, ab]$
$[C_{r,2}, \mathcal{R}]$	$[C_{r,2}, \mathcal{R}]$	$[C_{r,2}, Id]$	$[C_{r,2}, \mathcal{RT}]$	$[C_{r,2}, \mathcal{T}]$	$[C_{r,2}, \mathcal{B}]$	$[C_r, \omega^2]$	$[C_r, \omega]$	$[C_r, Id]$	$[C_r, \omega^3]$	$[C_t, Id]$	$[C_t, ab]$
$[C_{r,2}, \mathcal{T}]$	$[C_{r,2}, \mathcal{T}]$	$[C_{r,2}, \mathcal{RT}]$	$[C_{r,2}, Id]$	$[C_{r,2}, \mathcal{R}]$	$[C_{r,2}, \mathcal{B}]$	$[C_r, Id]$	$[C_r, \omega^3]$	$[C_r, \omega^2]$	$[C_r, \omega]$	$[C_t, b]$	$[C_t, a]$
$[C_{r,2}, \mathcal{RT}]$	$[C_{r,2}, \mathcal{RT}]$	$[C_{r,2}, \mathcal{T}]$	$[C_{r,2}, \mathcal{R}]$	$[C_{r,2}, Id]$	$[C_{r,2}, \mathcal{B}]$	$[C_r, \omega^2]$	$[C_r, \omega]$	$[C_r, Id]$	$[C_r, \omega^3]$	$[C_t, b]$	$[C_t, a]$
$[C_{r,2}, \mathcal{B}]$	$[C_{r,2}, \mathcal{RT}]$ $\oplus [C_{r,2}, \mathcal{T}]$ $\oplus [C_{r,2}, \mathcal{R}]$ $\oplus [C_{r,2}, Id]$	$[C_r, \omega^3]$ $\oplus [C_r, \omega]$	$[C_r, \omega^2]$ $\oplus [C_r, Id]$	$[C_r, \omega^3]$ $\oplus [C_r, \omega]$	$[C_r, \omega^2]$ $\oplus [C_r, Id]$	$[C_t, ab]$ $\oplus [C_t, a]$	$[C_t, Id]$ $\oplus [C_t, b]$				

TABLE V. The second part of fusion table for the \mathbb{D}_4 quantum double model. The complete fusion table is a 22×22 table. This table shows columns 12 to 22.

\otimes	$[C_t, b]$	$[C_t, ab]$	$[C_{tr}, Id]$	$[C_{tr}, a]$	$[C_{tr}, b]$	$[C_{tr}, ab]$	$[C_{r,2}, Id]$	$[C_{r,2}, \mathcal{R}]$	$[C_{r,2}, \mathcal{T}]$	$[C_{r,2}, \mathcal{RT}]$	$[C_{r,2}, \mathcal{B}]$
$[Id]$	$[C_t, b]$	$[C_t, ab]$	$[C_{tr}, Id]$	$[C_{tr}, a]$	$[C_{tr}, b]$	$[C_{tr}, ab]$	$[C_{r,2}, Id]$	$[C_{r,2}, \mathcal{R}]$	$[C_{r,2}, \mathcal{T}]$	$[C_{r,2}, \mathcal{RT}]$	$[C_{r,2}, \mathcal{B}]$
$[\mathcal{R}]$	$[C_t, b]$	$[C_t, ab]$	$[C_{tr}, b]$	$[C_{tr}, ab]$	$[C_{tr}, Id]$	$[C_{tr}, a]$	$[C_{r,2}, \mathcal{R}]$	$[C_{r,2}, Id]$	$[C_{r,2}, \mathcal{RT}]$	$[C_{r,2}, \mathcal{T}]$	$[C_{r,2}, \mathcal{B}]$
$[\mathcal{T}]$	$[C_t, Id]$	$[C_t, a]$	$[C_{tr}, b]$	$[C_{tr}, ab]$	$[C_{tr}, Id]$	$[C_{tr}, a]$	$[C_{r,2}, \mathcal{T}]$	$[C_{r,2}, \mathcal{RT}]$	$[C_{r,2}, Id]$	$[C_{r,2}, \mathcal{R}]$	$[C_{r,2}, \mathcal{B}]$
$[\mathcal{RT}]$	$[C_t, Id]$	$[C_t, a]$	$[C_{tr}, Id]$	$[C_{tr}, a]$	$[C_{tr}, b]$	$[C_{tr}, ab]$	$[C_{r,2}, \mathcal{RT}]$	$[C_{r,2}, \mathcal{T}]$	$[C_{r,2}, \mathcal{R}]$	$[C_{r,2}, Id]$	$[C_{r,2}, \mathcal{B}]$
$[\mathcal{B}]$	$[C_t, ab]$ $\oplus [C_t, a]$	$[C_t, Id]$ $\oplus [C_t, b]$	$[C_{tr}, ab]$ $\oplus [C_{tr}, a]$	$[C_{tr}, Id]$ $\oplus [C_{tr}, b]$	$[C_{tr}, ab]$ $\oplus [C_{tr}, a]$	$[C_{tr}, Id]$ $\oplus [C_{tr}, b]$	$[C_{r,2}, \mathcal{B}]$	$[C_{r,2}, \mathcal{B}]$	$[C_{r,2}, \mathcal{B}]$	$[C_{r,2}, \mathcal{B}]$	$[C_{r,2}, \mathcal{RT}]$ $\oplus [C_{r,2}, \mathcal{T}]$ $\oplus [C_{r,2}, \mathcal{R}]$ $\oplus [C_{r,2}, Id]$
$[C_r, Id]$	$[C_{tr}, Id]$ $\oplus [C_{tr}, b]$	$[C_{tr}, ab]$ $\oplus [C_{tr}, a]$	$[C_t, Id]$ $\oplus [C_t, b]$	$[C_t, ab]$ $\oplus [C_t, a]$	$[C_t, Id]$ $\oplus [C_t, b]$	$[C_t, ab]$ $\oplus [C_t, a]$	$[C_r, Id]$	$[C_r, \omega^2]$	$[C_r, Id]$	$[C_r, \omega^2]$	$[C_r, \omega^3]$ $\oplus [C_r, \omega]$
$[C_r, \omega]$	$[C_{tr}, ab]$ $\oplus [C_{tr}, a]$	$[C_{tr}, Id]$ $\oplus [C_{tr}, b]$	$[C_t, ab]$ $\oplus [C_t, a]$	$[C_t, Id]$ $\oplus [C_t, b]$	$[C_t, ab]$ $\oplus [C_t, a]$	$[C_t, Id]$ $\oplus [C_t, b]$	$[C_r, \omega^3]$	$[C_r, \omega]$	$[C_r, \omega^3]$	$[C_r, \omega]$	$[C_r, \omega^2]$ $\oplus [C_r, Id]$
$[C_r, \omega^2]$	$[C_{tr}, Id]$ $\oplus [C_{tr}, b]$	$[C_{tr}, ab]$ $\oplus [C_{tr}, a]$	$[C_t, Id]$ $\oplus [C_t, b]$	$[C_t, ab]$ $\oplus [C_t, a]$	$[C_t, Id]$ $\oplus [C_t, b]$	$[C_t, ab]$ $\oplus [C_t, a]$	$[C_r, \omega^2]$	$[C_r, Id]$	$[C_r, \omega^2]$	$[C_r, Id]$	$[C_r, \omega^3]$ $\oplus [C_r, \omega]$
$[C_r, \omega^3]$	$[C_{tr}, ab]$ $\oplus [C_{tr}, a]$	$[C_{tr}, Id]$ $\oplus [C_{tr}, b]$	$[C_t, ab]$ $\oplus [C_t, a]$	$[C_t, Id]$ $\oplus [C_t, b]$	$[C_t, ab]$ $\oplus [C_t, a]$	$[C_t, Id]$ $\oplus [C_t, b]$	$[C_r, \omega]$	$[C_r, \omega^3]$	$[C_r, \omega]$	$[C_r, \omega^3]$	$[C_r, \omega^2]$ $\oplus [C_r, Id]$
$[C_t, Id]$	$[C_{r,2}, \mathcal{RT}]$ $\oplus [C_{r,2}, \mathcal{T}]$ $\oplus [\mathcal{RT}]$ $\oplus [\mathcal{T}]$	$[C_{r,2}, \mathcal{B}]$ $\oplus [\mathcal{B}]$	$[C_r, \omega^2]$ $\oplus [C_r, Id]$	$[C_r, \omega^3]$ $\oplus [C_r, \omega]$	$[C_r, \omega^2]$ $\oplus [C_r, Id]$	$[C_r, \omega^3]$ $\oplus [C_r, \omega]$	$[C_t, Id]$	$[C_t, Id]$	$[C_t, b]$	$[C_t, b]$	$[C_t, ab]$ $\oplus [C_t, a]$
$[C_t, a]$	$[C_{r,2}, \mathcal{B}]$ $\oplus [\mathcal{B}]$	$[C_{r,2}, Id]$ $\oplus [C_{r,2}, \mathcal{R}]$ $\oplus [\mathcal{RT}]$ $\oplus [\mathcal{T}]$	$[C_r, \omega^3]$ $\oplus [C_r, \omega]$	$[C_r, \omega^2]$ $\oplus [C_r, Id]$	$[C_r, \omega^3]$ $\oplus [C_r, \omega]$	$[C_r, \omega^2]$ $\oplus [C_r, Id]$	$[C_t, ab]$	$[C_t, ab]$	$[C_t, a]$	$[C_t, a]$	$[C_t, Id]$ $\oplus [C_t, b]$
$[C_t, b]$	$[C_{r,2}, Id]$ $\oplus [C_{r,2}, \mathcal{R}]$ $\oplus [\mathcal{R}]$ $\oplus [Id]$	$[C_{r,2}, \mathcal{B}]$ $\oplus [\mathcal{B}]$	$[C_r, \omega^2]$ $\oplus [C_r, Id]$	$[C_r, \omega^3]$ $\oplus [C_r, \omega]$	$[C_r, \omega^2]$ $\oplus [C_r, Id]$	$[C_r, \omega^3]$ $\oplus [C_r, \omega]$	$[C_t, b]$	$[C_t, b]$	$[C_t, Id]$	$[C_t, Id]$	$[C_t, ab]$ $\oplus [C_t, a]$
$[C_t, ab]$	$[C_{r,2}, \mathcal{B}]$ $\oplus [\mathcal{B}]$	$[C_{r,2}, \mathcal{RT}]$ $\oplus [C_{r,2}, \mathcal{T}]$ $\oplus [\mathcal{R}]$ $\oplus [Id]$	$[C_r, \omega^3]$ $\oplus [C_r, \omega]$	$[C_r, \omega^2]$ $\oplus [C_r, Id]$	$[C_r, \omega^3]$ $\oplus [C_r, \omega]$	$[C_r, \omega^2]$ $\oplus [C_r, Id]$	$[C_t, a]$	$[C_t, a]$	$[C_t, ab]$	$[C_t, ab]$	$[C_t, Id]$ $\oplus [C_t, b]$
$[C_{tr}, Id]$	$[C_r, \omega^2]$ $\oplus [C_r, Id]$	$[C_r, \omega^3]$ $\oplus [C_r, \omega]$	$[C_{r,2}, \mathcal{RT}]$ $\oplus [C_{r,2}, Id]$ $\oplus [\mathcal{RT}]$ $\oplus [Id]$	$[C_{r,2}, \mathcal{B}]$ $\oplus [\mathcal{B}]$	$[C_{r,2}, \mathcal{T}]$ $\oplus [C_{r,2}, \mathcal{R}]$ $\oplus [\mathcal{T}]$ $\oplus [\mathcal{R}]$	$[C_{r,2}, \mathcal{B}]$ $\oplus [\mathcal{B}]$	$[C_{tr}, Id]$	$[C_{tr}, b]$	$[C_{tr}, b]$	$[C_{tr}, Id]$	$[C_{tr}, ab]$ $\oplus [C_{tr}, a]$
$[C_{tr}, a]$	$[C_r, \omega^3]$ $\oplus [C_r, \omega]$	$[C_r, \omega^2]$ $\oplus [C_r, Id]$	$[C_{r,2}, \mathcal{B}]$ $\oplus [\mathcal{B}]$	$[C_{r,2}, \mathcal{T}]$ $\oplus [C_{r,2}, \mathcal{R}]$ $\oplus [Id]$	$[C_{r,2}, \mathcal{B}]$ $\oplus [\mathcal{B}]$	$[C_{r,2}, \mathcal{RT}]$ $\oplus [C_{r,2}, Id]$ $\oplus [\mathcal{T}]$ $\oplus [\mathcal{R}]$	$[C_{tr}, ab]$	$[C_{tr}, a]$	$[C_{tr}, a]$	$[C_{tr}, ab]$	$[C_{tr}, Id]$ $\oplus [C_{tr}, b]$
$[C_{tr}, b]$	$[C_r, \omega^2]$ $\oplus [C_r, Id]$	$[C_r, \omega^3]$ $\oplus [C_r, \omega]$	$[C_{r,2}, \mathcal{T}]$ $\oplus [C_{r,2}, \mathcal{R}]$ $\oplus [\mathcal{T}]$ $\oplus [\mathcal{R}]$	$[C_{r,2}, \mathcal{B}]$ $\oplus [\mathcal{B}]$	$[C_{r,2}, \mathcal{RT}]$ $\oplus [C_{r,2}, Id]$ $\oplus [\mathcal{R}]$	$[C_{r,2}, \mathcal{B}]$ $\oplus [\mathcal{B}]$	$[C_{tr}, b]$	$[C_{tr}, Id]$	$[C_{tr}, Id]$	$[C_{tr}, b]$	$[C_{tr}, ab]$ $\oplus [C_{tr}, a]$
$[C_{tr}, ab]$	$[C_r, \omega^3]$ $\oplus [C_r, \omega]$	$[C_r, \omega^2]$ $\oplus [C_r, Id]$	$[C_{r,2}, \mathcal{B}]$ $\oplus [\mathcal{B}]$	$[C_{r,2}, \mathcal{RT}]$ $\oplus [C_{r,2}, Id]$ $\oplus [\mathcal{T}]$ $\oplus [\mathcal{R}]$	$[C_{r,2}, \mathcal{B}]$ $\oplus [\mathcal{B}]$	$[C_{r,2}, \mathcal{T}]$ $\oplus [C_{r,2}, \mathcal{R}]$ $\oplus [\mathcal{R}]$ $\oplus [Id]$	$[C_{tr}, a]$	$[C_{tr}, ab]$	$[C_{tr}, ab]$	$[C_{tr}, a]$	$[C_{tr}, Id]$ $\oplus [C_{tr}, b]$
$[C_{r,2}, Id]$	$[C_t, b]$	$[C_t, a]$	$[C_{tr}, Id]$	$[C_{tr}, ab]$	$[C_{tr}, b]$	$[C_{tr}, a]$	$[Id]$	$[\mathcal{R}]$	$[\mathcal{T}]$	$[\mathcal{RT}]$	$[\mathcal{B}]$
$[C_{r,2}, \mathcal{R}]$	$[C_t, b]$	$[C_t, a]$	$[C_{tr}, b]$	$[C_{tr}, a]$	$[C_{tr}, Id]$	$[C_{tr}, ab]$	$[\mathcal{R}]$	$[Id]$	$[\mathcal{RT}]$	$[\mathcal{T}]$	$[\mathcal{B}]$
$[C_{r,2}, \mathcal{T}]$	$[C_t, Id]$	$[C_t, ab]$	$[C_{tr}, b]$	$[C_{tr}, a]$	$[C_{tr}, Id]$	$[C_{tr}, ab]$	$[\mathcal{T}]$	$[\mathcal{RT}]$	$[Id]$	$[\mathcal{R}]$	$[\mathcal{B}]$
$[C_{r,2}, \mathcal{RT}]$	$[C_t, Id]$	$[C_t, ab]$	$[C_{tr}, Id]$	$[C_{tr}, ab]$	$[C_{tr}, b]$	$[C_{tr}, a]$	$[\mathcal{RT}]$	$[\mathcal{T}]$	$[\mathcal{R}]$	$[Id]$	$[\mathcal{B}]$
$[C_{r,2}, \mathcal{B}]$	$[C_t, ab]$ $\oplus [C_t, a]$	$[C_t, Id]$ $\oplus [C_t, b]$	$[C_{tr}, ab]$ $\oplus [C_{tr}, a]$	$[C_{tr}, Id]$ $\oplus [C_{tr}, b]$	$[C_{tr}, ab]$ $\oplus [C_{tr}, a]$	$[C_{tr}, Id]$ $\oplus [C_{tr}, b]$	$[\mathcal{B}]$	$[\mathcal{B}]$	$[\mathcal{B}]$	$[\mathcal{B}]$	$[Id]$ $\oplus [\mathcal{R}]$ $\oplus [\mathcal{T}]$ $\oplus [\mathcal{RT}]$

TABLE VI. Shrinking table for the 3d \mathbb{D}_4 quantum double model.

Loop	$[C_r, Id]$	$[C_r, \omega]$	$[C_r, \omega^2]$	$[C_r, \omega^3]$	$[C_t, Id]$	$[C_t, a]$	$[C_t, b]$	$[C_t, ab]$	$[C_{tr}, Id]$
\mathcal{S} (Loop)	$[Id] \oplus [\mathcal{T}]$	$[\mathcal{B}]$	$[\mathcal{R}] \oplus [\mathcal{RT}]$	$[\mathcal{B}]$	$[Id] \oplus [\mathcal{R}]$	$[\mathcal{B}]$	$[\mathcal{T}] \oplus [\mathcal{RT}]$	$[\mathcal{B}]$	$[Id] \oplus [\mathcal{RT}]$
Loop	$[C_{tr}, a]$	$[C_{tr}, b]$	$[C_{tr}, ab]$	$[C_{r,2}, Id]$	$[C_{r,2}, \mathcal{R}]$	$[C_{r,2}, \mathcal{T}]$	$[C_{r,2}, \mathcal{RT}]$	$[C_{r,2}, \mathcal{B}]$	
\mathcal{S} (Loop)	$[\mathcal{B}]$	$[\mathcal{R}] \oplus [\mathcal{T}]$	$[\mathcal{B}]$	$[Id]$	$[\mathcal{R}]$	$[\mathcal{T}]$	$[\mathcal{RT}]$	$[\mathcal{B}]$	

TABLE VII. Mapping table of f . We write $\mathbb{L}_{n_1 n_2 n_3}^{000}$ as $\mathbb{L}_{n_1 n_2 n_3}$ for simplicity.

a	1	P₁₀₀	P₀₁₀	P₁₁₀	P₀₀₁	L₁₀₀	L₁₀₀⁰⁰¹	L₁₀₀¹⁰⁰	L₁₀₀¹⁰¹	L₀₁₀	L₀₁₀⁰⁰¹
$f(\mathbf{a})$	$[Id]$	$[\mathcal{R}]$	$[\mathcal{T}]$	$[\mathcal{RT}]$	$[\mathcal{B}]$	$[C_r, Id]$	$[C_r, \omega]$	$[C_r, \omega^2]$	$[C_r, \omega^3]$	$[C_t, Id]$	$[C_t, a]$
a	L₀₁₀⁰¹⁰	L₀₁₀⁰¹¹	L₁₁₀	L₁₁₀⁰⁰¹	L₁₁₀¹⁰⁰	L₁₁₀¹⁰¹	L₀₀₁	L₀₀₁¹⁰⁰	L₀₀₁⁰¹⁰	L₀₀₁¹¹⁰	L₀₀₁⁰⁰¹
$f(\mathbf{a})$	$[C_t, b]$	$[C_t, ab]$	$[C_{tr}, Id]$	$[C_{tr}, a]$	$[C_{tr}, b]$	$[C_{tr}, ab]$	$[C_{r,2}, Id]$	$[C_{r,2}, \mathcal{R}]$	$[C_{r,2}, \mathcal{T}]$	$[C_{r,2}, \mathcal{RT}]$	$[C_{r,2}, \mathcal{B}]$

TABLE VIII. Mapping table of $\tilde{f} \equiv f \circ F$, where the mapping F is defined as $F(\mathbb{P}_{n_1 n_2 n_3}) = \mathbb{P}_{n_2 n_1 n_3}$ and $F(\mathbb{L}_{n_1 n_2 n_3}^{m_1 m_2 m_3}) = \mathbb{L}_{n_2 n_1 n_3}^{m_2 m_1 m_3}$.

a	1	P₁₀₀	P₀₁₀	P₁₁₀	P₀₀₁	L₁₀₀	L₁₀₀⁰⁰¹	L₁₀₀¹⁰⁰	L₁₀₀¹⁰¹	L₀₁₀	L₀₁₀⁰⁰¹
$\tilde{f}(\mathbf{a})$	$[Id]$	$[\mathcal{T}]$	$[\mathcal{R}]$	$[\mathcal{RT}]$	$[\mathcal{B}]$	$[C_t, Id]$	$[C_t, a]$	$[C_t, b]$	$[C_t, ab]$	$[C_r, Id]$	$[C_r, \omega]$
a	L₀₁₀⁰¹⁰	L₀₁₀⁰¹¹	L₁₁₀	L₁₁₀⁰⁰¹	L₁₁₀¹⁰⁰	L₁₁₀¹⁰¹	L₀₀₁	L₀₀₁¹⁰⁰	L₀₀₁⁰¹⁰	L₀₀₁¹¹⁰	L₀₀₁⁰⁰¹
$\tilde{f}(\mathbf{a})$	$[C_r, \omega^2]$	$[C_r, \omega^3]$	$[C_{tr}, Id]$	$[C_{tr}, a]$	$[C_{tr}, b]$	$[C_{tr}, ab]$	$[C_{r,2}, Id]$	$[C_{r,2}, \mathcal{T}]$	$[C_{r,2}, \mathcal{R}]$	$[C_{r,2}, \mathcal{RT}]$	$[C_{r,2}, \mathcal{B}]$

and the shrinking rules

$$\tilde{f}(\mathcal{S}(\mathbb{L}_{100})) = \tilde{f}(1 \oplus \mathbb{P}_{010}) = [Id] \oplus [\mathcal{R}], \quad (180)$$

$$\begin{aligned} \mathcal{S}(\tilde{f}(\mathbb{L}_{100})) &= \mathcal{S}([C_t, Id]) = [Id] \oplus [\mathcal{R}] \\ &= \tilde{f}(\mathcal{S}(\mathbb{L}_{100})). \end{aligned} \quad (181)$$

The explicit form of the isomorphism \tilde{f} is shown in Table VIII. The isomorphism \tilde{f} relates the gauge fluxes that are minimally coupled to 2-form fields B^1 , B^2 and B^3 to conjugacy classes C_t , C_r and $C_{r,2}$ respectively. Gauge charges that are minimally coupled to 1-form fields A^1 , A^2 and A^3 are related to the irreps \mathcal{T} , \mathcal{R} , and \mathcal{B} respectively.

Eqs. (167) and (168) demonstrate that the \mathbb{D}_4 quantum double model and the BF field theory with an AAB twist and gauge group $G = (\mathbb{Z}_2)^3$ share identical fusion and shrinking structures. The isomorphism f establishes the \mathbb{D}_4 quantum double model as the microscopic construction of the BF field theory with an AAB twist and gauge group $G = (\mathbb{Z}_2)^3$. This correspondence bridges two complementary approaches to topological order: the long wavelength continuum field theory and the microscopic lattice model. The agreement of their topological data not only provides strong support for the field-theoretic derivation of the fusion and shrinking rules but also re-

veals how these rules are encoded in the microscopic degrees of freedom of a local lattice Hamiltonian.

VII. DISCUSSION

A. Summary

Understanding higher-dimensional non-Abelian topological orders requires a unified framework that connects continuum topological field theories with explicit microscopic constructions. In this work, we establish such a connection in three dimensions by providing a complete microscopic realization of particle and loop excitations, their fusion and shrinking processes, and the associated consistency relations, thereby placing the field-theoretical principles of three-dimensional topological order on a firm lattice footing.

Concretely, we explicitly construct lattice creation operators for all topological excitations in the three-dimensional quantum double model and establish the corresponding connecting rules that allow excitations to be transported and deformed on the lattice. These operators enable us to implement both fusion and shrinking processes microscopically. Fusion of excitations is realized as the tensor-product decomposition of their lo-

cal Hilbert spaces, with the coefficients appearing in the resulting direct-sum decomposition defining the fusion rules. Likewise, shrinking rules are obtained from the direct-sum decomposition of the local Hilbert space after the shrinking process.

We compute all fusion and shrinking rules for the three-dimensional \mathbb{D}_3 and \mathbb{D}_4 quantum double models and show that the \mathbb{D}_4 model exhibits fusion and shrinking structures identical to those of the (3+1)D BF field theory with an AAB twist and gauge group $G = (\mathbb{Z}_2)^3$. This establishes the \mathbb{D}_4 quantum double model as a concrete microscopic construction of this continuum topological field theory, which was originally introduced in connection with Borromean-rings braiding [42].

Our explicit lattice construction further allows deterministic control over non-Abelian shrinking processes: by selecting the internal degrees of freedom of non-Abelian loop operators, specific shrinking channels can be selectively realized. Moreover, by analyzing the complete fusion and shrinking tables of the quantum double model, we verify that shrinking rules are fully consistent with fusion rules—namely, performing fusion followed by shrinking yields the same outcome as shrinking first and then fusing. This fusion–shrinking consistency condition, previously derived within continuum field-theoretical analyses [69, 77, 78], has been successfully demonstrated microscopically on the lattice.

Finally, the coexistence and compatibility of fusion and shrinking rules naturally underpin the diagrammatic framework developed in Ref. [78], in which fusion and shrinking processes are represented diagrammatically and constrained by algebraic relations such as fusion pentagon equations and (hierarchical) shrinking–fusion hexagon equations. Our microscopic construction not only confirms the validity of this framework but also provides an explicit microscopic foundation for its abstract structures. These algebraic relations play an essential role in ensuring the anomaly-free nature of higher-dimensional topological orders and may offer a computationally efficient route toward a systematic categorical classification [79–86].

B. Outlook

Several promising research directions emerge from this work. First, the interplay among braiding, fusion, and shrinking constitutes a more complete set of topological data for characterizing higher-dimensional topological orders. While the present work establishes and verifies the consistency between fusion and shrinking, it remains an open question whether analogous consistency relations also exist when braiding statistics are incorporated, such as multi-loop braiding or particle–loop–loop braiding in the three-dimensional quantum double model or within the Hamiltonian formulation of (3+1)D Dijkgraaf–Witten theory [87, 88]. Constructing combined braiding–fusion–shrinking processes may therefore

reveal deeper topological consistency conditions. Within such an extended framework, a number of directions become accessible, including hole dynamics in topological spin backgrounds [89–94], external-field-induced global phase diagrams [95–97], and parton constructions [98–102].

Building on this perspective, extending the existing diagrammatic framework provides another fruitful avenue. The fusion–shrinking consistency naturally gives rise to a hierarchy of diagrammatic representations [78]. Elementary fusion and shrinking diagrams correspond to vectors in fusion and shrinking spaces, while more complicated diagrams are generated through stacking and tensoring operations. Transformations among diagrams are mediated by unitary F -symbols and Δ -symbols, constrained by the pentagon equations and the (hierarchical) shrinking–fusion hexagon equations. Incorporating braiding into this formalism is expected to generate a richer set of algebraic constraints, potentially shedding light on the deeper categorical structures underlying three-dimensional topological orders.

Motivated by the correspondence between the \mathbb{D}_4 quantum double model and the BF field theory with an AAB twist and gauge group $G = (\mathbb{Z}_2)^3$, we further conjecture that this correspondence originates from an underlying algebraic relationship between the group \mathbb{D}_4 of the quantum double model and the gauge group $(\mathbb{Z}_2)^3$ of the BF field theory. Specifically, the AAB twist involves two 1-form gauge fields A and one 2-form gauge field B , which naturally correspond to a $(\mathbb{Z}_2)^2$ subgroup and a \mathbb{Z}_2 subgroup, respectively. A potential connection to the group \mathbb{D}_4 arises through a nontrivial central extension,

$$1 \rightarrow \mathbb{Z}_2 \rightarrow \mathbb{D}_4 \rightarrow (\mathbb{Z}_2)^2 \rightarrow 1. \quad (182)$$

This perspective may provide guidance for identifying microscopic counterparts of BF field theories with an AAB twist and more general gauge groups $\mathbb{Z}_{N_1} \times \mathbb{Z}_{N_2} \times \mathbb{Z}_{N_3}$. In particular, an important open question is the identification of corresponding lattice models for such generalized $BF+AAB$ field theories.

Another important direction is to deepen our understanding of generalized symmetries [103–111] in microscopic constructions of three-dimensional topological orders. Invertible and non-invertible 1-form and 2-form symmetries encode essential information about the algebraic structure of topological orders, their boundary theories, and their phase transitions. As a first step, we have initiated investigations of generalized symmetries in a three-dimensional non-Abelian topological order from the continuum field-theoretical perspective [112]. Future work includes constructing generalized symmetry operators directly on the lattice, with careful attention to onsite realizability and higher-form anomaly constraints [113, 114].

As all topological orders considered in this work are bosonic, an important future direction is the microscopic construction of three-dimensional topological orders with fermions. Such phases can be described by BF theories

with a BB twist [40, 44, 59, 60]. More generally, one can systematically construct and classify fermionic topological orders through gauging fermionic SPT phases [115–125]. Bridging microscopic constructions and continuum field theory in the presence of fermionic degrees of freedom is an important challenge and is expected to extend the diagrammatic framework of higher-dimensional topological orders [78] to include fermionic structures. Recent work has shown that thermal states of the three-dimensional fermionic toric code remain long-range entangled below a finite temperature [126]. Such finite-temperature topological order in fewer than four spatial dimensions originates from anomalous two-form symmetries associated with emergent fermionic particle excitations, and further exploration of these phenomena in both microscopic models and field-theoretical descriptions is promising.

Like topological order, fracton ordered phases exhibit long-range entanglement; however, they are non-liquid states that require unconventional continuum field theories for their description. Given the framework established in this work for 3d topological orders, an intriguing future direction would be to investigate the correspondence between microscopic lattice models and the continuum field theories of fracton order [12–16, 127–129].

Finally, these theoretical advances naturally point toward the prospect of topological quantum computation in three dimensions. In two dimensions, the creation and manipulation of anyons underpin topological quantum computation, and recent experiments on programmable quantum processors based on trapped ions and superconducting qubits have demonstrated the preparation of non-Abelian topologically ordered states together with controlled anyon fusion and braiding [130–134]. Recent progress using sequential quantum circuits [133, 135–141] has further enabled concrete protocols for implementing ribbon operators of non-Abelian anyons [142], providing a pathway toward universal topological quantum computation in two-dimensional quantum double models [143]. Extending these ideas to three dimensions, one may envision designing quantum circuits or higher-order cellular automata [144, 145] to create, braid, fuse, and shrink loop and membrane excitations, thereby exploring the computational power encoded in their non-Abelian fusion and shrinking dynamics.

ACKNOWLEDGMENTS

This work was in part supported by National Natural Science Foundation of China (NSFC) under Grants No. 12474149 and No. 12274250, Research Center for Magnetoelectric Physics of Guangdong Province under Grant No. 2024B0303390001, and Guangdong Provincial Key Laboratory of Magnetoelectric Physics and Devices under Grant No. 2022B1212010008.

Appendix A: Diagrammatics, pentagon and hexagon equations

In this appendix, we introduce unitary F - and Δ -symbols to transform diagrams. They satisfy a series of stringent algebraic equations known as the pentagon equation and the shrinking-fusion hexagon equation [78]. Any violation of these equations indicates quantum anomaly in 3d topological orders.

In Sec. II B, we illustrate how to construct more complicated diagrams by stacking basic diagrams. Besides Fig. 3, we can also construct the diagram that describes the fusion of three excitations as shown in Fig. 17. The difference between the diagrams shown in Figs. 3 and 17 is the order of the fusion process. Physically, fusion rules satisfy associativity, i.e., fusing b and c first should give the same final output as fusing a and b first. Therefore, the diagram shown in Fig. 17 also represents a set of basis vectors that span the same space V_d^{abc} . The two different bases represented by Fig. 3 and Fig. 17 can be transformed to each other by a unitary matrix known as the F -symbol, which is defined in Fig. 18. We can express the equation in Fig. 18 as:

$$\begin{aligned} & |(a, b); e, \mu\rangle \otimes |e, c; d, \nu\rangle \\ &= \sum_{f, \lambda, \eta} [F_d^{abc}]_{e\mu\nu, f\lambda\eta} |a, f; d, \eta\rangle \otimes |(b, c); f, \lambda\rangle. \end{aligned} \quad (\text{A1})$$

The summation over f exhausts all excitations in the set Φ_0^{3+1} , $\lambda = \{1, 2, \dots, N_f^{bc}\}$ and $\eta = \{1, 2, \dots, N_d^{af}\}$. Since the F -symbol is unitary, we have

$$\sum_{f, \lambda, \eta} [F_d^{abc}]_{e\mu\nu, f\lambda\eta} \left([F_d^{abc}]_{e'\mu'\nu', f\lambda\eta} \right)^* = \delta_{ee'} \delta_{\mu\mu'} \delta_{\nu\nu'} \quad (\text{A2})$$

which allow us to implement the inverse transformation. Since the total space V_d^{abc} is isomorphic to $\oplus_f V_d^{af} \otimes V_f^{bc}$ in Fig. 17, the dimension of the total space is given by

$$\dim(V_d^{abc}) = \sum_f N_d^{af} N_f^{bc}. \quad (\text{A3})$$

By comparing Eq. (15) and Eq. (A3), we obtain a constraint on fusion coefficients:

$$\sum_e N_e^{ab} N_d^{ec} = \sum_f N_d^{af} N_f^{bc}. \quad (\text{A4})$$

We employ a similar tensor product approach to construct fusion diagrams that involve more excitations. Applying the F -symbols inside these diagrams leads to a basis transformation. For example, consider fusing four excitations, we have two different ways to transform the far left diagram to the far right diagram as shown in Fig. 19, which gives a very strong algebraic constraint on

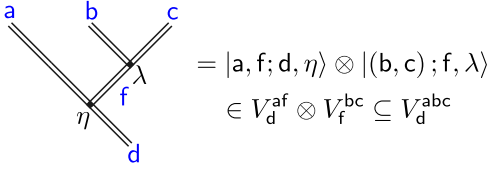


FIG. 17. A different diagram of fusing three excitations in 3d. The associativity of fusion rules guarantees that this diagram describes the same physics as the diagram shown in Fig. 3. The only difference between them is just a change of basis.

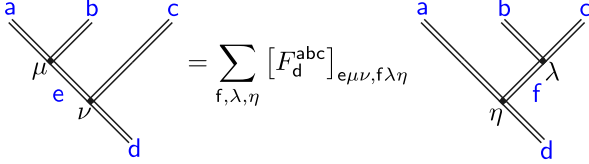


FIG. 18. Definition of the F -symbol in 3d. The left and right diagrams represent different bases for the same space V_d^{abc} , and we use the unitary F -symbol to change the basis. Transforming these diagrams to each other does not change any physics.

the F -symbols, known as the pentagon equation:

$$\begin{aligned} & \sum_{\sigma=1}^{N_e^{fh}} [F_e^{fcd}]_{g\nu\lambda, h\gamma\sigma} [F_e^{abh}]_{f\mu\sigma, i\rho\delta} \\ &= \sum_j \sum_{\omega=1}^{N_g^{aj}} \sum_{\theta=1}^{N_j^{bc}} \sum_{\tau=1}^{N_i^{jd}} [F_g^{abc}]_{f\mu\nu, j\theta\omega} [F_e^{ajd}]_{g\omega\lambda, i\tau\delta} [F_i^{bcd}]_{j\theta\tau, h\gamma\rho}. \end{aligned} \quad (\text{A5})$$

A similar pentagon equation can also be derived in the diagrammatic representations of 2d anyons. Actually, if we draw all previous fusion diagrams in a single-line fashion, our fusion diagrams automatically reduce to 2d anyonic fusion diagrams. Considering fusion diagrams for more excitations does not give any independent constraint beyond the pentagon equation.

Now we construct diagrams that incorporate both fusion and shrinking processes. Consider $\mathcal{S}(a) \otimes \mathcal{S}(b)$ and $\mathcal{S}(a \otimes b)$, their corresponding diagrams are shown in Figs. 4 and 20 respectively. Since we have the consistency condition Eq. (8), these two processes have the same final output and we consider them as different bases in the same space. The diagram in Fig. 4 is defined as $|d, e; c, \lambda\rangle \otimes |b; e, \nu\rangle \otimes |a; d, \mu\rangle$, where different d, e, μ, ν , and λ label different orthogonal vectors. This set of orthogonal vectors spans the space denoted as $V_c^{\mathcal{S}(a) \otimes \mathcal{S}(b)}$, which is isomorphic to $\oplus_{d,e} V_c^{de} \otimes V_e^b \otimes V_d^a$ due to our tensor product construction. Similarly, the diagram shown in Fig. 20 is defined as $|f; c, \gamma\rangle \otimes |a, b; f, \delta\rangle$, where f, δ , and γ label different orthogonal vectors. The corresponding space $V_c^{\mathcal{S}(a \otimes b)} = V_c^{\mathcal{S}(a) \otimes \mathcal{S}(b)}$ is isomorphic to $\oplus_f V_c^f \otimes V_f^{ab}$,

which recovers the constraint in Eq. (12):

$$\begin{aligned} \dim \left(V_c^{\mathcal{S}(a) \otimes \mathcal{S}(b)} \right) &= \dim \left(V_c^{\mathcal{S}(a \otimes b)} \right) \\ &= \sum_{d,e} N_c^{de} S_e^b S_d^a = \sum_f S_c^f N_f^{ab}. \end{aligned} \quad (\text{A6})$$

The two sets of vectors shown in Fig. 20 correspond to two different bases of the total space $V_c^{\mathcal{S}(a) \otimes \mathcal{S}(b)} = V_c^{\mathcal{S}(a \otimes b)}$. We expect that these two bases can transform to each other by a unitary matrix, called the Δ -symbol. The definition of the Δ -symbol is shown in Fig. 21. We explicitly write down the transformations in Fig. 21 as:

$$\begin{aligned} & |d, e; c, \lambda\rangle \otimes |b; e, \nu\rangle \otimes |a; d, \mu\rangle \\ &= \sum_{f, \delta, \gamma} [\Delta_c^{ab}]_{de\mu\nu\lambda, f\delta\gamma} |f; c, \gamma\rangle \otimes |a, b; f, \delta\rangle, \\ & |f; c, \gamma\rangle \otimes |a, b; f, \delta\rangle \\ &= \sum_{\substack{d, e, \\ \mu, \nu, \lambda}} \left([\Delta_c^{ab}]_{de\mu\nu\lambda, f\delta\gamma} \right)^* |d, e; c, \lambda\rangle \otimes |b; e, \nu\rangle \otimes |a; d, \mu\rangle. \end{aligned} \quad (\text{A7})$$

(A8)

Unitarity of the Δ -symbol demands:

$$\begin{aligned} & \sum_{f, \delta, \gamma} [\Delta_c^{ab}]_{de\mu\nu\lambda, f\delta\gamma} \left([\Delta_c^{ab}]_{d'e'\mu'\nu'\lambda', f\delta\gamma} \right)^* \\ &= \delta_{dd'} \delta_{ee'} \delta_{\mu\mu'} \delta_{\nu\nu'} \delta_{\lambda\lambda'}, \end{aligned} \quad (\text{A9})$$

$$\begin{aligned} & \sum_{\substack{d, e, \\ \mu, \nu, \lambda}} [\Delta_c^{ab}]_{de\mu\nu\lambda, f\delta\gamma} \left([\Delta_c^{ab}]_{de\mu\nu\lambda, f'\delta'\gamma'} \right)^* \\ &= \delta_{ff'} \delta_{\delta\delta'} \delta_{\gamma\gamma'}. \end{aligned} \quad (\text{A10})$$

The consistency condition between the fusion and shrinking rules further leads to a strong constraint on both F -symbols and Δ -symbols called the shrinking-fusion hexagon equation. Consider three excitations going through fusion and shrinking processes as shown in Fig. 22. By applying the F -symbols and Δ -symbols inside of the diagrams, we find two paths to transform the far left diagram to the far right diagram. By comparing the coefficients calculated from the upper and lower paths in Fig. 22, we obtain the shrinking-fusion hexagon equation:

$$\begin{aligned} & \sum_i \sum_{\alpha=1}^{N_i^{fg}} \sum_{\beta=1}^{N_d^{ei}} \sum_{\xi=1}^{S_i^j} [F_d^{efg}]_{h\delta\gamma, i\alpha\beta} [\Delta_i^{bc}]_{fg\nu\lambda\alpha, j\tau\xi} [\Delta_d^{aj}]_{ei\mu\xi\beta, k\theta\epsilon} \\ &= \sum_t \sum_{\sigma=1}^{N_t^{ab}} \sum_{\rho=1}^{S_h^{tc}} \sum_{\omega=1}^{N_k^{tc}} [\Delta_h^{ab}]_{ef\mu\nu\delta, t\sigma\rho} [\Delta_d^{tc}]_{hg\rho\lambda\gamma, k\omega\epsilon} [F_k^{abc}]_{t\sigma\omega, j\tau\theta}. \end{aligned} \quad (\text{A11})$$

The shrinking-fusion hexagon equation is understood as the consistency relation between F -symbols and Δ -symbols. We can further consider applying F -symbols

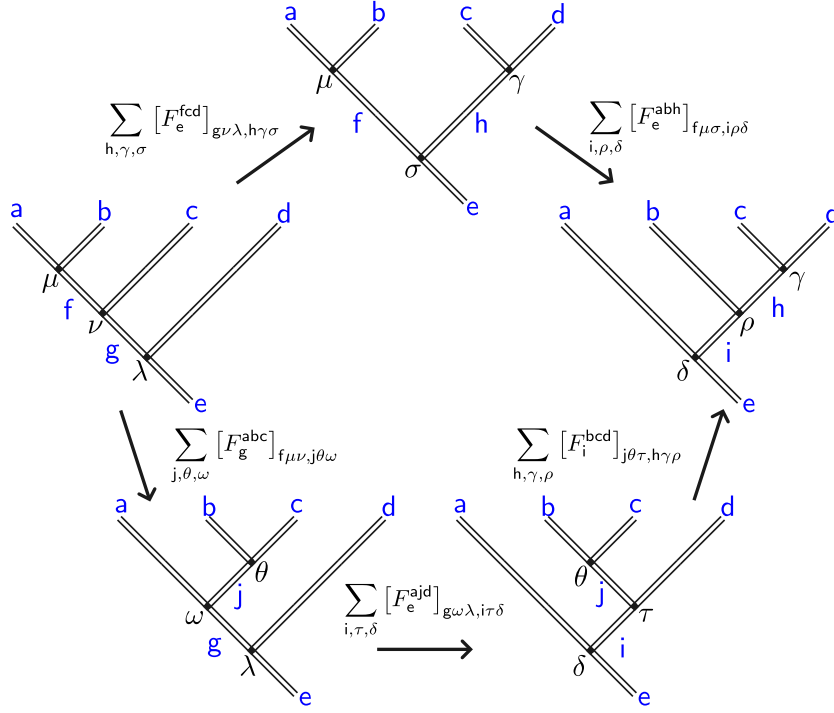


FIG. 19. Diagrammatic representation of the pentagon equation (A5). Starting from the far left diagram, we can go to the far right diagram through either the upper path or the lower path. Comparing these two different paths, we derive the pentagon equation.

$$\begin{array}{c}
 \begin{array}{c} a \\ \parallel \\ \delta \\ \parallel \\ f \\ \parallel \\ \gamma \\ \parallel \\ c \end{array} \begin{array}{c} b \\ \parallel \\ \delta \\ \parallel \\ f \\ \parallel \\ \gamma \\ \parallel \\ c \end{array} \\
 = |f; c, \gamma\rangle \otimes |a, b; f, \delta\rangle \\
 \in V_c^f \otimes V_f^{ab} \subseteq V_c^{\mathcal{S}(a \otimes b)}
 \end{array}$$

FIG. 20. The diagram describing $\mathcal{S}(a \otimes b)$ in 3d. This diagram is constructed by stacking a basic fusion diagram and a basic shrinking diagram. The corresponding vector is obtained by tensor product construction.

and Δ -symbols to transform diagrams that involve more excitations, such as $\mathcal{S}(a) \otimes \mathcal{S}(b) \otimes \mathcal{S}(c) \otimes \mathcal{S}(d)$. However, no more independent equations are obtained from these more complicated diagrams.

Since being able to use the F -symbols and Δ -symbols to change basis indicates the constraints on fusion and shrinking coefficients (i.e., Eq. (12) and Eq. (A4) hold), we conclude that the pentagon Eq. (A5) and shrinking-fusion hexagon Eq. (A11) are stronger constraints. These equations describe not only the behavior of fusion and shrinking coefficients but also the transformations of bases. We conjecture that the pentagon equation and shrinking-fusion hexagon equation are universal for all anomaly-free 3d topological orders. Our construction of the diagrammatics for 3d topological orders can be generalized to higher dimensions, and the details can be found in Ref. [78].

$$\begin{array}{c}
 \begin{array}{c} a \\ \parallel \\ \mu \\ \parallel \\ d \\ \parallel \\ \lambda \\ \parallel \\ c \end{array} \begin{array}{c} b \\ \parallel \\ \nu \\ \parallel \\ e \\ \parallel \\ \chi \\ \parallel \\ c \end{array} \\
 = \sum_{f, \delta, \gamma} [\Delta_c^{ab}]_{de\mu\nu\lambda, f\delta\gamma} \begin{array}{c} a \\ \parallel \\ \delta \\ \parallel \\ f \\ \parallel \\ \gamma \\ \parallel \\ c \end{array} \\
 = \sum_{d, e, \mu, \nu, \lambda} \left([\Delta_c^{ab}]_{de\mu\nu\lambda, f\delta\gamma} \right)^* \begin{array}{c} a \\ \parallel \\ \mu \\ \parallel \\ d \\ \parallel \\ \lambda \\ \parallel \\ c \end{array} \begin{array}{c} b \\ \parallel \\ \nu \\ \parallel \\ e \\ \parallel \\ \chi \\ \parallel \\ c \end{array}
 \end{array}$$

FIG. 21. Definition of the Δ -symbol in 3d. The left diagram and the right diagram describe the same physics in different bases. Similar to the F -symbol, the Δ -symbol is also unitary and we use it to change bases.

Appendix B: Details about basic operators

In this appendix, we provide some technical details about basic operators in Sec. III.

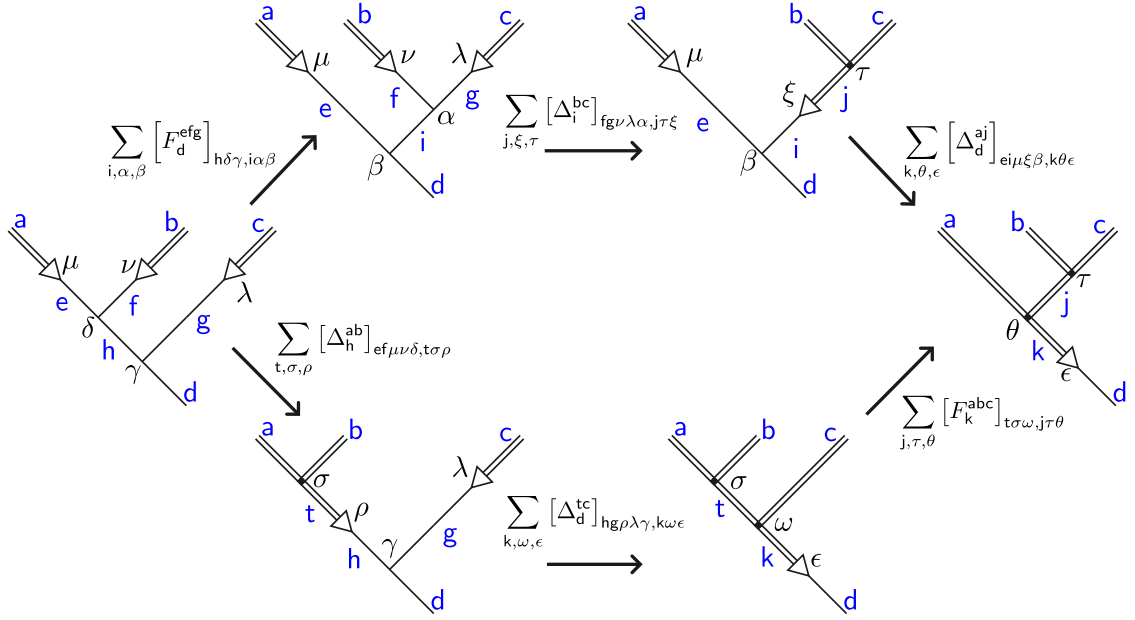


FIG. 22. Diagrammatic representations of the shrinking-fusion hexagon equation (A11). Two different paths can be constructed to transform the far left diagram to the far right diagram. Comparing these two different paths, we obtain the shrinking-fusion hexagon equation.

1. Proof of Eq. (30)

Consider a string $L = L_1 \cup L_2 \cup L_3$, if we connect L_2 and L_3 first, by using Eq. (29), we have

$$T_{L_1 \cup (L_2 \cup L_3)}^g = \sum_h T_{L_2 \cup L_3}^{\bar{h}g} T_{L_1}^h = \sum_{h,m} T_{L_3}^{\bar{m}h\bar{g}} T_{L_2}^m T_{L_1}^h, \quad (\text{B1})$$

where the bracket $(L_2 \cup L_3)$ is introduced to emphasize that L_2 and L_3 are connected first. If we connect L_1 and L_2 first, then we have

$$T_{(L_1 \cup L_2) \cup L_3}^g = \sum_m T_{L_3}^{\bar{m}g} T_{L_1 \cup L_2}^m = \sum_{h,m} T_{L_3}^{\bar{m}g} T_{L_2}^{\bar{h}m} T_{L_1}^h. \quad (\text{B2})$$

Rewrite $T_{L_3}^{\bar{m}g}$ as $T_{L_3}^{\bar{m}h\bar{g}}$, then replace the sum over m with the sum over $\bar{h}m$, we have

$$\begin{aligned} T_{(L_1 \cup L_2) \cup L_3}^g &= \sum_h \sum_{\bar{h}m} T_{L_3}^{\overline{(\bar{h}m)}\bar{h}g} T_{L_2}^{(\bar{h}m)} T_{L_1}^h \\ &= \sum_{h,m'} T_{L_3}^{\bar{m}'\bar{h}g} T_{L_2}^{m'} T_{L_1}^h = T_{L_1 \cup (L_2 \cup L_3)}^g, \end{aligned} \quad (\text{B3})$$

where the second line is obtained by relabeling $\bar{h}m$ as m' . Thus, we conclude that the order of connection is irrelevant.

2. Proof of Eqs. (31), (32) and (33)

Suppose $L = (v_0, v_1, \dots, v_n)$ starts at the vertex v_0 , goes through n edges denoted by $v_i v_{i+1}$ and finally ends at v_n . We set the arrow of $v_i v_{i+1}$ points from v_i to v_{i+1} . Then we write T_L^g as

$$T_L^g = \sum_{h_1, h_2, \dots, h_{n-1}} T_{v_{n-1}v_n}^{\bar{h}_{n-1}g} \dots T_{v_i v_{i+1}}^{\bar{h}_i h_{i+1}} \dots T_{v_1 v_2}^{\bar{h}_1 h_2} T_{v_0 v_1}^{h_1}. \quad (\text{B4})$$

Notice that the vertex operator $A_{v_i}^k$ commutes with all $T_{v_j v_{j+1}}^g$ when $j \neq i-1, i$ because they act on different edges. Since the action of $A_{v_i}^k$ on the edges $v_{i-1}v_i$ and $v_i v_{i+1}$ is given by $L_{v_{i-1}v_i}^k = L_k^-$ and $L_{v_i v_{i+1}}^k = L_k^+$, from Eq. (19) we can see

$$A_{v_i}^k T_{v_i v_{i+1}}^{\bar{h}_i h_{i+1}} = T_{v_i v_{i+1}}^{\bar{h}_i h_{i+1}} A_{v_i}^k, \quad (\text{B5})$$

$$A_{v_i}^k T_{v_{i-1}v_i}^{\bar{h}_{i-1} h_i} = T_{v_{i-1}v_i}^{\bar{h}_{i-1} h_i} A_{v_i}^k. \quad (\text{B6})$$

Thus, we have

$$\begin{aligned}
& A_{v_i}^k T_L^g \\
&= \sum_{\substack{h_1, \dots, h_i, \\ \dots, h_{n-1}}} T_{v_{n-1}v_n}^{\bar{h}_{n-1}g} \dots A_{v_i}^k T_{v_i v_{i+1}}^{\bar{h}_i h_{i+1}} T_{v_{i-1}v_i}^{\bar{h}_{i-1} h_i} \dots T_{v_0 v_1}^{h_1} \\
&= \sum_{\substack{h_1, \dots, h_i, \\ \dots, h_{n-1}}} T_{v_{n-1}v_n}^{\bar{h}_{n-1}g} \dots T_{v_i v_{i+1}}^{k \bar{h}_i h_{i+1}} T_{v_{i-1}v_i}^{\bar{h}_{i-1} h_i \bar{k}} A_{v_i}^k \dots T_{v_0 v_1}^{h_1} \\
&= \left[\sum_{\substack{h_1, \dots, (h_i \bar{k}), \\ \dots, h_{n-1}}} T_{v_{n-1}v_n}^{\bar{h}_{n-1}g} \dots T_{v_i v_{i+1}}^{k \bar{h}_i h_{i+1}} T_{v_{i-1}v_i}^{\bar{h}_{i-1} h_i \bar{k}} \dots T_{v_0 v_1}^{h_1} \right] A_{v_i}^k \\
&= T_L^g A_{v_i}^k, \tag{B7}
\end{aligned}$$

where $i \neq 0, n$. When $i = 0$ or $i = n$, similar to Eq. (B6), we obtain

$$A_{v_0}^k T_{v_0 v_1}^{h_1} = T_{v_0 v_1}^{k h_1} A_{v_0}^k, \tag{B8}$$

$$A_{v_n}^k T_{v_{n-1} v_n}^{\bar{h}_{n-1} g} = T_{v_{n-1} v_n}^{\bar{h}_{n-1} g \bar{k}} A_{v_n}^k. \tag{B9}$$

Thus, we have

$$\begin{aligned}
& A_{v_0}^k T_L^g \\
&= \sum_{\substack{h_1, \dots, h_j, \\ \dots, h_{n-1}}} T_{v_{n-1}v_n}^{\bar{h}_{n-1}g} \dots T_{v_1 v_2}^{\bar{h}_1 h_2} A_{v_0}^k T_{v_0 v_1}^{h_1} \\
&= \sum_{\substack{h_1, \dots, h_j, \\ \dots, h_{n-1}}} T_{v_{n-1}v_n}^{\bar{h}_{n-1}g} \dots T_{v_1 v_2}^{\bar{h}_1 h_2} T_{v_i v_{i+1}}^{k h_1} A_{v_0}^k \\
&= \left[\sum_{\substack{(k h_1), \dots, (k h_j), \\ \dots, (k h_{n-1})}} T_{v_{n-1}v_n}^{\bar{k} h_{n-1} k g} \dots T_{v_i v_{i+1}}^{\bar{k} h_i k h_{i+1}} \dots T_{v_0 v_1}^{k h_1} \right] A_{v_0}^k \\
&= T_L^{k g} A_{v_0}^k, \tag{B10}
\end{aligned}$$

and

$$\begin{aligned}
A_{v_n}^k T_L^g &= \sum_{h_1, \dots, h_j, \dots, h_{n-1}} A_{v_n}^k T_{v_{n-1}v_n}^{\bar{h}_{n-1}g} \dots T_{v_0 v_1}^{h_1} \\
&= \sum_{h_1, \dots, h_j, \dots, h_{n-1}} T_{v_{n-1}v_n}^{\bar{h}_{n-1}g \bar{k}} \dots T_{v_0 v_1}^{h_1} A_{v_n}^k \\
&= T_L^{g \bar{k}} A_{v_n}^k. \tag{B11}
\end{aligned}$$

Since the vertex term $A_v = \frac{1}{|G|} \sum_k A_v^k$, we conclude that T_L^g does not commute with A_{v_0} and A_{v_n} :

$$A_{v_0} T_L^g = \frac{1}{|G|} \sum_k A_{v_0}^k T_L^g = \frac{1}{|G|} \sum_k T_L^{k g} A_{v_0}^k \neq T_L^g A_{v_0}, \tag{B12}$$

$$A_{v_n} T_L^g = \frac{1}{|G|} \sum_k A_{v_n}^k T_L^g = \frac{1}{|G|} \sum_k T_L^{g \bar{k}} A_{v_n}^k \neq T_L^g A_{v_n}. \tag{B13}$$

3. Proof of Eqs. (37), (38) and (39)

We consider Eq. (37) first. Using Eq. (34), we have

$$\begin{aligned}
A_{v=\partial_0 L}^g |R; i, j\rangle &= A_{v=\partial_0 L}^g W_L(R; i, j) |\text{GS}\rangle \\
&= A_{v=\partial_0 L}^g \sum_{h \in G} \Gamma_{ij}^{R^*}(h) T_L^h |\text{GS}\rangle. \tag{B14}
\end{aligned}$$

Notice Eq. (32), we obtain

$$\begin{aligned}
A_{v=\partial_0 L}^g |R; i, j\rangle &= \sum_{h \in G} \Gamma_{ij}^{R^*}(h) T_L^{gh} A_{v=\partial_0 L}^g |\text{GS}\rangle \\
&= \sum_{h \in G} \Gamma_{ij}^{R^*}(h) T_L^{gh} |\text{GS}\rangle, \tag{B15}
\end{aligned}$$

where we absorb the $A_{v=\partial_0 L}^g$ into the ground state in the last step. By writing the matrix element $\Gamma_{ij}^{R^*}(g)$ as $\sum_k \Gamma_{ik}^{R^*}(\bar{g}) \Gamma_{kj}^{R^*}(gh)$, we can finally prove Eq. (37):

$$\begin{aligned}
A_{v=\partial_0 L}^g |R; i, j\rangle &= \sum_k \Gamma_{ik}^{R^*}(\bar{g}) \sum_{h \in G} \Gamma_{kj}^{R^*}(gh) T_L^{gh} |\text{GS}\rangle \\
&= \sum_k \Gamma_{ik}^{R^*}(\bar{g}) W_L(R; k, j) |\text{GS}\rangle \\
&= \sum_k \Gamma_{ki}^R(g) |R; k, j\rangle, \tag{B16}
\end{aligned}$$

where we have used $\Gamma_{ik}^{R^*}(\bar{g}) = \Gamma_{ki}^R(g)$. Similarly, we prove Eq. (38) as follows:

$$\begin{aligned}
A_{v=\partial_1 L}^g |R; i, j\rangle &= A_{v=\partial_1 L}^g \sum_{h \in G} \Gamma_{ij}^{R^*}(h) T_L^h |\text{GS}\rangle \\
&= \sum_{h \in G} \Gamma_{ij}^{R^*}(h) T_L^{h \bar{g}} A_{v=\partial_1 L}^g |\text{GS}\rangle \\
&= \sum_k \sum_{h \in G} \Gamma_{kj}^{R^*}(g) \Gamma_{ik}^{R^*}(h \bar{g}) T_L^{h \bar{g}} |\text{GS}\rangle \\
&= \sum_k \Gamma_{kj}^{R^*}(g) W_L(R; i, k) |\text{GS}\rangle \\
&= \sum_k \Gamma_{kj}^{R^*}(g) |R; i, k\rangle. \tag{B17}
\end{aligned}$$

As for Eq. (39), notice that the plaquette operator $B_{p,s}^h$ is a projector, while the T_L^h term does not change any group element. Thus, the plaquette operator $B_{p,s}^h$ automatically commutes with the string operator $W_L(R; i, j)$ for all (p, s) . We can directly absorb the plaquette operator $B_{p,s}^h$ into the ground state and have

$$\begin{aligned}
B_{p,s}^h |R; i, j\rangle &= B_{p,s}^h W_L(R; i, j) |\text{GS}\rangle \\
&= W_L(R; i, j) \delta_{h,e} |\text{GS}\rangle \\
&= \delta_{h,e} |R; i, j\rangle. \tag{B18}
\end{aligned}$$

4. Proof of Eq. (40)

Consider

$$\begin{aligned}
& \sum_k W_{L_2}(R; k, j) W_{L_1}(R; i, k) \\
&= \sum_k \sum_{g, h \in G} \Gamma_{kj}^{R^*}(h) T_{L_2}^h \Gamma_{ik}^{R^*}(g) T_{L_1}^g \\
&= \sum_{g, h} \Gamma_{ij}^{R^*}(gh) T_{L_2}^h T_{L_1}^g \\
&= \sum_m \sum_g \Gamma_{ij}^{R^*}(m) T_{L_2}^{\bar{g}m} T_{L_1}^g. \tag{B19}
\end{aligned}$$

By using Eq. (29), we have

$$\begin{aligned}
\sum_m \sum_g \Gamma_{ij}^{R^*}(m) T_{L_2}^{\bar{g}m} T_{L_1}^g &= \sum_m \Gamma_{ij}^{R^*}(m) T_{L_1 \cup L_2}^m \\
&= W_{L=L_1 \cup L_2}(R; i, j). \tag{B20}
\end{aligned}$$

Thus, we obtain the connecting rule of $W_{L=L_1 \cup L_2}(R; i, j)$:

$$W_{L=L_1 \cup L_2}(R; i, j) = \sum_k W_{L_2}(R; k, j) W_{L_1}(R; i, k). \tag{B21}$$

5. The commutation relations between B_p and L_M^c

When p lives in the bulk of the membrane M , we have $[B_p, L_M^c] = 0$. For simplicity, we consider the plaquette $v_0 v_1 v_1' v_0'$ shown in Fig. 12. Suppose the edges $v_0 v_0'$, $v_0 v_1$, and $v_1 v_1'$ are assigned with group elements g_1 , g_2 , and g_3 respectively, then we label this configuration as $|g_1, g_2, g_3\rangle$. Before the action of the operator $L_{M_2}^h$, the ordered product on the path $v_0' v_0 v_1 v_1'$ is $\bar{g}_1 g_2 g_3$. After the action of the operator $L_{M_2}^h$, the configuration becomes

$$\begin{aligned}
L_{M_2}^h |g_1, g_2, g_3\rangle &= \sum_{g_0} L_{v_1 v_1'}^{\bar{g}_0 h g_0} T_{v_0 v_1}^{g_0} L_{v_0 v_0'}^h |g_1, g_2, g_3\rangle \\
&= \sum_{g_0} \delta_{g_0, g_2} |h g_1, g_0, \bar{g}_0 h g_0 g_3\rangle \\
&= |h g_1, g_2, \bar{g}_2 h g_2 g_3\rangle. \tag{B22}
\end{aligned}$$

Now, the ordered product becomes

$$\overline{h g_1 g_2 \bar{g}_2 h g_2 g_3} = \bar{g}_1 \bar{h} g_2 \bar{g}_2 h g_2 g_3 = \bar{g}_1 g_2 g_3. \tag{B23}$$

Since the operator $L_{M_2}^h$ does not change the ordered product on the path $v_0' v_0 v_1 v_1'$, it automatically commutes with the plaquette term $B_{p=v_0 v_1 v_1' v_0'}$. For an arbitrary plaquette p living in the bulk of a membrane M , we can similarly prove that $[B_p, L_M^c] = 0$.

6. The commutation relations between A_v and L_M^c

When $v \neq v_0$ and $c \notin Z(G)$, where L_M^c is constructed by acting L_c^\pm on $v_0 v_0'$ first, we have $[A_v, L_M^c] = 0$. From Eq. (45), we can see that any L_M^c has the form of

$$L_M^c = \sum \cdots \left(\sum_g L_{vv'}^{\bar{g}cg} T_{v_0 v}^g \right) \cdots L_{v_0 v_0'}^c, \tag{B24}$$

where \cdots represents some terms that commute with A_v^h because they do not act on edges that contain vertex v . $T_{v_0 v}^g$ acts on an arbitrary string with endpoints denoted by v_0 and v . Thus, we only need to consider the term $\sum_g L_{vv'}^{\bar{g}cg} T_{v_0 v}^g$. Denote an arbitrary state on the edge vv' by $|k\rangle$ and consider the arrow of vv' points from v to v' , we have

$$L_{vv'}^c A_v^h |k\rangle = |chk\rangle = |h\bar{h}chk\rangle = A_v^h L_{vv'}^{\bar{h}ch} |k\rangle, \tag{B25}$$

$$L_{vv'}^c A_v^h |k\rangle = |ck\bar{h}\rangle = A_v^h L_{vv'}^c |k\rangle. \tag{B26}$$

Thus, we conclude that $L_{vv'}^c A_v^h = A_v^h L_{vv'}^{\bar{h}ch}$ and $[L_{vv'}^c, A_v^h] = 0$, where v lives on the direct part of the membrane M . By using Eq. (33), we verify that A_v^h commutes with $\sum_g L_{vv'}^{\bar{g}cg} T_{v_0 v}^g$ as follows:

$$\begin{aligned}
& \sum_{g \in G} L_{vv'}^{\bar{g}cg} T_{v_0 v}^g A_v^h \\
&= \sum_{g \in G} L_{vv'}^{\bar{g}cg} A_v^h T_{v_0 v}^{gh} \\
&= A_v^h \sum_{g \in G} L_{vv'}^{\bar{h}\bar{g}cgh} T_{v_0 v}^{gh} \\
&= A_v^h \sum_{gh \in G} L_{vv'}^{\bar{h}\bar{g}cgh} T_{v_0 v}^{gh} \\
&= A_v^h \sum_{m \in G} L_{vv'}^{\bar{m}cm} T_{v_0 v}^m. \tag{B27}
\end{aligned}$$

Thus, we have $[A_v, L_M^c] = 0$, where $v \neq v_0$.

7. Proof of Eqs. (52), (53), (54) and (55)

First, we consider that when $v_0 v$ in Eq. (B24) is an edge, the L_M^c can be written as

$$L_M^c = \sum \cdots \left(\sum_{g_0} L_{vv'}^{\bar{g}_0 c g_0} T_{v_0 v}^{g_0} \right) L_{v_0 v_0'}^c. \tag{B28}$$

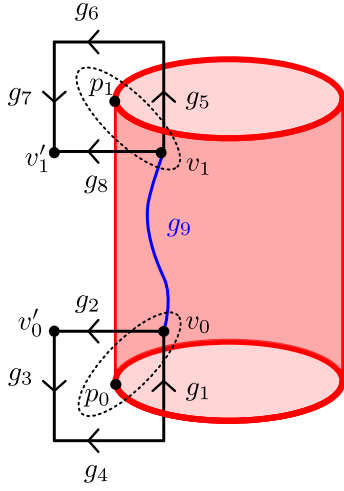


FIG. 23. Two sites $s_0 = (v_0, p_0)$ and $s_1 = (v_1, p_1)$ on the boundaries of M . $v_0 v_1$ denotes a string that starts and ends at v_0 and v_1 . The ordered product of elements along this string is labeled by g_9 .

By using Eq. (32) and $A_{v_0}^g L_{v_0 v_0'}^c = L_{v_0 v_0'}^{g c \bar{g}} A_{v_0}^g$, we have

$$\begin{aligned}
A_{v_0}^g L_M^c &= \sum \dots \left(\sum_{g_0} L_{v v'}^{\bar{g}_0 c g_0} A_{v_0}^g T_{v_0 v}^{g_0} \right) L_{v_0 v_0'}^c \\
&= \sum \dots \left(\sum_{g_0} L_{v v'}^{\bar{g}_0 c g_0} T_{v_0 v}^{g_0} \right) L_{v_0 v_0'}^{g c \bar{g}} A_{v_0}^g \\
&= \left[\sum \dots \left(\sum_{g_0} L_{v v'}^{\bar{g}_0 \bar{g} g c \bar{g} g_0} T_{v_0 v}^{g_0} \right) L_{v_0 v_0'}^{g c \bar{g}} \right] A_{v_0}^g \\
&= L_M^{g c \bar{g}} A_{v_0}^g. \tag{B29}
\end{aligned}$$

As shown in Fig. 23, we consider a cylindrical membrane M and construct the operator L_M^c as

$$L_M^c = \sum \left(\sum_{g_0} L_{v_1 v_1'}^{\bar{g}_0 c g_0} T_{v_0 v_1}^{g_0} \right) \dots L_{v_0 v_0'}^c, \tag{B30}$$

where the plaquette p_0 (p_1) and the vertex v_0 (v_1) form a site s_0 (s_1). Before we act the operator L_M^c , an arbitrary configuration on plaquettes p_0 is labeled by $|g_1, g_2, g_3, g_4\rangle$, an arbitrary configuration on plaquettes p_1 and the ordered product on the string with endpoints v_0 and v_1 are labeled by $|g_5, g_6, g_7, g_8, g_9\rangle$. Since L_M^c acts on $|g_1, g_2, g_3, g_4\rangle$ as $L_{v_0 v_0'}^c$, we consider acting B_{p_0, s_0}^h and L_M^c on $|g_1, g_2, g_3, g_4\rangle$ as

$$\begin{aligned}
B_{p_0, s_0}^h L_M^c |g_1, g_2, g_3, g_4\rangle &= B_{p_0, s_0}^h L_{v_0 v_0'}^c |g_1, g_2, g_3, g_4\rangle \\
&= B_{p_0, s_0}^h |g_1, c g_2, g_3, g_4\rangle \\
&= \delta_{h, c g_2 g_3 \bar{g}_4 g_1} |g_1, c g_2, g_3, g_4\rangle. \tag{B31}
\end{aligned}$$

Notice that

$$\begin{aligned}
L_M^c B_{p_0, s_0}^{c h} |g_1, g_2, g_3, g_4\rangle &= L_M^c \delta_{c h, g_2 g_3 \bar{g}_4 g_1} |g_1, g_2, g_3, g_4\rangle \\
&= \delta_{c h, g_2 g_3 \bar{g}_4 g_1} L_{v_0 v_0'}^c |g_1, g_2, g_3, g_4\rangle \\
&= \delta_{c h, g_2 g_3 \bar{g}_4 g_1} |g_1, c g_2, g_3, g_4\rangle \\
&= \delta_{h, c g_2 g_3 \bar{g}_4 g_1} |g_1, c g_2, g_3, g_4\rangle, \tag{B32}
\end{aligned}$$

we conclude that

$$B_{p_0, s_0}^h L_M^c = L_M^c B_{p_0, s_0}^{c h}. \tag{B33}$$

Now we consider acting B_{p_1, s_1}^h and $L_M^c T_{v_0 v_1}^g$ on $|g_5, g_6, g_7, g_8, g_9\rangle$. Notice that L_M^c acts on $|g_5, g_6, g_7, g_8, g_9\rangle$ as $\sum_{g_0} L_{v_1 v_1'}^{\bar{g}_0 c g_0} T_{v_0 v_1}^{g_0}$, we have

$$\begin{aligned}
&B_{p_1, s_1}^h L_M^c T_{v_0 v_1}^g |g_5, g_6, g_7, g_8, g_9\rangle \\
&= B_{p_1, s_1}^h \sum_{g_0} L_{v_1 v_1'}^{\bar{g}_0 c g_0} T_{v_0 v_1}^{g_0} T_{v_0 v_1}^g |g_5, g_6, g_7, g_8, g_9\rangle \\
&= B_{p_1, s_1}^h \sum_{g_0} \delta_{g_0, g_9} \delta_{g_9, g} |g_5, g_6, g_7, \bar{g}_0 c g_0 g_8, g_0\rangle \\
&= \delta_{g_9, g} B_{p_1, s_1}^h |g_5, g_6, g_7, \bar{g}_9 c g_9 g_8, g_9\rangle \\
&= \delta_{g_9, g} \delta_{h, g_5 g_6 g_7 \bar{g}_9 c g_9 g_8} |g_5, g_6, g_7, \bar{g}_9 c g_9 g_8, g_9\rangle. \tag{B34}
\end{aligned}$$

Since

$$\begin{aligned}
&L_M^c T_{v_0 v_1}^g B_{p_1, s_1}^{h \bar{g} c g} |g_5, g_6, g_7, g_8, g_9\rangle \\
&= L_M^c \delta_{g_9, g} \delta_{h \bar{g} c g, g_5 g_6 g_7 \bar{g}_8} |g_5, g_6, g_7, g_8, g_9\rangle \\
&= \delta_{g_9, g} \delta_{h \bar{g} c g, g_5 g_6 g_7 \bar{g}_8} \sum_{g_0} L_{v_1 v_1'}^{\bar{g}_0 c g_0} T_{v_0 v_1}^{g_0} |g_5, g_6, g_7, g_8, g_9\rangle \\
&= \delta_{g_9, g} \delta_{h \bar{g} c g, g_5 g_6 g_7 \bar{g}_8} |g_5, g_6, g_7, \bar{g}_9 c g_9 g_8, g_9\rangle \\
&= \delta_{g_9, g} \delta_{h, g_5 g_6 g_7 \bar{g}_9 c g_9 g_8} |g_5, g_6, g_7, \bar{g}_9 c g_9 g_8, g_9\rangle, \tag{B35}
\end{aligned}$$

we conclude that

$$B_{p_1, s_1}^h L_M^c T_{v_0 v_1}^g = L_M^c T_{v_0 v_1}^g B_{p_1, s_1}^{h \bar{g} c g}. \tag{B36}$$

By using Eqs. (32) and (B29), we prove Eq. (52) as follows:

$$\begin{aligned}
&A_{v_0}^g W_M(C, R; c, j; c', j') |GS\rangle \\
&= \sum_{h \in Z_r} \Gamma_{j j'}^{R*}(h) A_{v_0}^g L_M^c T_P^{g c h \bar{q} c'} |GS\rangle \\
&= \sum_{h \in Z_r} \Gamma_{j j'}^{R*}(h) L_M^{g c \bar{g}} T_P^{g q c h \bar{q} c'} A_{v_0}^g |GS\rangle \\
&= \sum_{h \in Z_r} \Gamma_{j j'}^{R*}(h) L_M^{g c \bar{g}} T_P^{g q c h \bar{q} c'} |GS\rangle. \tag{B37}
\end{aligned}$$

We prove that for any $g \in G$, $\bar{q}_g c \bar{g} g q_c \in Z_r$ in Eq. (C10). Since $h \in Z_r$, we have $\bar{q}_g c \bar{g} g q_c h \in Z_r$. By writing $T_P^{g q c h \bar{q} c'}$ as $T_P^{q_g c \bar{g} \bar{q}_g c \bar{g} g q_c h \bar{q} c'}$ and expanding $\Gamma_{j j'}^{R*}(h)$ as

$$\Gamma_{j j'}^{R*}(h) = \sum_i \Gamma_{j i}^{R*}(\bar{q}_c \bar{g} g q_c \bar{g}) \Gamma_{i j'}^{R*}(\bar{q}_g c \bar{g} g q_c h), \tag{B38}$$

we have

$$\begin{aligned}
& \sum_{h \in Z_r} \Gamma_{jj'}^{R*}(h) L_M^{gc\bar{g}} T_P^{gq_c h \bar{q}_{c'}} |GS\rangle \\
&= \sum_{h \in Z_r} \sum_i \Gamma_{ji}^{R*}(\bar{q}_c \bar{g} q_{gc} \bar{g}) \Gamma_{ij'}^{R*}(\bar{q}_{gc} \bar{g} g q_c h) \\
&\quad \times L_M^{gc\bar{g}} T_P^{q_{gc} \bar{g} \bar{q}_{gc} g q_c h \bar{q}_{c'}} |GS\rangle \\
&= \sum_i \Gamma_{ji}^{R*}(\bar{q}_c \bar{g} q_{gc} \bar{g}) \sum_{h' \in Z_r} \Gamma_{ij'}^{R*}(h') L_M^{gc\bar{g}} T_P^{q_{gc} \bar{g} h' \bar{q}_{c'}} |GS\rangle \\
&= \sum_i \Gamma_{ji}^{R*}(\bar{q}_c \bar{g} q_{gc} \bar{g}) W_M(C, R; gc\bar{g}, i; c', j') |GS\rangle, \quad (B39)
\end{aligned}$$

where h' is defined as $\bar{q}_{gc} \bar{g} g q_c h$. Notice that $\Gamma_{ji}^{R*}(\bar{q}_c \bar{g} q_{gc} \bar{g}) = \Gamma_{ij}^R(\bar{q}_{gc} \bar{g} g q_c)$, we obtain

$$\begin{aligned}
& A_{v_0}^g W_M(C, R; c, j; c', j') |GS\rangle \\
&= \sum_i \Gamma_{ij}^R(\bar{q}_{gc} \bar{g} g q_c) W_M(C, R; gc\bar{g}, i; c', j') |GS\rangle. \quad (B40)
\end{aligned}$$

Now, by using Eq. (B33), we prove Eq. (53) as follows:

$$\begin{aligned}
& B_{p_0, s_0}^h W_M(C, R; c, j; c', j') |GS\rangle \\
&= \sum_{g \in Z_r} \Gamma_{jj'}^{R*}(g) B_{p_0, s_0}^h L_M^c T_P^{q_c g \bar{q}_{c'}} |GS\rangle \\
&= \sum_{g \in Z_r} \Gamma_{jj'}^{R*}(g) L_M^c T_P^{q_c g \bar{q}_{c'}} B_{p_0, s_0}^{\bar{h}} |GS\rangle \\
&= \delta_{\bar{c}h, e} \sum_{g \in Z_r} \Gamma_{jj'}^{R*}(g) L_M^c T_P^{q_c g \bar{q}_{c'}} |GS\rangle \\
&= \delta_{c, h} W_M(C, R; c, j; c', j') |GS\rangle. \quad (B41)
\end{aligned}$$

Similarly, we use Eq. (33) to prove Eq. (54):

$$\begin{aligned}
& A_{v_1}^g W_M(C, R; c, j; c', j') |GS\rangle \\
&= \sum_{h \in Z_r} \Gamma_{jj'}^{R*}(h) A_{v_1}^g L_M^c T_P^{q_c h \bar{q}_{c'}} |GS\rangle \\
&= \sum_{h \in Z_r} \Gamma_{jj'}^{R*}(h) L_M^c T_P^{q_c h \bar{q}_{c'}} A_{v_1}^g |GS\rangle \\
&= \sum_{h \in Z_r} \Gamma_{jj'}^{R*}(h) L_M^c T_P^{q_c h \bar{q}_{c'}} |GS\rangle \\
&= \sum_{h \bar{q}_{c'} \bar{g} q_{gc'} \bar{g} \in Z_r} \sum_i \Gamma_{ji}^{R*}(h \bar{q}_{c'} \bar{g} q_{gc'} \bar{g}) \Gamma_{ij'}^{R*}(\bar{q}_{gc'} \bar{g} g q_c) \\
&\quad \times L_M^c T_P^{q_c h \bar{q}_{c'} \bar{g} q_{gc'} \bar{g} \bar{q}_{gc'} \bar{g}} |GS\rangle \\
&= \sum_i \Gamma_{ij'}^{R*}(\bar{q}_{gc'} \bar{g} g q_c) W_M(C, R; c, j; gc'\bar{g}, i) |GS\rangle, \quad (B42)
\end{aligned}$$

As for Eq. (55), we use Eq. (B36) to obtain that

$$\begin{aligned}
& B_{p_1, s_1}^h W_M(C, R; c, j; c', j') |GS\rangle \\
&= \sum_{g \in Z_r} \Gamma_{jj'}^{R*}(g) B_{p_1, s_1}^h L_M^c T_P^{q_c g \bar{q}_{c'}} |GS\rangle \\
&= \sum_{g \in Z_r} \Gamma_{jj'}^{R*}(g) L_M^c T_P^{q_c g \bar{q}_{c'}} B_{p_1, s_1}^{\overline{h q_c g \bar{q}_{c'} c q_c g \bar{q}_{c'}}} |GS\rangle \\
&= \sum_{g \in Z_r} \Gamma_{jj'}^{R*}(g) L_M^c T_P^{q_c g \bar{q}_{c'}} \delta_{\overline{h q_c g \bar{q}_{c'} c q_c g \bar{q}_{c'}, e}} |GS\rangle. \quad (B43)
\end{aligned}$$

Notice $c = q_c r \bar{q}_c$ and $g \in Z_r$, we have

$$\begin{aligned}
\delta_{h q_{c'} \bar{g} \bar{q}_c c q_c g \bar{q}_{c'}, e} &= \delta_{h q_{c'} \bar{g} r g \bar{q}_{c'}, e} \\
&= \delta_{h q_{c'} r \bar{q}_{c'}, e} = \delta_{hc', e}. \quad (B44)
\end{aligned}$$

Thus, we conclude that

$$\begin{aligned}
& B_{p_1, s_1}^h W_M(C, R; c, j; c', j') |GS\rangle \\
&= \delta_{h, \bar{c}'} W_M(C, R; c, j; c', j') |GS\rangle. \quad (B45)
\end{aligned}$$

Appendix C: Irreducible Representations of Quantum Double

The quantum double DG of a finite group G is an algebra with two sets of generators $\{A_g \mid g \in G\}$, $\{B_h \mid h \in G\}$, which satisfy:

$$\begin{aligned}
A_{g_1} A_{g_2} &= A_{g_1 g_2}, \\
B_{h_1} B_{h_2} &= \delta_{h_1, h_2} B_{h_2}, \\
A_g B_h &= B_{g h \bar{g}} A_g. \quad (C1)
\end{aligned}$$

A set of basis of DG is given by $\{D_{(h, g)} = B_h A_g\}$, which satisfies:

$$\begin{aligned}
D_{(h_1, g_1)} D_{(h_2, g_2)} &= B_{h_1} A_{g_1} B_{h_2} A_{g_2} = B_{h_1} B_{g_1 h_2 \bar{g}_1} A_{g_1} A_{g_2} \\
&= \delta_{h_1, g_1 h_2 \bar{g}_1} B_{h_1} A_{g_1 g_2} \\
&= \delta_{h_1, g_1 h_2 \bar{g}_1} D_{(h_1, g_1 g_2)}. \quad (C2)
\end{aligned}$$

The group G can be written as:

$$G = \bigcup_i C_i, \quad (C3)$$

where C_i is a conjugacy class. We can choose a representative r in the class and denote the class by C_r , then we have

$$r \in C_r = \{q_c r \bar{q}_c \mid q_c \in G\}. \quad (C4)$$

Any element $c \in C_r$ can be written as $q_c r \bar{q}_c$, $q_c \in G$. We choose a specific set of q_c and demand that $q_r = e$ when $c = r$. The choices of q_c are not unique, if $c = q_c r \bar{q}_c = q'_c r \bar{q}'_c$, then

$$r = \bar{q}_c q'_c r \bar{q}'_c q_c = (\bar{q}_c q'_c) r \overline{\bar{q}_c q'_c}, \quad (C5)$$

i.e.,

$$\bar{q}_c q'_c \in Z_r, \quad (C6)$$

where Z_r is the centralizer of r . We write $\bar{q}_c q'_c = z \in Z_r$, then

$$q'_c = q_c z \quad \text{for some } z \in Z_r. \quad (C7)$$

That is, for given $c \in C_r$ and r , all q_c that satisfy $c = q_c r \bar{q}_c$ form a coset of G :

$$\{q_c \mid q_c r \bar{q}_c = c \in C_r\} = q_c Z_r. \quad (C8)$$

Thus, we can rewrite the G as:

$$G = \bigcup_{c \in C_r} q_c Z_r, \quad (\text{C9})$$

where r and q_c are preselected.

We prove that for any $g \in G$, $c \in C_r$, we have $\bar{q}_{gc\bar{g}} g q_c \in Z_r$:

$$\begin{aligned} (\bar{q}_{gc\bar{g}} g q_c) r (\overline{\bar{q}_{gc\bar{g}} g q_c}) &= (\bar{q}_{gc\bar{g}} g q_c) r (\bar{q}_c \bar{g} q_{c\bar{g}}) \\ &= \bar{q}_{gc\bar{g}} g c \bar{g} q_{c\bar{g}} = r. \end{aligned} \quad (\text{C10})$$

In the last step, we use:

$$q_c r \bar{q}_c = c \implies r = \bar{q}_c c q_c, \quad \forall q_c \in G, \forall c \in C_r. \quad (\text{C11})$$

Each irrep of DG is labeled by a pair (C, R) , where C is the conjugacy class, R is the irrep of the centralizer Z_r . The corresponding representation space is given by $V^{(C,R)} = \mathbb{C}[C] \otimes V^R$, where $\mathbb{C}[C]$ is an algebra with the basis $\{c \in C\}$ and V^R is the representation space of the irrep R . A set of basis of $V^{(C,R)}$ is given by

$$\{|c\rangle \otimes |j\rangle \mid c \in C, j = 1, \dots, \dim(R)\}. \quad (\text{C12})$$

Denote the irrep of DG as $\Pi^{(C,R)}$, then the action of DG on $V^{(C,R)}$ is given by

$$\Pi^{(C,R)}(B_h) (|c\rangle \otimes |j\rangle) = \delta_{h,c} |c\rangle \otimes |j\rangle, \quad (\text{C13})$$

$$\begin{aligned} \Pi^{(C,R)}(A_g) (|c\rangle \otimes |j\rangle) &= |gc\bar{g}\rangle \otimes R(\bar{q}_{gc\bar{g}} g q_c) |j\rangle \\ &= |gc\bar{g}\rangle \otimes \left[\sum_i \Gamma_{ij}^R (\bar{q}_{gc\bar{g}} g q_c) |i\rangle \right] \\ &= \sum_i \Gamma_{ij}^R (\bar{q}_{gc\bar{g}} g q_c) |gc\bar{g}\rangle \otimes |i\rangle. \end{aligned} \quad (\text{C14})$$

Obviously we have

$$\Pi^{(C,R)}(B_{h_1}) \Pi^{(C,R)}(B_{h_2}) = \delta_{h_1, h_2} \Pi^{(C,R)}(B_{h_2}), \quad (\text{C15})$$

$$\Pi^{(C,R)}(A_g) \Pi^{(C,R)}(B_h) = \Pi^{(C,R)}(B_{gh\bar{g}}) \Pi^{(C,R)}(A_g), \quad (\text{C16})$$

Then we verify that $\Pi^{(C,R)}(A_{g_1}) \Pi^{(C,R)}(A_{g_2}) = \Pi^{(C,R)}(A_{g_1 g_2})$:

$$\begin{aligned} &\Pi^{(C,R)}(A_{g_1}) \Pi^{(C,R)}(A_{g_2}) |c\rangle \otimes |j\rangle \\ &= \Pi^{(C,R)}(A_{g_1}) \left[\sum_i \Gamma_{ij}^R (\bar{q}_{g_2 c \bar{g}_2} g_2 q_c) |g_2 c \bar{g}_2\rangle \otimes |i\rangle \right] \\ &= \sum_i \Gamma_{ij}^R (\bar{q}_{g_2 c \bar{g}_2} g_2 q_c) \sum_k \Gamma_{ki}^R (\bar{q}_{g_1, g_2 c \bar{g}_2 \bar{g}_1} g_1 q_{g_2 c \bar{g}_2}) \\ &\quad \times |g_1 g_2 c \bar{g}_2 \bar{g}_1\rangle \otimes |k\rangle \\ &= \sum_{i,k} \Gamma_{ki}^R (\bar{q}_{g_1 g_2 c \bar{g}_2 \bar{g}_1} g_1 q_{g_2 c \bar{g}_2}) \Gamma_{ij}^R (\bar{q}_{g_2 c \bar{g}_2} g_2 q_c) \\ &\quad \times |g_1 g_2 c \bar{g}_2 \bar{g}_1\rangle \otimes |k\rangle \\ &= \sum_k \Gamma_{kj}^R (\bar{q}_{g_1 g_2 c \bar{g}_2 \bar{g}_1} g_1 q_{g_2 c \bar{g}_2}) |g_1 g_2 c \bar{g}_2 \bar{g}_1\rangle \otimes |k\rangle \\ &= \Pi^{(C,R)}(A_{g_1 g_2}) |c\rangle \otimes |j\rangle. \end{aligned} \quad (\text{C17})$$

Given two irreps and their corresponding representation spaces $(\Pi^{(C_1, R_1)}, V^{(C_1, R_1)})$ and $(\Pi^{(C_2, R_2)}, V^{(C_2, R_2)})$, the tensor product representation and the corresponding representation space $(\Pi^{(C_1, R_1)} \otimes \Pi^{(C_2, R_2)}, V^{(C_1, R_1)} \otimes V^{(C_2, R_2)})$ is constructed by means of the co-multiplication Δ . Explicitly, we define

$$\Delta(D_{(h,g)}) = \sum_{k \in G} D_{(h\bar{k}, g)} \otimes D_{(k, g)}. \quad (\text{C18})$$

Then for $v \in V^{(C_1, R_1)}$ and $w \in V^{(C_2, R_2)}$, the action on $v \otimes w$ is given by

$$\begin{aligned} &\Pi^{(C_1, R_1)} \otimes \Pi^{(C_2, R_2)} (\Delta(D_{(h,g)})) v \otimes w \\ &= \sum_{k \in G} \Pi^{(C_1, R_1)} (D_{(h\bar{k}, g)}) v \otimes \Pi^{(C_2, R_2)} (D_{(k, g)}) w. \end{aligned} \quad (\text{C19})$$

The tensor product representation is generally reducible and can be decomposed as

$$\Pi^{(C_1, R_1)} \otimes \Pi^{(C_2, R_2)} = \bigoplus_{(C_3, R_3)} N_{(C_3, R_3)}^{(C_1, R_1)(C_2, R_2)} \Pi^{(C_3, R_3)}, \quad (\text{C20})$$

where the coefficient is given by

$$\begin{aligned} &N_{(C_3, R_3)}^{(C_1, R_1)(C_2, R_2)} \\ &= \frac{1}{|G|} \sum_{h, g} \text{tr} \left[\Pi^{(C_1, R_1)} \otimes \Pi^{(C_2, R_2)} (\Delta(D_{(h,g)})) \right] \\ &\quad \times \left\{ \text{tr} \left[\Pi^{(C_3, R_3)} (D_{(h,g)}) \right] \right\}^*. \end{aligned} \quad (\text{C21})$$

Appendix D: Details of shrinking rules in \mathbb{D}_3 quantum double model

In this appendix, we provide technical details about computing shrinking rules in the \mathbb{D}_3 quantum double model. For simplicity, we omit C_e for particles, c and j labels when they only have one possible value in the following discussion. For $[C_r, \omega]$, the operators are given by

$$\begin{aligned} W_M(C_r, \omega; r, r) &= \sum_{g \in Z_r} \Gamma^{\omega^*}(g) L_M^r T_P^g \\ &= L_M^r T_P^e + \omega^2 L_M^r T_P^r + \omega L_M^r T_P^{r^2}, \end{aligned} \quad (\text{D1})$$

$$\begin{aligned} W_M(C_r, \omega; r^2, r) &= \sum_{g \in Z_r} \Gamma^{\omega^*}(g) L_M^{r^2} T_P^{tg} \\ &= L_M^{r^2} T_P^t + \omega^2 L_M^{r^2} T_P^{tr} + \omega L_M^{r^2} T_P^{tr^2}, \end{aligned} \quad (\text{D2})$$

where $\omega = \exp\left(\frac{2\pi i}{3}\right)$ and $\omega^* = \omega^2$. Note that only the first degree of freedom, i.e., c in Eq. (51), is related to

the local space $V_{(C,R)}$ on the boundary $\partial_0 M$. Thus, we need to exhaust the first degree of freedom. Here we fix the second degree of freedom as $c' = r$. One can also consider $c' = r^2$, which does not affect the final result. After the shrinking process, we have

$$\begin{aligned} \mathcal{S}(W_M(C_r, \omega; r, r)) &= T_P^e + \omega^2 T_P^r + \omega T_P^{r^2} \\ &= W_P(B; 1, 1), \end{aligned} \quad (\text{D3})$$

$$\begin{aligned} \mathcal{S}(W_M(C_r, \omega; r^2, r)) &= T_P^t + \omega^2 T_P^{tr} + \omega T_P^{tr^2} \\ &= W_P(B; 2, 1), \end{aligned} \quad (\text{D4})$$

where the operators for particle $[B]$ are given by

$$\begin{aligned} W_P(B; 1, 1) &= \sum_{g \in G} \Gamma_{11}^{B*}(g) L_M^e T_P^g \\ &= T_P^e + \omega^2 T_P^r + \omega T_P^{r^2}, \end{aligned} \quad (\text{D5})$$

$$\begin{aligned} W_P(B; 2, 2) &= \sum_{g \in G} \Gamma_{22}^{B*}(g) L_M^e T_P^g \\ &= T_P^e + \omega T_P^r + \omega^2 T_P^{r^2}, \end{aligned} \quad (\text{D6})$$

$$\begin{aligned} W_P(B; 1, 2) &= \sum_{g \in G} \Gamma_{12}^{B*}(g) L_M^e T_P^g \\ &= T_P^t + \omega T_P^{tr} + \omega^2 T_P^{tr^2}, \end{aligned} \quad (\text{D7})$$

$$\begin{aligned} W_P(B; 2, 1) &= \sum_{g \in G} \Gamma_{21}^{B*}(g) L_M^e T_P^g \\ &= T_P^t + \omega^2 T_P^{tr} + \omega T_P^{tr^2}. \end{aligned} \quad (\text{D8})$$

The two operators $W_P(B; 1, 1)$ and $W_P(B; 2, 1)$ are related to the vectors $|1\rangle_{(B)}$ and $|2\rangle_{(B)}$, which span the space $V_{(B)}$. Thus, we have

$$\mathcal{S}(V_{(C_r, \omega)}) = V_{(B)}, \quad (\text{D9})$$

which gives the Abelian shrinking rule

$$\mathcal{S}([C_r, \omega]) = [B]. \quad (\text{D10})$$

For $[C_r, \omega^2]$, we consider

$$\begin{aligned} W_M(C_r, \omega^2; r, r) &= \sum_{g \in Z_r} \Gamma^\omega(g) L_M^r T_P^g \\ &= L_M^r T_P^e + \omega L_M^r T_P^r + \omega^2 L_M^r T_P^{r^2}, \end{aligned} \quad (\text{D11})$$

$$\begin{aligned} W_M(C_r, \omega^2; r^2, r) &= \sum_{g \in Z_r} \Gamma^\omega(g) L_M^{r^2} T_P^{tg} \\ &= L_M^{r^2} T_P^t + \omega L_M^{r^2} T_P^{tr} + \omega^2 L_M^{r^2} T_P^{tr^2}. \end{aligned} \quad (\text{D12})$$

After the shrinking process, we have

$$\begin{aligned} \mathcal{S}(W_M(C_r, \omega^2; r, r)) &= T_P^e + \omega T_P^r + \omega^2 T_P^{r^2} \\ &= W_P(B; 2, 2), \end{aligned} \quad (\text{D13})$$

$$\begin{aligned} \mathcal{S}(W_M(C_r, \omega^2; r^2, r)) &= T_P^t + \omega T_P^{tr} + \omega^2 T_P^{tr^2} \\ &= W_P(B; 1, 2). \end{aligned} \quad (\text{D14})$$

The two operators $W_P(B; 2, 2)$ and $W_P(B; 1, 2)$ are also related to the vectors $|2\rangle_{(B)}$ and $|1\rangle_{(B)}$. Thus, we have

$$\mathcal{S}(V_{(C_r, \omega^2)}) = V_{(B)}, \quad (\text{D15})$$

which leads to the shrinking rule

$$\mathcal{S}([C_r, \omega^2]) = [B]. \quad (\text{D16})$$

For $[C_t, Id]$, consider

$$\begin{aligned} W_M(C_t, Id; t, t) &= \sum_{g \in Z_t} \Gamma^{Id}(g) L_M^t T_P^g \\ &= L_M^t T_P^e + L_M^t T_P^t, \end{aligned} \quad (\text{D17})$$

$$\begin{aligned} W_M(C_t, Id; tr, t) &= \sum_{g \in Z_t} \Gamma^{Id}(g) L_M^{tr} T_P^{rg} \\ &= L_M^{tr} T_P^r + L_M^{tr} T_P^{tr^2}, \end{aligned} \quad (\text{D18})$$

$$\begin{aligned} W_M(C_t, Id; tr^2, t) &= \sum_{g \in Z_t} \Gamma^{Id}(g) L_M^{tr^2} T_P^{r^2g} \\ &= L_M^{tr^2} T_P^{r^2} + L_M^{tr^2} T_P^{tr}. \end{aligned} \quad (\text{D19})$$

After the shrinking process, we have

$$\begin{aligned} \mathcal{S}(W_M(C_t, Id; t, t)) &= T_P^e + T_P^t \\ &= \frac{1}{3} (W_P(B; 1, 1) + W_P(B; 1, 2) + W_P(B; 2, 1) \\ &\quad + W_P(B; 2, 2) + W_P(Id)), \end{aligned} \quad (\text{D20})$$

$$\begin{aligned} \mathcal{S}(W_M(C_t, Id; tr, t)) &= T_P^r + T_P^{tr^2} \\ &= \frac{1}{3} (\omega W_P(B; 1, 1) + \omega W_P(B; 1, 2) + \omega^2 W_P(B; 2, 1) \\ &\quad + \omega^2 W_P(B; 2, 2) + W_P(Id)), \end{aligned} \quad (\text{D21})$$

$$\begin{aligned} \mathcal{S}(W_M(C_t, Id; tr^2, t)) &= T_P^{r^2} + T_P^{tr} \\ &= \frac{1}{3} (\omega^2 W_P(B; 1, 1) + \omega^2 W_P(B; 1, 2) + \omega W_P(B; 2, 1) \\ &\quad + \omega W_P(B; 2, 2) + W_P(Id)). \end{aligned} \quad (\text{D22})$$

Thus, $\mathcal{S}(V_{(C_t, Id)})$ has two invariant subspaces $V_{(Id)}$ and $V_{(B)}$, which leads to the decomposition

$$\mathcal{S}(V_{(C_t, Id)}) = V_{(Id)} \oplus V_{(B)}, \quad (\text{D23})$$

and the shrinking rule

$$\mathcal{S}([C_t, Id]) = [Id] \oplus [B]. \quad (\text{D24})$$

For $[C_t, -]$, consider

$$\begin{aligned} W_M(C_t, -; t, t) &= \sum_{g \in Z_t} \Gamma^{-*}(g) L_M^t T_P^g \\ &= L_M^t T_P^e - L_M^t T_P^t, \end{aligned} \quad (\text{D25})$$

$$\begin{aligned} W_M(C_t, -; tr, t) &= \sum_{g \in Z_t} \Gamma^{-*}(g) L_M^{tr} T_P^{rg} \\ &= L_M^{tr} T_P^r - L_M^{tr} T_P^{tr^2}, \end{aligned} \quad (\text{D26})$$

$$\begin{aligned} W_M(C_t, -; tr^2, t) &= \sum_{g \in Z_t} \Gamma^{-*}(g) L_M^{tr^2} T_P^{r^2g} \\ &= L_M^{tr^2} T_P^{r^2} - L_M^{tr^2} T_P^{tr}. \end{aligned} \quad (\text{D27})$$

After the shrinking process, we have

$$\begin{aligned} \mathcal{S}(W_M(C_t, -; t, t)) &= T_P^e - T_P^t \\ &= \frac{1}{3} (W_P(B; 1, 1) - W_P(B; 1, 2) - W_P(B; 2, 1) \\ &\quad + W_P(B; 2, 2) + W_P(A)), \end{aligned} \quad (\text{D28})$$

$$\begin{aligned} \mathcal{S}(W_M(C_t, -; tr, t)) &= T_P^r - T_P^{tr^2} \\ &= \frac{1}{3} (\omega W_P(B; 1, 1) - \omega W_P(B; 1, 2) - \omega^2 W_P(B; 2, 1) \\ &\quad + \omega^2 W_P(B; 2, 2) + W_P(A)), \end{aligned} \quad (\text{D29})$$

$$\begin{aligned} \mathcal{S}(W_M(C_t, -; tr^2, t)) &= T_P^{r^2} - T_P^{tr} \\ &= \frac{1}{3} (\omega^2 W_P(B; 1, 1) - \omega^2 W_P(B; 1, 2) - \omega W_P(B; 2, 1) \\ &\quad + \omega W_P(B; 2, 2) + W_P(A)). \end{aligned} \quad (\text{D30})$$

The space $\mathcal{S}(V_{(C_t, -)})$ decomposes as

$$\mathcal{S}(V_{(C_t, -)}) = V_{(A)} \oplus V_{(B)}, \quad (\text{D31})$$

which leads to the shrinking rule

$$\mathcal{S}([C_t, -]) = [A] \oplus [B]. \quad (\text{D32})$$

All the shrinking rules in the 3d \mathbb{D}_3 quantum double model are shown in Table III.

-
- [1] B. Zeng, X. Chen, D.-L. Zhou, and X.-G. Wen, Quantum information meets quantum matter – from quantum entanglement to topological phase in many-body systems (2018), [arXiv:1508.02595 \[cond-mat.str-el\]](#).
- [2] E. Witten, Quantum field theory and the jones polynomial, [Commun. Math. Phys. **121**, 351 \(1989\)](#).
- [3] V. Turaev, *Quantum Invariants of Knots and 3-manifolds*, De Gruyter studies in mathematics (Walter de Gruyter GmbH, 2016).
- [4] B. Blok and X. G. Wen, Effective theories of the fractional quantum hall effect at generic filling fractions, [Phys. Rev. B **42**, 8133 \(1990\)](#).
- [5] C. Nayak, S. H. Simon, A. Stern, M. Freedman, and S. Das Sarma, Non-abelian anyons and topological quantum computation, [Rev. Mod. Phys. **80**, 1083 \(2008\)](#).
- [6] X.-G. Wen, *Quantum field theory of many-body systems: from the origin of sound to an origin of light and electrons* (Oxford University Press, 2004).
- [7] A. Kitaev, Fault-tolerant quantum computation by anyons, [Annals of Physics **303**, 2 \(2003\)](#).
- [8] A. Kitaev, Anyons in an exactly solved model and beyond, [Annals of Physics **321**, 2 \(2006\)](#), January Special Issue.
- [9] H. Bombin and M. A. Martin-Delgado, Family of non-abelian kitaev models on a lattice: Topological condensation and confinement, [Phys. Rev. B **78**, 115421 \(2008\)](#).
- [10] M. Koch-Janusz, M. Levin, and A. Stern, Exactly soluble lattice models for non-abelian states of matter in two dimensions, [Phys. Rev. B **88**, 115133 \(2013\)](#).
- [11] S. H. Simon, *Topological quantum* (Oxford University Press, 2023).
- [12] S. Vijay, J. Haah, and L. Fu, A new kind of topological quantum order: A dimensional hierarchy of quasiparticles built from stationary excitations, [Phys. Rev. B **92**, 235136 \(2015\)](#).
- [13] X. Ma, W. Shirley, M. Cheng, M. Levin, J. McGreevy, and X. Chen, Fractional order in infinite-component chern-simons gauge theories, [Phys. Rev. B **105**, 195124 \(2022\)](#).
- [14] K. Slagle, Foliated quantum field theory of fracton order, [Phys. Rev. Lett. **126**, 101603 \(2021\)](#).
- [15] B.-X. Li and P. Ye, Infinite-component BF field theory: Nexus of fracton order, Toeplitz braiding, and non-Hermitian amplification, [arXiv e-prints, arXiv:2511.09301 \(2025\)](#), [arXiv:2511.09301 \[cond-mat.str-el\]](#).
- [16] B.-X. Li, Y. Zhou, and P. Ye, Three-dimensional fracton topological orders with boundary toeplitz braiding, [Phys. Rev. B **110**, 205108 \(2024\)](#).
- [17] R. Shankar, Renormalization-group approach to interacting fermions, [Rev. Mod. Phys. **66**, 129 \(1994\)](#).
- [18] J. M. Leinaas and J. Myrheim, On the theory of identical particles, [Il Nuovo Cimento B \(1971-1996\) **37**, 1 \(1977\)](#).

- [19] F. Wilczek, Magnetic flux, angular momentum, and statistics, *Phys. Rev. Lett.* **48**, 1144 (1982).
- [20] F. Wilczek, Quantum mechanics of fractional-spin particles, *Phys. Rev. Lett.* **49**, 957 (1982).
- [21] Y.-S. Wu, General theory for quantum statistics in two dimensions, *Phys. Rev. Lett.* **52**, 2103 (1984).
- [22] T. Lan, L. Kong, and X.-G. Wen, Classification of $(3 + 1)$ D bosonic topological orders: The case when pointlike excitations are all bosons, *Phys. Rev. X* **8**, 021074 (2018).
- [23] T. Lan and X.-G. Wen, Classification of $3 + 1$ D bosonic topological orders (ii): The case when some pointlike excitations are fermions, *Phys. Rev. X* **9**, 021005 (2019).
- [24] J.-L. Huang, J. McGreevy, and B. Shi, Knots and entanglement, *SciPost Phys.* **14**, 141 (2023).
- [25] X. Wen, H. He, A. Tiwari, Y. Zheng, and P. Ye, Entanglement entropy for $(3+1)$ -dimensional topological order with excitations, *Phys. Rev. B* **97**, 085147 (2018).
- [26] J. C. Baez and J. P. Muniain, *Gauge fields, knots and gravity*, Vol. 4 (World Scientific Publishing Company, 1994).
- [27] L. H. Kauffman, *Knots and physics*, Vol. 1 (World scientific, 2001).
- [28] A. Hatcher, *Algebraic topology* (Cambridge university press, New York, 2001).
- [29] J. Milnor, Link groups, *Annals of Mathematics* **59**, 177 (1954).
- [30] R. Kobayashi, Y. Li, H. Xue, P.-S. Hsin, and Y.-A. Chen, Generalized statistics on lattices, *Phys. Rev. X* **16**, 011010 (2026).
- [31] L. Fidkowski, J. Haah, and M. B. Hastings, Gravitational anomaly of $(3 + 1)$ -dimensional F_2 toric code with fermionic charges and fermionic loop self-statistics, *Phys. Rev. B* **106**, 165135 (2022).
- [32] Y.-A. Chen and P.-S. Hsin, Exactly solvable lattice Hamiltonians and gravitational anomalies, *SciPost Phys.* **14**, 089 (2023).
- [33] T. Hansson, V. Oganesyan, and S. Sondhi, Superconductors are topologically ordered, *Annals of Physics* **313**, 497 (2004).
- [34] G. T. Horowitz, Exactly soluble diffeomorphism invariant theories, *Communications in Mathematical Physics* **125**, 417 (1989).
- [35] G. T. Horowitz and M. Srednicki, A quantum field theoretic description of linking numbers and their generalization, *Communications in Mathematical Physics* **130**, 83 (1990).
- [36] P. Ye, T. L. Hughes, J. Maciejko, and E. Fradkin, Composite particle theory of three-dimensional gapped fermionic phases: Fractional topological insulators and charge-loop excitation symmetry, *Phys. Rev. B* **94**, 115104 (2016).
- [37] B. Moy, H. Goldman, R. Sohal, and E. Fradkin, Theory of oblique topological insulators, *SciPost Phys.* **14**, 023 (2023).
- [38] P. Ye and X.-G. Wen, Constructing symmetric topological phases of bosons in three dimensions via fermionic projective construction and dyon condensation, *Phys. Rev. B* **89**, 045127 (2014).
- [39] P. Putrov, J. Wang, and S.-T. Yau, Braiding statistics and link invariants of bosonic/fermionic topological quantum matter in $2+1$ and $3+1$ dimensions, *Annals of Physics* **384**, 254 (2017).
- [40] Q.-R. Wang, M. Cheng, C. Wang, and Z.-C. Gu, Topological quantum field theory for abelian topological phases and loop braiding statistics in $(3+1)$ -dimensions, *Phys. Rev. B* **99**, 235137 (2019).
- [41] P. Ye and Z.-C. Gu, Topological quantum field theory of three-dimensional bosonic abelian-symmetry-protected topological phases, *Phys. Rev. B* **93**, 205157 (2016).
- [42] A. P. O. Chan, P. Ye, and S. Ryu, Braiding with borromean rings in $(3 + 1)$ -dimensional spacetime, *Phys. Rev. Lett.* **121**, 061601 (2018).
- [43] Z.-F. Zhang and P. Ye, Compatible braidings with hopf links, multiloop, and borromean rings in $(3 + 1)$ -dimensional spacetime, *Phys. Rev. Res.* **3**, 023132 (2021).
- [44] P. Ye and Z.-C. Gu, Vortex-line condensation in three dimensions: A physical mechanism for bosonic topological insulators, *Phys. Rev. X* **5**, 021029 (2015).
- [45] P. Ye and J. Wang, Symmetry-protected topological phases with charge and spin symmetries: Response theory and dynamical gauge theory in two and three dimensions, *Phys. Rev. B* **88**, 235109 (2013).
- [46] M. G. Alford and F. Wilczek, Aharonov-Bohm interaction of cosmic strings with matter, *Phys. Rev. Lett.* **62**, 1071 (1989).
- [47] L. M. Krauss and F. Wilczek, Discrete gauge symmetry in continuum theories, *Phys. Rev. Lett.* **62**, 1221 (1989).
- [48] M. G. Alford, Kai-Ming Lee, J. March-Russell, and J. Preskill, Quantum field theory of non-abelian strings and vortices, *Nuclear Physics B* **384**, 251 (1992).
- [49] J. Preskill and L. M. Krauss, Local discrete symmetry and quantum-mechanical hair, *Nuclear Physics B* **341**, 50 (1990).
- [50] C. Wang and M. Levin, Braiding statistics of loop excitations in three dimensions, *Phys. Rev. Lett.* **113**, 080403 (2014).
- [51] J. C. Wang, Z.-C. Gu, and X.-G. Wen, Field-theory representation of gauge-gravity symmetry-protected topological invariants, group cohomology, and beyond, *Phys. Rev. Lett.* **114**, 031601 (2015).
- [52] J. C. Wang and X.-G. Wen, Non-abelian string and particle braiding in topological order: Modular $SL(3, \mathbb{Z})$ representation and $(3 + 1)$ -dimensional twisted gauge theory, *Phys. Rev. B* **91**, 035134 (2015).
- [53] C.-M. Jian and X.-L. Qi, Layer construction of 3d topological states and string braiding statistics, *Phys. Rev. X* **4**, 041043 (2014).
- [54] S. Jiang, A. Mesaros, and Y. Ran, Generalized modular transformations in $(3+1)$ D topologically ordered phases and triple linking invariant of loop braiding, *Phys. Rev. X* **4**, 031048 (2014).
- [55] C. Wang, C.-H. Lin, and M. Levin, Bulk-boundary correspondence for three-dimensional symmetry-protected topological phases, *Phys. Rev. X* **6**, 021015 (2016).
- [56] A. Tiwari, X. Chen, and S. Ryu, Wilson operator algebras and ground states of coupled BF theories, *Phys. Rev. B* **95**, 245124 (2017).
- [57] A. Kapustin and R. Thorngren, Anomalies of discrete symmetries in various dimensions and group cohomology, (2014), [arXiv:1404.3230 \[hep-th\]](https://arxiv.org/abs/1404.3230).
- [58] X. Chen, A. Tiwari, and S. Ryu, Bulk-boundary correspondence in $(3+1)$ -dimensional topological phases, *Phys. Rev. B* **94**, 045113 (2016).
- [59] A. Kapustin and N. Seiberg, Coupling a QFT to a TQFT and Duality, *JHEP* **04**, 001, [arXiv:1401.0740 \[hep-th\]](https://arxiv.org/abs/1401.0740).

- [60] Z.-F. Zhang, Q.-R. Wang, and P. Ye, Continuum field theory of three-dimensional topological orders with emergent fermions and braiding statistics, *Phys. Rev. Res.* **5**, 043111 (2023).
- [61] X.-L. Qi and S.-C. Zhang, Topological insulators and superconductors, *Rev. Mod. Phys.* **83**, 1057 (2011).
- [62] M. F. Lapa, C.-M. Jian, P. Ye, and T. L. Hughes, Topological electromagnetic responses of bosonic quantum hall, topological insulator, and chiral semimetal phases in all dimensions, *Phys. Rev. B* **95**, 035149 (2017).
- [63] P. Ye, M. Cheng, and E. Fradkin, Fractional s -duality, classification of fractional topological insulators, and surface topological order, *Phys. Rev. B* **96**, 085125 (2017).
- [64] E. Witten, Fermion path integrals and topological phases, *Rev. Mod. Phys.* **88**, 035001 (2016).
- [65] B. Han, H. Wang, and P. Ye, Generalized wen-zee terms, *Phys. Rev. B* **99**, 205120 (2019).
- [66] S.-Q. Ning, Z.-X. Liu, and P. Ye, Fractionalizing global symmetry on looplike topological excitations, *Phys. Rev. B* **105**, 205137 (2022).
- [67] S.-Q. Ning, Z.-X. Liu, and P. Ye, Symmetry enrichment in three-dimensional topological phases, *Phys. Rev. B* **94**, 245120 (2016).
- [68] P. Ye, Three-dimensional anomalous twisted gauge theories with global symmetry: Implications for quantum spin liquids, *Phys. Rev. B* **97**, 125127 (2018).
- [69] Z.-F. Zhang, Q.-R. Wang, and P. Ye, Non-abelian fusion, shrinking, and quantum dimensions of abelian gauge fluxes, *Phys. Rev. B* **107**, 165117 (2023).
- [70] T. Johnson-Freyd and M. Yu, Topological Orders in (4+1)-Dimensions, *SciPost Phys.* **13**, 068 (2022).
- [71] T. Johnson-Freyd, On the classification of topological orders, *Communications in Mathematical Physics* **393**, 989 (2022).
- [72] X. Chen, A. Dua, P.-S. Hsin, C.-M. Jian, W. Shirley, and C. Xu, Loops in 4+1d topological phases, *SciPost Phys.* **15**, 001 (2023).
- [73] Z. Wan, J. Wang, and Y. Zheng, Quantum 4d yang-mills theory and time-reversal symmetric 5d higher-gauge topological field theory, *Phys. Rev. D* **100**, 085012 (2019).
- [74] C.-M. Jian, X.-C. Wu, Y. Xu, and C. Xu, Physics of symmetry protected topological phases involving higher symmetries and its applications, *Phys. Rev. B* **103**, 064426 (2021).
- [75] Y. Feng, H. Xue, Y. Li, M. Cheng, R. Kobayashi, P.-S. Hsin, and Y.-A. Chen, Anyonic membranes and pontyagin statistics, *Phys. Rev. Lett.* **136**, 086601 (2026).
- [76] Z.-F. Zhang and P. Ye, Topological orders, braiding statistics, and mixture of two types of twisted BF theories in five dimensions, *JHEP* **04**, 138, [arXiv:2104.07067](https://arxiv.org/abs/2104.07067) [[hep-th](https://arxiv.org/archive/hep)].
- [77] Y. Huang, Z.-F. Zhang, and P. Ye, Fusion rules and shrinking rules of topological orders in five dimensions, *JHEP* **11**, 210, [arXiv:2306.14611](https://arxiv.org/abs/2306.14611) [[hep-th](https://arxiv.org/archive/hep)].
- [78] Y. Huang, Z.-F. Zhang, and P. Ye, Diagrammatics, pentagon equations, and hexagon equations of topological orders with loop- and membrane-like excitations, *JHEP* **2025** (6), 238, [arXiv:2405.19077](https://arxiv.org/abs/2405.19077) [[hep-th](https://arxiv.org/archive/hep)].
- [79] M. A. Levin and X.-G. Wen, String-net condensation: A physical mechanism for topological phases, *Phys. Rev. B* **71**, 045110 (2005).
- [80] L. Kong, T. Lan, X.-G. Wen, Z.-H. Zhang, and H. Zheng, Classification of topological phases with finite internal symmetries in all dimensions, *Journal of High Energy Physics* **2020**, 93 (2020).
- [81] C. Delcamp and A. Tiwari, From gauge to higher gauge models of topological phases, *Journal of High Energy Physics* **2018**, 1 (2018).
- [82] L. Kong, Y. Tian, and S. Zhou, The center of monoidal 2-categories in 3+1d dijkgraaf-witten theory, *Advances in Mathematics* **360**, 106928 (2020).
- [83] C. Delcamp and A. Tiwari, On 2-form gauge models of topological phases, *Journal of High Energy Physics* **2019**, 1 (2019).
- [84] H. Chen, Drinfel'd double symmetry of the 4d kitaev model, *Journal of High Energy Physics* **2023**, 141 (2023).
- [85] A. Debray, W. Ye, and M. Yu, How to build anomalous (3+1)d topological quantum field theories, (2025), [arXiv:2510.24834](https://arxiv.org/abs/2510.24834) [[math-ph](https://arxiv.org/archive/math)].
- [86] L. Kong and X.-G. Wen, Braided fusion categories, gravitational anomalies, and the mathematical framework for topological orders in any dimensions, (2014), [arXiv:1405.5858](https://arxiv.org/abs/1405.5858) [[cond-mat.str-el](https://arxiv.org/archive/cond)].
- [87] Y. Wan, J. C. Wang, and H. He, Twisted gauge theory model of topological phases in three dimensions, *Phys. Rev. B* **92**, 045101 (2015).
- [88] J. Huxford, D. X. Nguyen, and Y. B. Kim, Twisted lattice gauge theory: Membrane operators, three-loop braiding, and topological charge, *Phys. Rev. B* **110**, 035117 (2024).
- [89] P. Ye, C.-S. Tian, X.-L. Qi, and Z.-Y. Weng, Confinement-deconfinement interplay in quantum phases of doped mott insulators, *Phys. Rev. Lett.* **106**, 147002 (2011).
- [90] P. Ye and Q.-R. Wang, Monopoles, confinement and charge localization in the t-j model with dilute holes, *Nuclear Physics B* **874**, 386 (2013).
- [91] Y. Ma, P. Ye, and Z.-Y. Weng, Low-temperature pseudogap phenomenon: precursor of high- T_c superconductivity, *New Journal of Physics* **16**, 083039 (2014).
- [92] J.-W. Mei, Possible fermi liquid in the lightly doped kitaev spin liquid, *Phys. Rev. Lett.* **108**, 227207 (2012).
- [93] X.-Y. Song, A. Vishwanath, and Y.-H. Zhang, Doping the chiral spin liquid: Topological superconductor or chiral metal, *Phys. Rev. B* **103**, 165138 (2021).
- [94] Z.-T. Xu, Z.-C. Gu, and S. Yang, Global phase diagram of doped quantum spin liquid on the Kagome lattice, [arXiv e-prints](https://arxiv.org/abs/2404.05685), [arXiv:2404.05685](https://arxiv.org/abs/2404.05685) (2024), [arXiv:2404.05685](https://arxiv.org/archive/cond) [[cond-mat.str-el](https://arxiv.org/archive/cond)].
- [95] G.-Y. Zhu, J.-Y. Chen, P. Ye, and S. Trebst, Topological fracton quantum phase transitions by tuning exact tensor network states, *Phys. Rev. Lett.* **130**, 216704 (2023).
- [96] C. Zhou, M.-Y. Li, Z. Yan, P. Ye, and Z. Y. Meng, Detecting subsystem symmetry protected topological order through strange correlators, *Phys. Rev. B* **106**, 214428 (2022).
- [97] C. Zhou, M.-Y. Li, Z. Yan, P. Ye, and Z. Y. Meng, Evolution of dynamical signature in the x-cube fracton topological order, *Phys. Rev. Res.* **4**, 033111 (2022).
- [98] X.-G. Wen, Mean-field theory of spin-liquid states with finite energy gap and topological orders, *Phys. Rev. B* **44**, 2664 (1991).
- [99] P. Ye and X.-G. Wen, Projective construction of two-dimensional symmetry-protected topological phases with $u(1)$, $so(3)$, or $su(2)$ symmetries, *Phys. Rev. B* **87**,

- 195128 (2013).
- [100] Y.-M. Lu and D.-H. Lee, Spin quantum hall effects in featureless nonfractionalized spin-1 magnets, *Phys. Rev. B* **89**, 184417 (2014).
- [101] C. Wang, A. Nahum, and T. Senthil, Topological paramagnetism in frustrated spin-1 mott insulators, *Phys. Rev. B* **91**, 195131 (2015).
- [102] M. Barkeshli and X.-G. Wen, $u(1) \times u(1) \rtimes Z_2$ chernsimons theory and Z_4 parafermion fractional quantum hall states, *Phys. Rev. B* **81**, 045323 (2010).
- [103] D. Gaiotto, A. Kapustin, N. Seiberg, and B. Willett, Generalized global symmetries, *Journal of High Energy Physics* **2015**, 172 (2015).
- [104] X.-G. Wen, Emergent anomalous higher symmetries from topological order and from dynamical electromagnetic field in condensed matter systems, *Phys. Rev. B* **99**, 205139 (2019).
- [105] J. McGreevy, Generalized symmetries in condensed matter, *Annual Review of Condensed Matter Physics* **14**, 57 (2023).
- [106] C. Cordova, T. T. Dumitrescu, K. Intriligator, and S.-H. Shao, Snowmass white paper: Generalized symmetries in quantum field theory and beyond, [arXiv:2205.09545](https://arxiv.org/abs/2205.09545).
- [107] S. Schafer-Nameki, ICTP lectures on (non-)invertible generalized symmetries, [arXiv:2305.18296](https://arxiv.org/abs/2305.18296).
- [108] L. Bhardwaj, L. E. Bottini, L. Fraser-Talente, L. Gladden, D. S. W. Gould, A. Platschorre, and H. Tillim, Lectures on generalized symmetries, [arXiv:2307.07547](https://arxiv.org/abs/2307.07547).
- [109] R. Luo, Q.-R. Wang, and Y.-N. Wang, Lecture notes on generalized symmetries and applications, *Physics Reports* **1065**, 1 (2024).
- [110] F. Benini, C. Córdova, and P.-S. Hsin, On 2-group global symmetries and their anomalies, *Journal of High Energy Physics* **2019**, 118 (2019).
- [111] Y.-N. Wang and Y. Zhang, Fermionic higher-form symmetries, *SciPost Phys.* **15**, 142 (2023).
- [112] Z.-F. Zhang, Y. Huang, Q.-R. Wang, and P. Ye, Field-Theoretical Construction of Conserved Currents, Non-Invertible Symmetries, and Mixed Anomalies in Three-Dimensional Non-Abelian Topological Order, [arXiv e-prints](https://arxiv.org/abs/2601.01523), [arXiv:2601.01523](https://arxiv.org/abs/2601.01523) [cond-mat.str-el].
- [113] Y. Feng, Y.-A. Chen, P.-S. Hsin, and R. Kobayashi, Onsiteability of higher-form symmetries, (2025), [arXiv:2510.23701](https://arxiv.org/abs/2510.23701).
- [114] Y. Feng, R. Kobayashi, Y.-A. Chen, and S. Ryu, Higher-form anomalies on lattices, (2025), [arXiv:2509.12304](https://arxiv.org/abs/2509.12304).
- [115] Q.-R. Wang and Z.-C. Gu, Towards a complete classification of symmetry-protected topological phases for interacting fermions in three dimensions and a general group supercohomology theory, *Phys. Rev. X* **8**, 011055 (2018).
- [116] S.-Q. Ning, X.-Y. Ren, Q.-R. Wang, Y. Qi, and Z.-C. Gu, Classification of Interacting Topological Crystalline Superconductors in Three Dimensions and Beyond, [arXiv e-prints](https://arxiv.org/abs/2512.25069), [arXiv:2512.25069](https://arxiv.org/abs/2512.25069) [cond-mat.str-el].
- [117] Q.-R. Wang and Z.-C. Gu, Construction and classification of symmetry-protected topological phases in interacting fermion systems, *Phys. Rev. X* **10**, 031055 (2020).
- [118] J.-H. Zhang, S.-Q. Ning, Y. Qi, and Z.-C. Gu, Construction and classification of crystalline topological superconductor and insulators in three-dimensional interacting fermion systems, *Phys. Rev. X* **15**, 031029 (2025).
- [119] C.-T. Hsieh, G. Y. Cho, and S. Ryu, Global anomalies on the surface of fermionic symmetry-protected topological phases in (3+1) dimensions, *Phys. Rev. B* **93**, 075135 (2016).
- [120] A. Kapustin, R. Thorngren, A. Turzillo, and Z. Wang, Fermionic symmetry protected topological phases and cobordisms, *Journal of High Energy Physics* **2015**, 1 (2015).
- [121] M. Cheng, N. Tantivasadakarn, and C. Wang, Loop braiding statistics and interacting fermionic symmetry-protected topological phases in three dimensions, *Phys. Rev. X* **8**, 011054 (2018).
- [122] K. Loo and Q.-R. Wang, Systematic construction of interfaces and anomalous boundaries for fermionic symmetry-protected topological phases, *Phys. Rev. B* **111**, 205102 (2025).
- [123] Z.-C. Gu and X.-G. Wen, Symmetry-protected topological orders for interacting fermions: Fermionic topological nonlinear σ models and a special group supercohomology theory, *Phys. Rev. B* **90**, 115141 (2014).
- [124] J.-R. Zhou, Q.-R. Wang, C. Wang, and Z.-C. Gu, Non-abelian three-loop braiding statistics for 3d fermionic topological phases, *Nature Communications* **12**, 3191 (2021).
- [125] Y.-A. Chen, T. D. Ellison, and N. Tantivasadakarn, Disentangling supercohomology symmetry-protected topological phases in three spatial dimensions, *Phys. Rev. Res.* **3**, 013056 (2021).
- [126] S.-T. Zhou, M. Cheng, T. Rakovszky, C. von Keyserlingk, and T. D. Ellison, Finite-temperature quantum topological order in three dimensions, *Phys. Rev. Lett.* **135**, 040402 (2025).
- [127] M.-Y. Li and P. Ye, Fracton physics of spatially extended excitations, *Phys. Rev. B* **101**, 245134 (2020).
- [128] M.-Y. Li and P. Ye, Fracton physics of spatially extended excitations. ii. polynomial ground state degeneracy of exactly solvable models, *Phys. Rev. B* **104**, 235127 (2021).
- [129] M.-Y. Li and P. Ye, Hierarchy of entanglement renormalization and long-range entangled states, *Phys. Rev. B* **107**, 115169 (2023).
- [130] M. Iqbal, N. Tantivasadakarn, R. Verresen, S. L. Campbell, J. M. Dreiling, C. Figgatt, J. P. Gaebler, J. Johansen, M. Mills, S. A. Moses, J. M. Pino, A. Ransford, M. Rowe, P. Siegfried, R. P. Stutz, M. Foss-Feig, A. Vishwanath, and H. Dreyer, Non-abelian topological order and anyons on a trapped-ion processor, *Nature* **626**, 505 (2024), [arXiv:2305.03766](https://arxiv.org/abs/2305.03766) [quant-ph].
- [131] S. Xu, Z.-Z. Sun, K. Wang, H. Li, Z. Zhu, H. Dong, J. Deng, X. Zhang, J. Chen, Y. Wu, C. Zhang, F. Jin, X. Zhu, Y. Gao, A. Zhang, N. Wang, Y. Zou, Z. Tan, F. Shen, J. Zhong, Z. Bao, W. Li, W. Jiang, L.-W. Yu, Z. Song, P. Zhang, L. Xiang, Q. Guo, Z. Wang, C. Song, H. Wang, and D.-L. Deng, Non-abelian braiding of fibonacci anyons with a superconducting processor, *Nature Physics* **20**, 1469 (2024), [arXiv:2404.00091](https://arxiv.org/abs/2404.00091) [quant-ph].
- [132] Google Quantum AI and Collaborators, Non-abelian braiding of graph vertices in a superconducting processor, *Nature* **618**, 264 (2023), [arXiv:2210.10255](https://arxiv.org/abs/2210.10255) [quant-ph].
- [133] Y.-J. Liu, K. Shtengel, A. Smith, and F. Pollmann, Methods for simulating string-net states and anyons on a digital quantum computer, *PRX Quantum* **3**, 040315

- (2022).
- [134] Z. K. Mineev, K. Najafi, S. Majumder, J. Wang, A. Stern, E.-A. Kim, C.-M. Jian, and G. Zhu, Realizing string-net condensation: Fibonacci anyon braiding for universal gates and sampling chromatic polynomials, *Nature Communications* **16**, 6225 (2025).
- [135] C. Schön, E. Solano, F. Verstraete, J. I. Cirac, and M. M. Wolf, Sequential generation of entangled multiqubit states, *Phys. Rev. Lett.* **95**, 110503 (2005).
- [136] C. Schön, K. Hammerer, M. M. Wolf, J. I. Cirac, and E. Solano, Sequential generation of matrix-product states in cavity qed, *Phys. Rev. A* **75**, 032311 (2007).
- [137] M. C. Bañuls, D. Pérez-García, M. M. Wolf, F. Verstraete, and J. I. Cirac, Sequentially generated states for the study of two-dimensional systems, *Phys. Rev. A* **77**, 052306 (2008).
- [138] Z.-Y. Wei, D. Malz, and J. I. Cirac, Sequential generation of projected entangled-pair states, *Phys. Rev. Lett.* **128**, 010607 (2022).
- [139] S.-H. Lin, R. Dilip, A. G. Green, A. Smith, and F. Pollmann, Real- and imaginary-time evolution with compressed quantum circuits, *PRX Quantum* **2**, 010342 (2021).
- [140] X. Chen, A. Dua, M. Hermele, D. T. Stephen, N. Tantisadakarn, R. Vanhove, and J.-Y. Zhao, Sequential quantum circuits as maps between gapped phases, *Phys. Rev. B* **109**, 075116 (2024).
- [141] Y.-T. Hu, M.-Y. Li, and P. Ye, Preparing code states via seed-entangler-enriched sequential quantum circuits: Application to tetradigit topological error-correcting codes, *Phys. Rev. B* **112**, 165139 (2025).
- [142] A. Lyons, C. F. B. Lo, N. Tantisadakarn, A. Vishwanath, and R. Verresen, Protocols for creating anyons and defects via gauging, *Phys. Rev. Lett.* **135**, 200405 (2025).
- [143] C. F. Bowen Lo, A. Lyons, R. Verresen, A. Vishwanath, and N. Tantisadakarn, Universal Quantum Computation with the S_3 Quantum Double: A Pedagogical Exposition, *arXiv e-prints*, arXiv:2502.14974 (2025), arXiv:2502.14974 [quant-ph].
- [144] J.-Y. Zhang and P. Ye, Programmable anyon mobility through higher order cellular automata, (2025), arXiv:2508.13961 [quant-ph].
- [145] J.-Y. Zhang, M.-Y. Li, and P. Ye, Higher-order cellular automata generated symmetry-protected topological phases and detection through multi point strange correlators, *PRX Quantum* **5**, 030342 (2024).